AMORPHOUS TELECHELIC HYDROCARBON DIOLS AND ETHYLENE-BASED MODEL COPOLYMERS VIA ACYCLIC DIENE METATHESIS

By

JOHN E. SCHWENDEMAN

A DISSERTATION PRESENTED TO THE GRADUATE SCHOOL
OF THE UNIVERSITY OF FLORIDA IN PARTIAL FULFILLMENT
OF THE REQUIREMENTS FOR THE DEGREE OF
DOCTOR OF PHILOSOPHY

UNIVERSITY OF FLORIDA

2002

To Irina, Laura, Paul and Anne

ACKNOWLEDGMENTS

Prof. Ken Wagener has been a true advisor and mentor. His love of chemistry, constant enthusiasm, and insatiable desire to pass-on what he has learned have made working in his research group an enriching experience. I will always be grateful for what he has taught me about chemistry, life, and myself.

I would also like to thank all of the members of the Wagener group and the Butler Polymer Laboratories that have helped me along the way. Krystyna Brzezinska, Jim Pawlow, Mark Watson, Jason Smith, Fernando Gomez, Debby Tindall, and Cameron Church were senior group members that provided excellent models for my graduate student career and were always there for help and support. Pat O'Donnell, Ed Lehman, John Sworen, and Tim Hopkins have been good friends and have helped me in countless ways in the lab. I am grateful for all of the other members of the polymer group for maintaining instruments, organizing meetings, discussing chemistry, and being fun to work with. Special thanks go to Lorraine Williams for her cheerful disposition, no matter how great the workload that we put on her.

My gratitude goes to the National Science Foundation and Medtronic, Inc. for their financial support of my research. Our collaborators at Medtronic, Michael Benz, Ed DiDomenico, Randy Sparer, Matt Jolly, and Kelvin Bonnema, are appreciated for involving me in their interesting project.

I am deeply grateful for my family. My parents, Paul and Anne Schwendeman, have provided me with advice, love and support throughout my academic career and life.

The greatest reward for anything I may achieve is the pride I see in their faces. My family has grown in the time that I have spent at the University of Florida. I now have a beautiful and intelligent wife (and colleague), Irina, and an adorable daughter, Laura. They have contributed the love and happiness that helped me through the stressful times.

TABLE OF CONTENTS

page

ACKNOWLEDGMENTS iv

LIST OF TABLES ix

LIST OF FIGURES x

ABSTRACT xiv

CHAPTER

1 INTRODUCTION 1

1.1 Historical Context of ADMET 1
1.2 History of Metathesis Catalysts 2
1.3 The ADMET Reaction 5
1.4 Applications of ADMET 8
1.5 Experimental Considerations 10
1.5.1 Catalyst Selection Issues 10
1.5.2 Monomer and Solvent Preparation 13
1.5.3 ADMET Reaction Apparatus 14
1.5.4 General ADMET Polymerization Procedure 15
1.6 Diverse Materials via ADMET 17
1.6.1 Perfectly Linear, Alkyl Branched, and Functionalized Polyethylenes 18
1.6.2 Telechelic Oligomers and Block Copolymers 22
1.7 Outlook for ADMET 28

2 SYNTHESIS OF ADMET MONOMERS 29

2.1 Introduction 29
2.2 Synthesis of Symmetrical Geminal Dimethyl α,ω-Diene Monomers 30
2.2.1 First Attempt: The Grignard Reagent/Alkenyl Halide Coupling Method. .. 30
2.2.2 Second Attempt: Diester Reduction/Tosylation/Tosylate Reduction Method 32
2.2.3 Third Attempt: The Direct Geminal Dimethylation of Ketone 33, or Methylation of Tertiary Alcohol 32 Method. 34
2.2.4 Fourth Attempt: Successful Preparation of Monomer (22) by a Carboxylic Acid Reduction/Tosylation/Tosylate Reduction Reaction Sequence Method 36
2.3 Synthesis of Carboxylic Acid and Methyl Ester Bearing α,ω-Diene Monomers.. 42

2.4 Conclusion 45

3 SYNTHESIS, CHARACTERIZATION, AND THERMAL BEHAVIOR OF ADMET ETHYLENE-BASED MODEL COPOLYMERS 46

3.1 Introduction 46
3.2 ADMET Models of Ethylene/Isobutlyene (EIB) Copolymers 49
3.2.1 Background for EIB Copolymers 49
3.2.2 Synthesis and Characterization of the EIB Model Copolymers 52
3.2.3 Thermal Behavior of the EIB Model Copolymers 58
3.3 ADMET Model of Ethylene/Methyl Methacrylate (EMMA) Copolymers 62
3.3.1 Background for EMMA Copolymers 62
3.3.2 Synthesis and Characterization of the EMMA Model Copolymer 64
3.3.3 Thermal Behavior of the EMMA Model Copolymer 67
3.4 ADMET Model of Ethylene/Methacrylic Acid (EMAA) Copolymers 70
3.4.1 Background for EMAA Copolymers 70
3.4.2 Synthesis and Characterization of the EMAA Model Copolymer 71
3.4.3 Thermal Behavior of the EMAA Model Copolymer 77
3.5 Melting Point Comparisons for ADMET Ethylene-Based Model Copolymers 81
3.6 Conclusion 83

4 COMPLETELY AMORPHOUS TELECHELIC HYDROCARBON DIOLS 85

4.1 Introduction 85
4.2 Synthesis of the Telechelic Diol with Short Chain-Ends (42a) 88
4.2.1 The First and Second Attempts 89
4.2.2 The Third and Fourth Attempts 91
4.2.3 The Fifth Attempt: Success! 94
4.3 Synthesis of Telechelic Diols with Medium Length Chain-Ends (42b) 99
4.4 Synthesis of Telechelic Diols with Long Chain-Ends (42c) 108
4.5 Conclusion 116

5 EXPERIMENTAL 118

5.1 Instrumentation and Analysis 118
5.2 Materials 119
5.3 Synthesis of α,ω-Diene Monomers 120
5.3.1 Gem-Dimethyl and Carboxylic Acid Monomer Syntheses 120
5.3.1.1 Step 1: dialkenylation of propionic acid (carboxylic acid monomer synthesis) 120
5.3.1.2 Step 2: carboxylic acid reduction to the alcohol 123
5.3.1.3 Step 3: tosylation of the alcohol 125
5.3.1.4 Step 4: reduction of the tosylate 126
5.3.2 Ester Monomer Synthesis 128
5.4 Synthesis of ADMET Ethylene-Based Model Copolymers 129
5.4.1 Synthesis of the EIB Model Copolymers (36a-c) 129

5.4.1.1 Synthesis of the unsaturated gem-dimethyl substituted polymers (39a-c) 129
5.4.1.2 Synthesis of the saturated gem-dimethyl substituted polymers (36a-c) 131
5.4.2 Synthesis of the EMMA Model Copolymer (37) 133
5.4.2.1 Synthesis of the unsaturated ester-functionalized polymer (40) 133
5.4.2.2 Synthesis of the saturated ester-functionalized polymer (37) 134
5.4.3 Synthesis of the EMAA Model Copolymer (38) 134
5.4.3.1 Synthesis of the unsaturated carboxylic acid-functionalized polymer (41) 134
5.4.3.2 Synthesis of the saturated carboxylic acid-functionalized polymer (38) 135
5.5 Synthesis of Telechelic Hydrocarbon Diols 136
5.5.1 Synthesis of the Monofunctional Reactants (43b and 46) 136
5.5.1.1 Synthesis of monofunctional reactant 43b 136
5.5.1.2 Synthesis of monofunctional reactant 46 137
5.5.2 Synthesis of the Telechelic Diols (42a-c) 138
5.5.2.1 Synthesis of 42a by the ADMET polymerization-depolymerization method 138
5.5.2.2 Synthesis of 42b by the ADMET polymerization-depolymerization method 141
5.5.2.3 Synthesis of 44b by the direct ADMET polymerization method 143
5.5.2.4 Synthesis of 47 by the direct ADMET polymerization method 144

APPENDIX

A ADDITIONAL ^{1}H AND ^{13}C NMR SPECTRA 147

B ADDITIONAL IR SPECTRA 153

LIST OF REFERENCES 159

BIOGRAPHICAL SKETCH 168

LIST OF TABLES

Table page

1.1 Melting Transitions (T_m) of the ADMET model polyethylenes **5-12**, listed in order of increasing steric bulk of the pendant group (R). 21

3.1 Thermal transitions of the ADMET gem-dimethyl branched and methyl branched model polyethylenes. 62

3.2 Melting transitions of the ADMET EMMA model copolymer (37), Yakota's periodic EMMA copolymers, and Matsuo's and Macknight's random EMMA copolymers....69

3.3 Thermal transitions of the ADMET EMAA model copolymer (38), Yakota's periodic EMAA copolymers, and Coleman's and Macknight's random EMAA copolymers....80

3.4 Peak melting temperatures for an analogous series of ADMET ethylene-based model copolymers....82

LIST OF FIGURES

Figure page

1.1 Various metathesis reactions....3

1.2 Three well-defined metathesis catalysts. 4

1.3 The mechanism of ADMET polymerization. 7

1.4 A variety of polymers made by ADMET. 9

1.5 Apparatuses used in ADMET reactions....15

1.6 Perfectly linear, methyl branched, and functionalized ADMET polyethylenes with precisely placed pendant groups (R)....20

1.7 Schematic representations of a telechelic polymer and three types of copolymers made by ADMET. 23

1.8 Telechelic oligomers made by the ADMET depolymerization of 1,4-butadiene.....24

1.9 A silicon-containing ABA block copolymer made with an ADMET-produced chlorodimethylsilane-terminated telechelic polymer. 25

1.10 A polypeptide/hydrocarbon ABA block copolymer made with an ADMET-produced amine-terminated telechelic polymer....26

1.11 A segmented block copolymer made from a silicon-containing telechelic diene and a biphenyl diene. 27

1.12 A poly(tetrahydrofuran)/hydrocarbon segmented block copolymer made by ADMET. 27

2.1 The gem-dimethyl (22a-c), carboxylic acid functional (23c), and ester functional (24c) α,ω-diene monomers....29

2.2 The grignard reagent/alkenyl halide coupling method.. 31

2.3 The diester reduction/tosylation/tosylate reduction method. 33

2.4 Direct geminal dimethylation of ketone 33 or alcohol 32. 34

2.5 ^{13}C and ^{1}H NMR spectra of the product mixture of the reaction of ketone 33 with $Ti(CH_3)_2Cl_2$.....35

2.6 Successful reaction sequence (carboxylic acid reduction/tosylation/ tosylate reduction).....37

2.7 ^{1}H and ^{13}C NMR spectra of monomer 22a.....38

2.8 ^{1}H and ^{13}C NMR spectra of monomer 22b.....39

2.9 ^{1}H and ^{13}C NMR spectra of monomer 22c.....41

2.10 ^{1}H and ^{13}C NMR spectra of monomer 23c.....43

2.11 Synthesis of the ester functional monomer 24c.....44

2.12 ^{1}H and ^{13}C NMR spectra of monomer 24c.....44

3.1 Synthetic scheme for the ADMET-made EIB, EMMA, and EMAA model copolymers (**36a-c**, **37**, and **38**, respectively).....48

3.2 The concepts of regioregularity and stereoregularity in polymers.....50

3.3 ^{1}H (top) and ^{13}C (bottom) NMR spectra for the unsaturated polymer (**39a**).....54

3.4 ^{1}H (top) and ^{13}C (bottom) NMR spectra for the EIB model copolymer (**36a**).....56

3.5 IR spectra for the unsaturated polymer (**39a**) (top) and the EIB model copolymer (**36a**) (bottom).....57

3.6 DSC trace for the EIB model copolymer (**36a**).....59

3.7 DSC trace for the EIB model copolymer (**36b**).....60

3.8 DSC Trace for the EIB Model Copolymer (**36c**).....60

3.9 DSC trace showing the 'cold crystallization' phenomenon that was observed on the second scan of the EIB model copolymer (**36c**).....61

3.10 ^{1}H (top) and ^{13}C (bottom) NMR spectra for the EMMA model copolymer (**37**).....65

3.11 IR spectra for the unsaturated polymer (**40**) (top) and the EMMA model copolymer (**37**) (bottom).....67

3.12 DSC trace for the EMMA model copolymer (**37**).....68

3.13 ^{1}H NMR spectra for the first (top) and second (bottom) attempts to make the unsaturated polymer (**41**).....73

3.14 IR spectra for the monomer (**23c**) (previous page), and the first (top) and second (bottom) attempts to make the unsaturated polymer (**41**).....75

3.15 ^{1}H NMR spectrum for the EMAA model copolymer (**38**). 76

3.16 DSC trace for the EMAA model copolymer (**38**).....79

4.1 ADMET-made telechelic hydrocarbon diols (**42a-c**). 87

4.2 Synthetic scheme for the telechelic diols **42a** and **42b**.....89

4.3 ^{1}H NMR spectrum for the first attempt to make the unsaturated telechelic diacetate (**44a**).....90

4.4 Reaction apparatus used in the third and forth attemps to make the unsaturated telechelic diacetate (**44a**). 92

4.5 ^{1}H NMR spectrum for the third attempt to make the unsaturated telechelic diacetate (**44a**).....92

4.6 Olefin region of the ^{1}H NMR spectrum for the fourth attempt to make the unsaturated telechelic diacetate (**44a**).....93

4.7 The polymerization-depolymerization method and apparatus.....95

4.8 Chelation of catalyst **3** when MR **43a** is used.....96

4.9 ^{1}H NMR spectrum for the fifth attempt to make the unsaturated telechelic diacetate (**44a**).....97

4.10 ^{1}H NMR spectrum for the saturated telechelic diacetate (**45a**). 98

4.11 ^{13}C (top) and ^{1}H (bottom) NMR spectra for the telechelic diol (**42a**). 99

4.12 ^{13}C (top) and ^{1}H (bottom) NMR spectra for the unsaturated telechelic diacetate (**44b**) made by the polymerization-depolymerization method. 102

4.13 ^{1}H NMR spectrum for the saturated telechelic diacetate (**45b**). 103

4.14 ^{1}H NMR spectrum for the telechelic diol (**42b**).....104

4.15 DSC traces for the telechelics (**42b**, **44b**, and **45b**).....107

4.16 Synthetic scheme for the telechelic diol **42c**.....109

4.17 ^{13}C (top) and ^{1}H (bottom) NMR spectra for the unsaturated telechelic di(benzyl ether) (**47**) made with catalyst **3**. 110

4.18 ^{13}C (top) and ^{1}H (bottom) NMR spectra for the telechelic diol (**42c**) made using catalyst **3**. 111

4.19 ^{13}C (top) and ^{1}H (bottom) NMR spectra for the unsaturated telechelic di(benzyl ether) (**47**) made with catalyst **2**. 113

4.20 ^{13}C (top) and ^{1}H (bottom) NMR spectra for the telechelic diol (**42c**) made using catalyst **2**. 114

4.21 DSC traces for the telechelic diols (**42c's**) made using catalyst **3** (dashed line) and catalyst **2** (solid line). 115

Abstract of Dissertation Presented to the Graduate School
of the University of Florida in Partial Fulfillment of the
Requirements for the Degree of Doctor of Philosophy

AMORPHOUS TELECHELIC HYDROCARBON DIOLS
AND ETHYLENE-BASED MODEL COPOLYMERS
VIA ACYCLIC DIENE METATHESIS
By

John E. Schwendeman

December, 2002

Chair: Dr. Kenneth B. Wagener
Major Department: Chemistry

The synthesis, characterization, and thermal behavior of ADMET-made models of ethylene/isobutylene (EIB), ethylene/methyl methacrylate (EMMA) and ethylene/ methacrylic acid (EMAA) copolymers with sequence ordered pendant groups are described in Chapter 3. These model copolymers are compared to their random copolymer counterparts, which are made using chain-growth polymerization methods. They exhibit sharper melting transitions relative to the random copolymers, but their melting points occur at lower temperatures. Also, these new model copolymers are compared with a previously studied series of ADMET ethylene-based model copolymers, and support the previous finding that the melting points of the model periodic copolymers decrease with increasing steric bulk of their pendant groups. Only one of the model copolymers failed to crystallize, and this property was used advantageously to produce the amorphous telechelic hydrocarbon diols that are discussed in Chapter 4.

In Chapter 4, several methods are described for the production of perfectly bifunctional, completely amorphous telechelic hydrocarbon diols using ADMET chemistry. The hydrocarbon backbone is based on the symmetrical gem-dimethyl substituted α,ω-diene monomer that was used to make one of the EIB model copolymers. Three monofunctional reactants (MR's), each with a different methylene sequence length, were used to end-cap the polymer chains. All three MR's could be used to make difunctional telechelic diols, but the use of the shortest MR led to relatively poor molecular weight control and the use of the longest MR led to a semicrystalline material. The best results were obtained when the medium length MR was used in combination with the polymerization-depolymerization production method. The resulting telechelic diol was perfectly bifunctional within NMR and IR spectroscopy detection limits, and it was completely amorphous with a glass transition temperature at –56 °C.

Additionally, a simple two-step procedure was developed that was more efficient than the polymerization-depolymerization method. It involved the direct ADMET polymerization of the α,ω-diene monomer in the presence of a MR with a benzyl ether protecting group, followed by a one-pot hydrogenation-deprotection step. However, this method was only tested with the longest MR, which yielded the semicrystalline material. An improvement was suggested, involving the use of a shorter benzyl ether MR, that might lead to a perfectly difunctional, *completely amorphous* telechelic hydrocarbon diol using this simpler procedure.

CHAPTER 1
INTRODUCTION

1.1 Historical Context of ADMET

The phenomenon of olefin metathesis has been known for half of a century, but it was not until recently, concurrent with the discovery of well-defined catalysts, that the acyclic diene metathesis (ADMET) reaction could be utilized to make high molecular weight polymers. The term "olefin metathesis" was coined by Calderon in 1967, [1,2] and refers to a reaction in which the carbon atoms between a pair of double bonds are interchanged.[3-6] The chemistry, however, dates back to the discovery of transition metal catalysts for olefin polymerization by Ziegler and Natta in the late 1940s.[7,8]

In the mid-1950s, olefin metathesis reactions were observed by several research groups using Ziegler-Natta type catalysts,[9-11] but most of these early metathesis catalysts involved multi-component systems that were ill-defined, so the identity of the active catalyst and the reaction mechanism were unknown. Proof that the alkene double bond is broken and reassembled by the active catalyst did not exist until Dall'Asta and coworkers reported detailed labeling studies in the early 1960s.[12,13] Due to the nebulous nature of the active catalyst, the mechanism of the reaction remained unknown until 1971, when Chauvin and coworkers proposed that the key step in the reaction involves the formation of a metallocyclobutane ring intermediate from a metal carbene and an alkene.[14] Although not universally accepted at first, this mechanism eventually led to the rational design of more well-defined catalyst complexes and a better understanding of

structure-activity relationships, without which the ADMET reaction would not have been extensively developed. It is instructive to summarize the advancements in metathesis catalyst design that led to the discovery of ADMET polymerization, before we discuss the chemistry and utility of the ADMET reaction itself.

1.2 History of Metathesis Catalysts

Today, olefin metathesis has a variety of diverse applications, which stem from the mechanistically related reactions shown in Figure 1.1. These reactions include ring-opening metathesis (ROM), ring-closing metathesis (RCM), ring-opening metathesis polymerization (ROMP), cross-metathesis (CM), and ADMET polymerization. The development of these diverse reactions and their applications closely parallels the advancements in metathesis catalyst design. Until the early 1980s, the use of olefin metathesis was limited by the ill-defined, multi-component catalysts that were available. In general, these "classical" catalyst systems were composed of an early transition metal halide, such as WCl_6, and an alkylating agent, such as Bu_4Sn or $EtAlCl_2$, or a solid support. Revolutionary in their day, such catalysts were successful under certain conditions, such as high temperatures (100 °C). Since they are cheap and easy to prepare, they still have important commercial applications, such as the Shell Higher Olefin Process (SHOP) used in the production of large, functionalized olefins from simple alkenes.[3,8] The inherent disadvantages of the "classical" catalysts are that the identity and concentration of the active catalytic species could not be known or controlled, and the harsh conditions and Lewis acid activators made the metathesis of functionalized alkenes difficult.

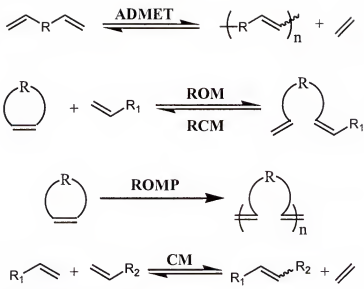

Figure 1.1 Various metathesis reactions.

The discoveries of organometallic carbene complexes in 1964[8] and the mechanism of olefin metathesis by Chauvin in 1971 eventually led to the rational design of progressively more advanced, well-defined catalyst systems. A significant breakthrough occurred in 1990 with Schrock's discovery of the well-defined, single-site tungsten and molybdenum (**1**) alkylidene catalysts (Figure 1.2).[15-20] The unprecedented activity of these catalysts greatly expanded the utility of the olefin metathesis reaction, allowing Wagener and coworkers to successfully polymerize 1,9-decadiene via the ADMET reaction in that same year.[21,22] However, these early transition metal-based complexes are highly oxophilic, making them susceptible to air and moisture poisoning if they are not employed under rigorously dry, oxygen-free conditions. They are also relatively intolerant of many functional groups, such as alcohols, aldehydes and carboxylic acids. These factors have limited the use of early transition metal-based catalysts, like **1**, for the metathesis of certain functionalized olefins.

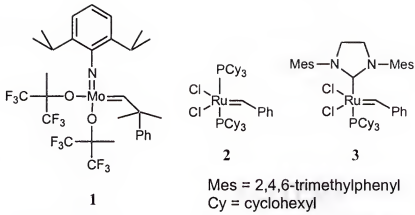

Figure 1.2 Three well-defined metathesis catalysts: Schrock's molybdenum alkylidene (**1**) and Grubbs' "first generation" (**2**) and "second generation" (**3**) benzylidene catalysts.

The development of well-defined ruthenium-based catalysts by Grubbs and coworkers in the early 1990s,[23-29] overcame many of the limitations of the Schrock-type catalysts. As a later transition metal, ruthenium tends to react preferentially with olefins in the presence of most other functional groups.[28] As early as the 1960s, it had been observed that $RuCl_3$(hydrate) could be used to obtain modest polymer yields in the ROMP of norbornene derivatives, even in the presence of ethanol and water.[28,30,31] Developments in the 1980s led researchers in the Grubbs group to examine the use of well-defined ruthenium alkylidene complexes as catalysts for olefin metathesis reactions. The most versatile and active of this "first generation" of Grubbs' carbene catalysts, ruthenium benzylidene **2** shown in Figure 1.2, is stable in air and is much more tolerant of water and most functional groups than catalysts based on early transition metal complexes, like **1**. However, catalyst **2** could not match the high activity of catalyst **1**. The discovery that N-heterocyclic carbene ligands could be used to improve the activity of the Grubbs-type ruthenium complex by Herrmann and coworkers in the late 1990s[32-34] prompted others to explore their use to bridge this gap in activity.[35] The Grubbs

group found that, by replacing only one of the phosphine ligands in **2** with a N-heterocyclic carbene ligand, high activity (similar to that of **1**) could be achieved without sacrificing the catalyst's functional group tolerance.[28,36-40] The most active of this "second generation" of Grubbs' catalysts (**3**) is shown in Figure 1.2.

Far from complete, the story of metathesis catalyst development is still unfolding. Challenges remaining include the formation of tetrasubstituted alkenes by CM, the ROMP of barrelenes, the tolerance of basic functional groups like nitriles and amines, and the stereoselective control of certain metathesis reactions.[28] Several research groups are working in each of these areas, and we anticipate future developments and the opportunities they will present for olefin metathesis.

1.3 The ADMET Reaction

The ADMET reaction has been the primary focus of research in the Wagener group since our successful polymerization of 1,9-decadiene with Schrock's tungsten alkylidene catalyst in 1990.[21,41] Previous research conducted by Wagener and coworkers in the late 1980s led to the demonstration that ADMET of α,ω-dienes meets the stringent requirements of step polymerization.[41] Subsequent studies sought to define the requirements for the reaction, including steric and electronic factors, functional groups tolerated by available catalysts, catalyst selection, and the necessary length and structural characteristics of the diene monomer. [41-56]

The mechanism of the ADMET reaction, first described by Wagener, Boncella, and Nel in 1991,[46] is shown in Figure 1.3. Essentially, ADMET is a step-growth polycondensation reaction that is driven by the removal of a small molecule, or condensate. Several features of this mechanism differentiate ADMET from its chain

polymerization relative, ROMP. Every step in the reaction cycle is reversible and in equilibrium, so it is the removal of the small olefinic by-product (typically ethylene since terminal dienes are most often employed) that irreversibly shifts the equilibrium from monomer to polymer. This is usually accomplished by using reduced pressure ($< 10^{-2}$ Torr), or in some cases an argon or nitrogen flow, to remove the condensate as it forms. ROMP, by contrast, is driven by the release of ring strain and no small molecule is produced during the reaction. Further, the ADMET cycle contains two metallocyclobutane intermediates (**4d** and **4f**), while the ROMP cycle has one. The first of these (**4d**) is formed when the monomer, or oligomer, associates with the alkylidene that bears another monomer or the growing polymer chain (**4c**). The second is **4f**, which is formed when the terminal olefin from an oligomer, or monomer, associates with the methylidene (**4e**). Upon collapse of **4f**, ethylene is removed and an alkylidene (**4c**) is formed that bears the growing polymer chain. The "true" catalyst in the reaction is the methylidene complex (**4e**), which is thought to be the most susceptible to decomposition of the alkylidene species present in the mechanism. Repetition of the cycle shown in Figure 1.3 leads to high molecular weight polymer at high conversion.

Similar to other polycondensation reactions, such as those used to produce polyesters and polyamides,[57] internal interchange reactions may occur during the ADMET reaction. This happens when an alkylidene on a polymer chain end (**4c**) reacts with an internal double bond in another polymer chain. While this results in two new polymer chains, there is no corresponding change in the overall molecular weight distribution. Typically, the observed molecular weight distribution is the Flory, or most

probable, distribution, in which the polydispersity index (M_w/M_n) approaches 2.0 at high conversion.[58]

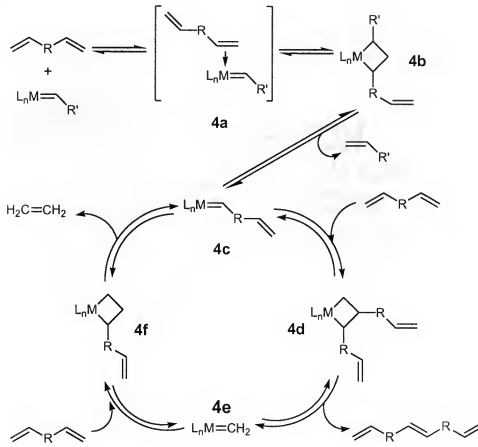

Figure 1.3 The mechanism of ADMET polymerization.

The molecular weights of ADMET polymers are typical for step-growth polymers, like the polyesters and polyamides mentioned above. Currently, the number average molecular weight (M_n) can range from 1,000 to 100,000 grams per mole in ADMET polymers, but it usually lies between 20,000 and 70,000 grams per mole. The molecular weight attainable depends on many factors, such as the efficiency of stirring and condensate removal, purity of reagents, catalyst efficiency and lifetime, monomer-catalyst compatibility, and the physical properties of the monomer and/or polymer. Many of these factors will be discussed in the sections that follow.

The general conditions for ADMET are like most other polycondensation reactions. The reaction is usually carried out in bulk monomer, where the monomer acts as both reactant and solvent. This maximizes the monomer concentration and shifts the equilibrium toward polymer formation. It also reduces the occurrence of intramolecular cyclization of the monomer by RCM, which becomes more kinetically favorable at lower diene concentrations. Cyclization is a common phenomenon in polycondensation chemistry,[57] but it can be substantially avoided in ADMET reactions by using α,ω-dienes with a chain length of ten atoms or more. If the dienes are any shorter, they may form thermodynamically stable five, six, and seven membered rings in preference to polymer. Ultimately, thermodynamics rather than kinetics determine whether cyclics or polymers are preferred for a given monomer, because ADMET polymerizations are carried out under equilibrium conditions over extended periods of time.

Another general reaction condition for ADMET polymerizations is the use of reduced pressure to remove the condensate. As mentioned above, this shifts the equilibrium irreversibly towards polymer formation, but it also serves to accelerate monomer conversion and increase the molecular weight of the polymer. These and other reaction conditions are discussed in more detail in Section 1.5.

1.4 Applications of ADMET

In the past decade, ADMET has moved smoothly from its development phase towards a broad realm of applications. With the advent of highly active, robust metathesis catalysts, such as **1**, **2**, and **3**, the challenge in ADMET chemistry has essentially been reduced to the synthesis and cost of the diene monomer. In other words, with few exceptions, if the diene monomer can be made, then a polymer can be produced by

ADMET. This chemistry provides access to a variety of polymers and polymer architectures that are not available using other polymerization methods. Figure 1.4 shows a variety of polymers produced recently in the Wagener group. [42-47,51,56,59] In addition to these, we have produced several alkyl branched and functionalized polymers with unprecedented regioregularity for the modeling of commercial ethylene copolymers, perfectly spaced graft (or comb) copolymers, reactive carbosilane polymers for use as solvent resistant elastomers with tunable properties, telechelic polymers for use in polymer modification or incorporation into block copolymers, and numerous other types of useful polymers.

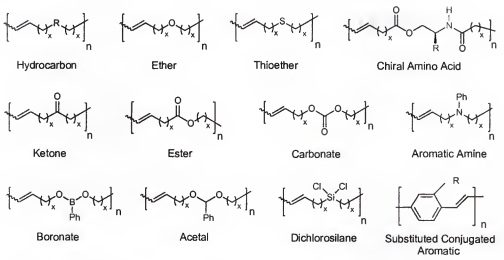

Figure 1.4 A variety of polymers made by ADMET.

Following a discussion of the general synthetic techniques used to create many of the polymers shown in Figure 1.4, Section 1.6 provides a more detailed description of some of these ADMET polymers and their unique properties. Several examples from other research groups are mentioned, but the focus is on recent research conducted in the Wagener laboratories that is relevant to the work presented in this dissertation.

1.5 Experimental Considerations

In this section, several issues that are critical to the successful experimental implementation of the ADMET reaction are discussed. Among these issues are the selection of the catalyst, the preparation of monomers and solvents, and the choice of the reaction apparatus to be used. After addressing these issues below, a description of a general ADMET polymerization procedure is provided to illustrate many of the factors that affect the success of the reaction.

1.5.1 Catalyst Selection Issues

The recent progress in ADMET polymerization is closely tied to developments in catalyst design. Representatives from three types of catalysts, "classical" catalysts, Schrock-type alkylidenes, and Grubbs-type carbenes, can be used in ADMET polymerizations. Each type has strengths and weaknesses, so the choice of catalyst for a given reaction is based on the particular diene to be polymerized and the physical properties of the polymer that will be formed, as well as other practical considerations.

By far the most widely used catalysts for ADMET are Schrock's molybdenum alkylidene (**1**) and Grubbs' ruthenium benzylidene (**2**) shown in Figure 1.2, because they are reliable and their chemistry is now well-established. Also shown in Figure 1.2 is the "second generation" Grubbs' catalyst (**3**), which has gained attention recently because it combines the high activity of **1** with the functional group tolerance of **2**. The multi-component "classical" catalysts are rarely employed in ADMET reactions, because their ill-defined nature can lead to unpredictable reactivity and undesired side reactions. However, their low cost and ease of preparation make "classical" catalysts useful for some applications.

So, which catalyst is right for a particular ADMET reaction? While some generalities can be made, the choice is complicated by subtleties in the mechanism and reactivity of each catalyst. For instance, kinetic studies comparing the reactivity of **1** with **2**, using 1,5-hexadiene as the monomer, showed that different products were formed for each catalyst under identical reaction conditions.[60] Linear polymer was the major product when catalyst **1** was used, while cyclics, such as 1,5-cyclooctadiene, were the major products when catalyst **2** was used. This result is attributed to mechanistic differences between these two catalysts. The same study showed that both catalysts produced primarily linear polymer when 1,9-decadiene was used as the monomer, but catalyst **1** accomplished the transformation an order of magnitude faster than **2**. In another recent study, a comparison of the kinetic behavior of the Grubbs' catalysts, **2** and **3,** showed that **3** is the more active catalyst by about an order of magnitude, but only at higher temperatures.[61] At 45, 60, and 75 °C catalyst **3** becomes progressively more active than **2** for the polymerization of 1,9-decadiene, but at 30 °C catalyst **2** is almost twice as fast as **3**. Also, an induction period was observed for catalyst **3** at all temperatures studied, which made it slower than **2** at the initial stage of the reaction. We attribute this to the slower rate of phosphine dissociation (a necessary step in the initiation of catalytic activity) for catalyst **3** than for **2**, which has been reported by Grubbs.[62,63]

We conclude that, generally, catalyst **1** and **3** are faster than **2**, but the reaction temperature is an important variable, particularly for catalyst **3**. Catalyst **3** is also more stable at higher temperatures than **1** or **2**. This is important in bulk ADMET polymerizations, where the viscosity of the growing polymer can impede stirring and the

diffusion of the condensate, limiting the ultimate molecular weight of the polymer. By increasing the reaction temperature, the viscosity can usually be lowered and higher molecular weights may be obtainable.

The choice of catalyst becomes even more complicated when monomers with functional groups are used. In general, catalysts **2** and **3** are more tolerant of air, water, and a wide range of functional groups, such as alcohols, esters and ketones, than is catalyst **1**. However, catalyst **1** is more tolerant than **2** of functionalities based on sulfur.[15-20] Additionally, the oxophilicity of molybdenum makes catalyst **1** highly susceptible to air and moisture poisoning. As a result, all solvents and monomers must be rigorously dried and degassed, and air-free Schlenk line techniques must be employed when catalyst **1** is used. The use of catalysts **2** and **3** is not hindered by these inconveniences. However, care should still be taken to keep reagents dry and air-free no matter which catalyst is used, as ADMET reaction times are often on the order of days, so catalyst decomposition can become an issue, particularly when solvents and elevated temperatures are used.

Recently, we have discovered a side reaction when the "second generation" Grubbs catalyst (**3**) is used under certain conditions. Olefin isomerization occurs, concurrent with the metathesis reaction, leading to a mixture of olefin products that differ by the position of the carbon-carbon double bond and/or the number of methylene units present in the molecular structure. By studying the reaction of **3** with simple olefins (1-octene and 2-octene) under typical ADMET conditions, we found that olefin isomerization is most pronounced at higher temperatures (50 °C and higher), while the extent of isomerization at 30 °C and below is significantly reduced.[64] We also determined that this phenomenon

is negligible when catalyst **2** is used and non-existent when catalyst **1** is used. Consequently, catalysts **1** and **2** are preferable for producing polymers with precise microstructures, such as those used in our polyethylene model studies discussed in Section 1.6.1 and the model ethylene copolymers described in Chapter 3. However, catalyst **3** is still highly useful for situations that require its high activity and functional group tolerance, and when extremely precise polymer microstructures are not so important.

Ultimately, optimal catalyst selection is based partly on generalizations of catalyst reactivity and partly on experience. In some cases, experimentation with several catalysts may be required to find the best one for a particular reaction.

1.5.2 Monomer and Solvent Preparation

The monomers and solvents used in ADMET reactions should be of high purity to avoid possible side reactions and premature catalyst decomposition. A variety of methods exist for the purification of monomers, and the choice, or combination of choices, depends on the physical properties of both the monomer and any impurities present. Among the methods most often employed are distillation (simple, fractional, or spinning band), recrystallization, column chromatography, and high performance liquid chromatography (HPLC).[65-67] Particular care must be taken when using catalyst **1** to ensure that monomers and solvents are devoid of water or dissolved oxygen. Drying is usually accomplished by vacuum distillation of a liquid monomer (or solvent) from an appropriate drying agent, or by heating a solid monomer under vacuum in the presence of a desiccant using an Abderhalden-type drying apparatus. Liquid monomers and solvents are then degassed by three freeze-pump-thaw cycles, as a final preparation, before they

are exposed to catalyst **1**. While purity is important, monomers and solvents need not be rigorously dry or air-free when the ruthenium-based catalysts **2** and **3** are used.

1.5.3 ADMET Reaction Apparatus

The glassware used in ADMET reactions has evolved from complex apparatuses to increasingly more simple ones. The elaborate break-seal glassware that was initially used to understand many monomer structure-reactivity relationships[46] has given way to simple Schlenk tubes or round-bottomed flasks. Today, a typical setup is merely a reaction flask, equipped with a magnetic stir bar and a Teflon valve (or glass stopcock). The valve allows for easy vacuum control when the apparatus is attached to a high vacuum line. An illustration of this simple apparatus is shown in Figure 1.5a.

Depending on the nature of the monomer or the polymer that is to be formed, several minor modifications to the apparatus can be made in order to maximize the molecular weight and/or polymer yield. For example, if the monomer is very volatile, or if a volatile solvent is used to dissolve a solid monomer (or polymer), then a dry ice/2-propanol filled, dewar-type condenser is attached to the reaction flask to prevent the loss of volatiles (Figure 1.5b). An alternative is the use of an argon or nitrogen flow to drive off the ethylene condensate. The apparatus is shown in Figure 1.5c, and it involves bubbling the gas through a needle directly into the reaction mixture and out through an oil-filled bubbler. However, this method is not as efficient at removing ethylene, so its use is usually restricted to cases where high vacuum is undesirable due to the volatility of certain reaction components.

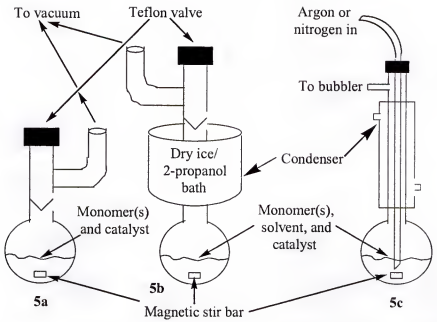

Figure 1.5 Apparatuses used in ADMET reactions.

The flexibility and simplicity of the apparatuses used in ADMET polymerizations have helped to make it a useful method for the preparation of a variety of macromolecules with diverse properties. The experimental method and apparatus can be critical to the ultimate efficiency and success of an ADMET reaction, so they should always be carefully considered and planed before beginning the reaction.

1.5.4 General ADMET Polymerization Procedure

Most often, ADMET reactions are conducted in the bulk state (where the catalyst is dissolved in pure monomer) and under reduced pressure (high vacuum), to drive the equilibrium towards polymer by maximizing the monomer concentration and removing the ethylene condensate. A typical procedure involves taking the purified, dried, and degassed monomer (see Section 1.5.2 above) and an oven dried reaction flask, with stir bar and Teflon valve, into an argon (or nitrogen) atmosphere glovebox, where the monomer is then weighed into the reaction flask. The appropriate catalyst (see Section

1.5.1) is weighed out to the desired monomer to catalyst ratio; usually 500-1000:1 for catalyst **1**, 100-500:1 for catalyst **2**, or 100-1000:1 for catalyst **3**. The catalyst is then added to the reaction flask, where it usually rapidly dissolves in the monomer with stirring, and the immediate evolution of ethylene is observed as it bubbles out of the solution. As quickly as possible, the reaction flask is closed, taken from the glovebox, and attached to a high vacuum line. Catalysts **2** and **3** can actually be handled in air, but the above precautions are often taken to ensure the longevity of the active catalyst and to maximize the molecular weight of the polymer.

Once the reaction flask is on the vacuum line, it is briefly (about 1 second) opened to vacuum at periodic intervals until the vigorous bubbling subsides and the viscosity (molecular weight) is such that stirring becomes more difficult. At this point, the flask is opened to full vacuum ($< 10^{-2}$ Torr) and the reaction temperature is gradually increased from the initial temperature, which is catalyst and monomer dependent. Usually, the reaction is started at room temperature for more volatile monomers, while initial temperatures of 30-40 °C may be used for monomers with higher boiling points. Due to its high activity, reactions using catalyst **1** are started at lower temperatures (20-30 °C) to avoid excessive bubbling that could cause the monomer to splatter on the sides of the reaction flask and lower the polymer yield. Since the rate of decomposition becomes accelerated at different temperatures for each of the catalysts, the maximum effective operating temperature under ADMET reaction conditions is different for each one. Catalyst **1** is used up to 50-55 °C, catalyst **2** is used up to 60-70 °C, and catalyst **3** can be used as high as 70-90 °C. Of course, these values depend on other variables, such as the presence of air, moisture, solvent, and monomer functional groups.

The reaction is considered complete when the evolution of ethylene (bubbling) is no longer observed and/or the mixture can no longer be stirred. The importance of a good magnetic stir bar and a powerful magnetic stirrer cannot be overstressed. As the viscosity (molecular weight) of the polymer increases, the percent conversion becomes increasingly limited by the diffusion of reactive end-groups. If the stir bar can no longer move through the thickening mixture, then the diffusion of end-groups may be sufficiently retarded to effectively halt the further increase of molecular weight. Once the reaction has reached this stage, it is cooled to room temperature and the catalyst is quenched by adding a terminating agent, such as ethyl vinyl ether or benzaldehyde, or by exposure to air. The polymer may then be isolated by precipitation and filtration, or by column chromatography. Additionally, Grubbs' catalyst (**2**) can be efficiently removed with the aid of water-soluble chelating phosphines.[46,68] Any residual solvent is then removed from the polymer by heating it under vacuum. The resulting ADMET polymer typically has a number average molecular weight in the range of 20,000 to 70,000 grams per mole and a polydispersity index of 2. The polymer can be characterized using various analytical techniques, such as nuclear magnetic resonance spectroscopy (NMR), infrared spectroscopy (IR), elemental analysis, gel-permeation chromatography (GPC), vapor pressure osmometry (VPO), membrane osmometry (MO), thermal gravimetric analysis (TGA), and differential scanning calorimetry (DSC).

1.6 Diverse Materials via ADMET

The versatility of the ADMET reaction for producing polymer structures and morphologies that are difficult or impossible to obtain by other methods is remarkable. ADMET has allowed the synthesis of perfectly linear polyethylene[69,70] and a variety of

alkyl branched[71] and functionalized polyethylenes[72-75] that have precisely placed pendant groups along the hydrocarbon backbone. Such polymers make excellent models for the study of structure-property relationships in commercial polymers and copolymers. A variety of end-functional (telechelic) polymers[47,76-81] have been made, both directly and by the ADMET depolymerization of unsaturated polymers, and some of these were used to make segmented[60,82] and ABA[80,81] block copolymers. Several hybrid organic/inorganic ADMET polymers, containing silicon,[44,56,59,82-87] tin,[88-90] germanium,[90,91] and phosphazine[92,93] as their inorganic components, have been recently produced. Graft copolymers with "perfect comb" structures are also accessible using ADMET polymerization.[94] It has even been possible to make certain conjugated polymers[95-97] and both main-chain and side-chain liquid crystalline polymers[98,99] via ADMET. Recently, biopolymers that contain chiral, amino acid moieties were added to the growing list of polymeric materials made via ADMET.[100] However, only the alkyl branched and functionalized polyethylenes, and telechelic oligomers and block copolymers will be discussed in more detail below, since they are the most pertinent to the research described in this dissertation.

1.6.1 Perfectly Linear, Alkyl Branched, and Functionalized Polyethylenes

In recent years, the Wagener group has focused considerable attention toward the modeling of polymers and copolymers made from ethylene. We have been studying the effect that precise placement of alkyl branches and functional groups along the polyethylene backbone has on the properties of this commercially important class of polymers. This work began with the production of perfectly linear polyethylene by the exhaustive hydrogenation of polyoctenamer made by ADMET of 1,9-decadiene (**5** in

Figure 1.6).[70,79] The linear ADMET polyethylene has a melting point (131-134 °C) that is comparable to industrially produced high-density polyethylene (133-138 °C) and approaches the theoretical value for infinitely long, perfectly linear polyethylene (141.5-146.5 °C) determined by Hoffman.[101,102]

In subsequent studies, we found that precise placement of branches along the polyethylene backbone has dramatic effects on the polymer's crystallization and melting behavior, which had not been observed previously. One such study involved the synthesis of a series of methyl branched polyethylenes (**6a-e**), where the methyl groups were placed precisely on every 9th, 11th, 15th, 19th, and 21st carbon atom of the backbone, respectively.[71] These precise structures are made possible by the clean condensation chemistry of ADMET using well-defined catalysts and symmetric methyl branched α,ω-diene monomers. As expected, we found that increasing the frequency of the methyl branches decreases the melting temperature (T_m) of the polymer. The melting temperatures, determined by DSC, ranged from 62 °C for the methyl branch on every 21st carbon (**6e**) to –14 °C for the methyl branch on every 9th carbon of the backbone (**6a**). In contrast to their ethylene/propylene copolymer counterparts, made by chain-growth polymerization techniques, these ADMET polymers all exhibited very sharp melting endotherms in their DSC traces. They also had substantially lower T_m ranges than the chain-made polymers with similar mole fractions of methyl branches. These observations are most likely due to the effect of precise, regular placement of the methyl branches on the polyethylene backbone for the ADMET models, which creates a type of semi-crystalline order that has not been found in chain-made, branched polyethylenes.

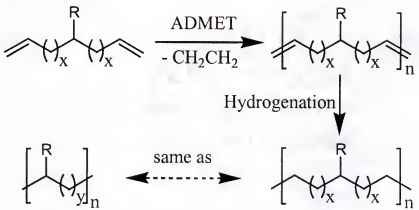

5	R = H (linear polyethylene)
6a-e	R = CH_3; y = 8, 10, 14, 18, and 20
7	R = (=O); y = 18
8a-d	R = OAc; y = 18, 20, 22, and 26
9a-b	R = CO_2CH_3; y = 18 and 22
10	R = $CO_2CH_2CH_3$; y = 18
11	R = C_6H_6; y = 18
12	R = Cl; y = 18

Figure 1.6 Perfectly linear, methyl branched, and functionalized ADMET polyethylenes with precisely placed pendant groups (R).

In other studies, the effects of precisely placed functional groups on the polyethylene backbone were examined, using the same methodology. Model copolymers of ethylene with carbon monoxide (**7**), vinyl acetate (**8a-d**), acrylates (**9a-b** and **10**), styrene (**11**), and vinyl chloride (**12**) were made via ADMET polymerization of symmetric α,ω-dienes followed by hydrogenation of the unsaturated polymer (see Figure 1.6).[72-76] Many of these reactions were performed using a tandem ADMET polymerization/heterogeneous hydrogenation method developed in our laboratories.[75] This process involves the addition of chromatographic grade silica gel to the Grubbs' ruthenium benzylidene (**2**) catalyzed reaction after the polymerization is complete, which results in a silica supported ruthenium species that catalyzes rapid and quantitative

hydrogenation of olefins. The method uses mild conditions (moderate pressures, room temperature) and has the added benefit of facilitating catalyst removal from the product.

The commercially relevant model ethylene copolymers, **7-12,** were compared to their chain-made counterparts, and to each other, to determine the effects that precise placement of the functional groups along the backbone and variation of the type of functional group have on their properties. ADMET produced functionalized polyethylene is different from a perfect ethylene/functional monomer model copolymer, in that the pendant functionality is separated by an even number of carbon atoms in the ADMET polymers instead of an odd number. However, we believe that this minor difference can be ignored for the comparison of our model copolymers to random copolymers with similar mole fractions of functional groups, due to the fairly large spacing of the pendant functional groups. Consistent with our methyl branch studies mentioned above, we found that our ADMET model copolymers exhibited sharper, more defined melting endotherms and their melting temperatures were lower than their chain-made counterparts.

Table 1.1 Melting Transitions (T_m) of the ADMET model polyethylenes **5-12**, listed in order of increasing steric bulk of the pendant group (R).

Polymer	Functional Group (R)	T_m [°C]
5	H	134
7	=O	134
12	Cl	77
6d	CH_3	56
8a	OAc	23
9a	CO_2CH_3	14
10	$CO_2CH_2CH_3$	13
11	C_6H_5	-12

The melting points of an analogous series of functionalized ADMET polyethylenes with perfectly spaced pendant groups on every 19th carbon atom of the backbone are shown in Table 1.1. The analogous methyl branched polyethylene (**6d**) and perfectly

linear ADMET polyethylene (**5**) are included for comparison. Significantly, the width of the melting point range spans nearly 150 °C within the series, and the melting points decrease with increasing steric bulk in the pendant groups. For the largest functional group studied, the phenyl group (polymer **11** in Table 1.1), crystallization is virtually nonexistent in the absence of annealing. However, a comparison of the model copolymers containing chloro and methyl groups (polymers **12** and **6d** in Table 1.1), which have similar steric requirements but differ in melting point by more than 20 °C, suggests that the size of the substituent is not the only factor that determines the melting point in ethylene copolymers. Future efforts will concentrate on expanding the number of precise models, and will include more detailed crystallographic and morphological studies in order to better understand the crystallization and melting behavior of functionalized polyethylene copolymers.

1.6.2 Telechelic Oligomers and Block Copolymers

Telechelic, or chain end-functional, polymers are useful because their reactive end-groups permit further modification and the production of phase-separated materials, such as ABA and segmented block copolymers. ADMET polymerization and depolymerization methods have been used in the synthesis of telechelic oligomers. Additionally, ADMET has been used to make block copolymers from telechelic dienes. Schematic representations of ABA and segmented block copolymers, as well as one of a telechelic polymer, are shown in Figure 1.7.

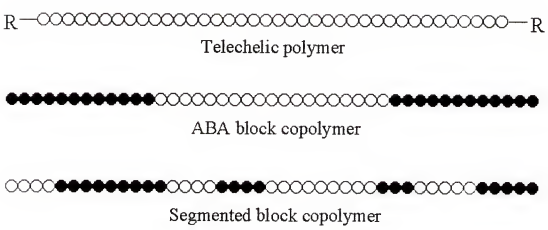

Figure 1.7 Schematic representations of a telechelic polymer and three types of copolymers made by ADMET.

The ADMET depolymerization of unsaturated polymers, such as 1,4-polybutadiene, has been used extensively in the Wagener group to synthesize telechelic oligomers. The metathesis depolymerization of 1,4-polybutadiene is accomplished, with or without the use of a monofunctional diene, by adding a well-defined catalyst (**1**, **2**, or **3**) and a small amount of solvent to the unsaturated polymer. When a monofunctional diene is used, such as ethylene or an end-functionalized monoene, telechelic oligomers with terminal alkene or other functional groups may be prepared.[77,78] Several examples, including ester, silylether, and imide terminated polymers, are shown in Figure 1.8. Macrocyclic intermediates are formed during the depolymerization reaction, followed by ring opening metathesis with the monoene to give the telechelic oligomer. The depolymerization of 1,4-polybutadiene has even been accomplished in the absence of added solvent, and this reaction has possible applications in the recycling of commercial elastomers to chemical feedstocks.[47,70,76] Other telechelics, with end-functionalities that are not well-tolerated by current catalysts, such as alcohols and acyclic amines, can be synthesized using protecting group strategies. Telechelics with acyclic amine end-

groups have recently been synthesized using the direct ADMET polymerization of α,ω-dienes in the presence of a functional group-protected α-olefin,[81,103] and telechelics with alcohol end-groups are featured in Chapter 4 of this dissertation.

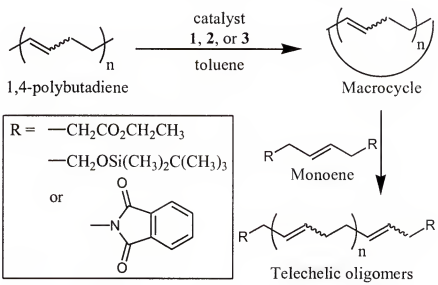

Figure 1.8 Telechelic oligomers made by the ADMET depolymerization of 1,4-butadiene.

Chlorodimethylsilane-terminated telechelics, made via the direct ADMET method, have been used to make ABA triblock copolymers through coupling reactions with hydroxyl-terminated poly(dimethylsiloxane) (Figure 1.9).[80] The biologically and structurally interesting polypeptide/hydrocarbon ABA triblock copolymer (**16**) shown in Figure 1.10 has also been prepared, using the amine-terminated telechelic oligomer (**13**) mentioned above.[81] The difunctional telechelic (**13**), made via ADMET, was used for the living polymerization of **14**, which was followed by hydrogenation of the olefins in **15** to give the ABA triblock copolymer (**16**).

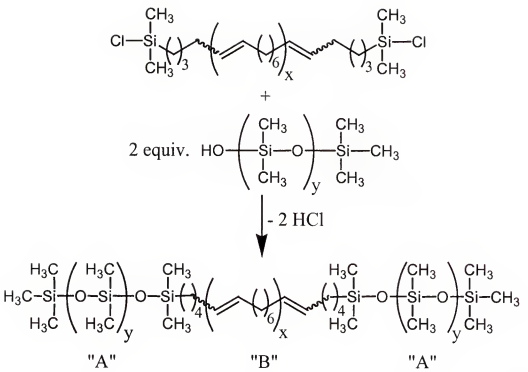

Figure 1.9 A silicon-containing ABA block copolymer made with an ADMET-produced chlorodimethylsilane-terminated telechelic polymer.

Segmented block copolymers, where alternating sections of "hard" and "soft" units are linked in the polymer chain, can also be prepared by ADMET chemistry. One example, shown in Figure 1.11, involves the copolymerization of telechelic diene oligomer **17** with the biphenyl diene monomer **18**, to produce the segmented block copolymer **19**.[82] The telechelic oligomer (**17**) is produced before copolymerization to prevent extensive self-metathesis of **18**, which would result in the formation of a low molecular weight insoluble solid. The copolymerization of **18** with **17** is advantageous, because it allows for a higher molecular weight material to be obtained, and it imparts excellent solubility and improved physical properties to the resultant copolymer. The copolymer (**19**) contains about 13 mole percent of the biphenylene subunit in the polymer backbone. Another example, shown in Figure 1.12, involves the ADMET copolymerization of a poly(tetrahydrofuran) telechelic diene (**20**) with 1,9-decadiene to

produce the well phase-separated segmented copolymer (**21**).[60] Such copolymers are useful materials due to the strength imparted by physical crosslinking within the hard segments combined with the toughness or elasticity provided by the phase-separated soft segment.

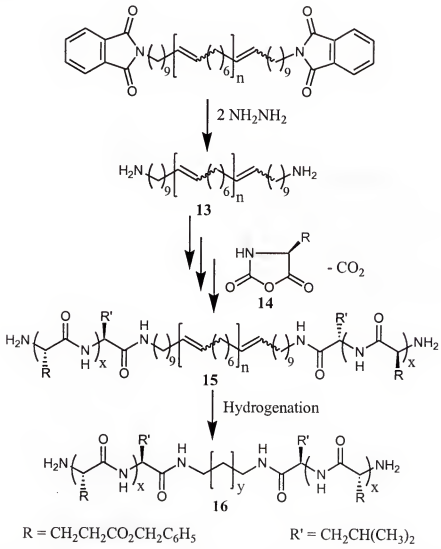

Figure 1.10 A polypeptide/hydrocarbon ABA block copolymer made with an ADMET-produced amine-terminated telechelic polymer.

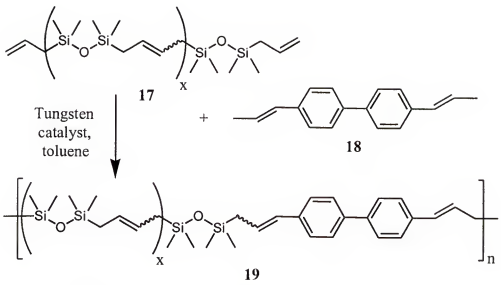

Figure 1.11 A segmented block copolymer made from a silicon-containing telechelic diene and a biphenyl diene.

The examples discussed above represent a fraction of the polymer materials and architectures available through the use of ADMET polymerization. The flexibility and versatility of this method is apparent from the number of diverse materials that have been made. This is due, in no small part, to the advent of well-defined metathesis catalysts and the creativity of the minds that define the possibilities.

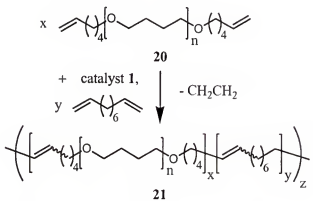

Figure 1.12 A poly(tetrahydrofuran)/hydrocarbon segmented block copolymer made by ADMET.

1.7 Outlook for ADMET

We have recounted the historical context for the discovery of the ADMET reaction, discussed many of the experimental preparations necessary for the successful implementation of the ADMET polymerization method, and demonstrated the applicability of this versatile reaction. As evidenced in Section 1.6, ADMET is an extremely flexible approach to the synthesis of a wide range of polymeric materials. With the well-defined metathesis catalysts that are available today, almost any functional group that can be incorporated into an α,ω-diene monomer can also be incorporated into a polymer. However, exceptions still exist, and there is room for improvement in catalyst design to permit the metathesis of basic functional groups, such as amines, as well as in experimental methods to allow higher molecular weights to be obtained when solid monomers are used. Aggressive efforts are being made in both of these areas, and we are confident that the utility of the ADMET reaction will continue to be demonstrated with, or without, these improvements.

CHAPTER 2
SYNTHESIS OF ADMET MONOMERS

2.1 Introduction

As mentioned in Section 1.4, the most challenging task encountered in the production of ADMET polymers is most often the synthesis of the requisite α,ω-diene monomers. The initial goal of the research described in this dissertation was to produce a series of gem-dimethyl branched polyethylene model polymers (EIB copolymers) to study the effects that perfectly regioregular, symmetrical branch points have on the crystallization and thermal behavior of polyethylene. To accomplish this goal using ADMET chemistry, the synthesis of a series of symmetrical gem-dimethyl α,ω-diene monomers (compounds **22a-c** in Figure 2.1), which differ only by the number of methylene 'spacers' between the gem-dimethyl pendant group and the terminal olefins, was required. In Section 2.2, the details of several trials that culminated in the successful completion of this substantial task are discussed.

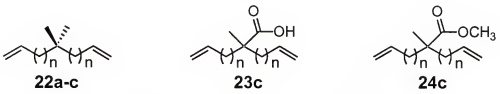

Figure 2.1 The gem-dimethyl (22a-c), carboxylic acid functional (23c), and ester functional (24c) α,ω-diene monomers.

The success of the symmetrical gem-dimethyl α,ω-diene monomer synthesis led to the expansion of the original research goals of this dissertation to include the synthesis of

completely amorphous telechelic hydrocarbon diols (Chapter 4), and the synthesis of two ethylene/functional monomer (EFM) model copolymers (Chapter 3). The gem-dimethyl monomer **22a** was advantageously used for the telechelic diol project, while the synthetic route used to make compounds **22a-c** serendipitously inspired the synthesis of monomers **23c** and **24c** (see Figure 2.1), which subsequently could be used in the production of ethylene/methacrylic acid (EMAA) and ethylene/methyl methacrylate (EMMA) model copolymers. The relatively simple preparations of monomers **23c** and **24c** are discussed in Section 2.3.

2.2 Synthesis of Symmetrical Geminal Dimethyl α,ω-Diene Monomers

Discussed below are three unsuccessful synthetic schemes for the production of the symmetrical gem-dimethyl α,ω-diene monomer, followed by the one that worked. The experimental details for the successful route, which is described in Section 2.2.4, are provided in Chapter 5.

2.2.1 First Attempt: The Grignard Reagent/Alkenyl Halide Coupling Method.

The first attempt to synthesize monomer **22a** (where n = 3) is outlined in Figure 2.2. The key step in this strategy is the Li_2CuCl_4 mediated cross-coupling of the alkenylmagnesium bromide (**28**) with the alkenyl bromide (**25a**). The methodology for this reaction was taken from the work pioneered by M. Tamura and J. Kochi in the early 1970s.[104] However, before this step could be attempted, it was necessary to synthesize the tertiary alkenyl bromide intermediate (**27**).

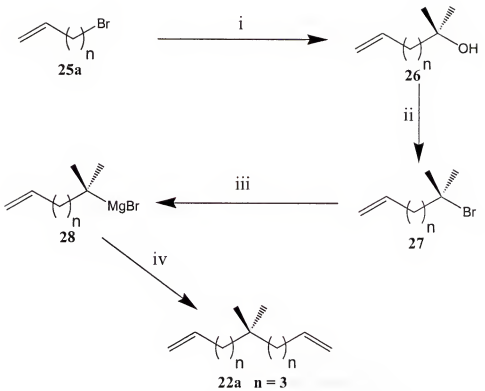

Figure 2.2 The Grignard reagent/alkenyl halide coupling method. Reagents and reaction conditions: i) a. Mg°, THF solvent; b. acetone; ii) 2.5 eq. Me_3SiCl and 2 eq. LiBr, acetonitrile solvent: iii) Mg°, THF solvent; iv) 25a and Li_2CuCl_4, THF solvent, -20 °C.

The tertiary alcohol (**26**) was synthesized by the alkenylmagnesium bromide alkylation of acetone, using classical Grignard chemistry. The alcohol (**26**) was then converted to the tertiary alkenyl bromide (**27**) using chlorotrimethylsilane and lithium bromide in acetonitrile. This method of bromination, developed by George A. Olah *et al.,* [105] was chosen for its mild nature (alkene tolerance) and high yield (nearly quantitative) of tertiary bromide. However, reactions carried out by this researcher yielded mixtures of tertiary alkenyl bromide (**27**), elimination product, and alkenyltrimethylsilyl ether, as seen in ^{1}H and ^{13}C NMR spectra. Product isolation and reaction optimization were not carried out, because other researchers in our laboratory discovered that the key step in this scheme, the Grignard reagent/alkyl bromide cross-coupling reaction, was

incompatible with terminal olefins. As a result, this strategy was set aside, while more promising alternatives were explored.

2.2.2 Second Attempt: Diester Reduction/Tosylation/Tosylate Reduction Method.

Based on previous work in our group,[58] the second attempt to synthesize monomer **22a** was a modification of a successful route to the monomethyl substituted dienes that were used to make regularly spaced methyl branched model polyethylenes (**6a-e**). Also, a similar methodology was used by Grubbs and coworkers to make a gem-dimethyl cyclobutene monomer, which they used to produce a ROMP version of an alternating ethylene/isobutylene copolymer.[106] Outlined in Figure 2.3, the strategy involves the stepwise addition of two equivalents of alkenyl bromide (**25a**) to diethyl malonate, using potassium *tert*-butoxide for enolate formation, to give the diester (**29**). The isolated yield for this step was about 50%. The diester was then reduced using six equivalents of 1.0 M $LiAlH_4$ in diethyl ether. In addition to the expected diol (**30**), incompletely reduced (aldehyde) product was detected in the NMR spectra. The diol product (**30**) could not be isolated by two successive fractional distillations, and its reaction with four more equivalents of $LiAlH_4$ failed to completely reduce the aldehyde group. However, using eight equivalents of $LiAlH_4$, the completely reduced diol (**30**) was obtained in about 80% yield.

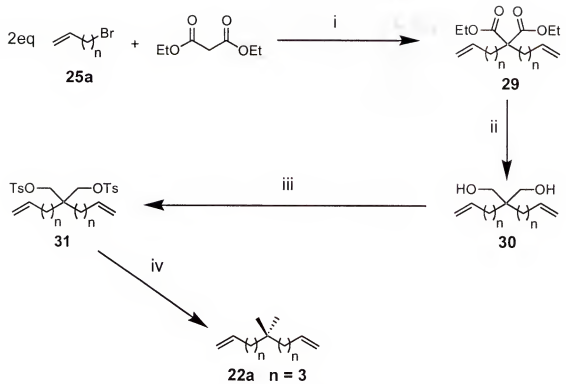

Figure 2.3 The diester reduction/tosylation/tosylate reduction method. Reagents and reaction conditions: i) two successive additions of potassium *t*-butoxide and 25a, DME solvent; ii) several equivalents of 1.0 M $LiAlH_4$ in diethyl ether; iii) 4 eq. of TosCl and 6 eq. of pyridine, chloroform solvent, 0 °C; iv) several equivalents of 1.0 M $LiAlH_4$ in diethyl ether.

The problems encountered in the second step of this reaction sequence can be attributed to the difficulty of transforming two sterically encumbered functional groups simultaneously. Large excesses of reagents are required in such cases, and product isolation can be problematic. Since the remaining two steps in this method involve transformations of two sterically encumbered functional groups, this strategy was deemed impractical for the synthesis of a series of gem-dimethyl monomers. Accordingly, two alternative schemes were devised; one that might yield monomer **22** in only two steps (Third Attempt), and another with four steps that only requires manipulations of one sterically encumbered functional group (Fourth Attempt).

2.2.3 Third Attempt: The Direct Geminal Dimethylation of Ketone 33, or Methylation of Tertiary Alcohol 32 Method.

Figure 2.4 outlines an elegant two step procedure that utilizes classical Grignard chemistry to form the tertiary alcohol (**32**), followed by methylation with $Ti(CH_3)_2Cl_2$ to give the monomer (**22**). In the early 1980s, Reetz and Westermann[107-110] developed the methodology for the key methylation step in this reaction sequence. They found that geminal dimethylation of ketones, and methylation of tertiary alcohols and halides, could be accomplished using organotitanium reagents. The organotitanium reagent ($Ti(CH_3)_2Cl_2$) was prepared by adding one equivalent of $Zn(CH_3)_2$ (dissolved in dry dichloromethane) to a solution of $TiCl_4$ in dichloromethane at –30 °C under an argon atmosphere. Two equivalents of this reagent were required for the reaction with the ketone (**33**).

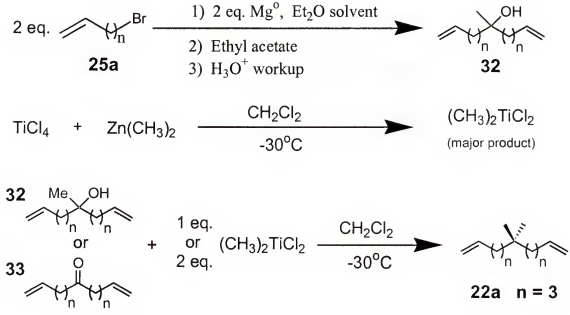

Figure 2.4 Direct geminal dimethylation of ketone 33 or alcohol 32.

^1H and ^{13}C NMR analysis (see Figure 2.5) of the complex product mixture (many spots on TLC plate) seem to indicate the oligomerization of the ketone (**33**) through its

olefin groups. While the carbonyl peak is absent in the ^{13}C NMR spectrum of the product, indicating dimethylation was probably successful, this method is clearly not appropriate for the synthesis of the symmetrical diene monomer (**22**).

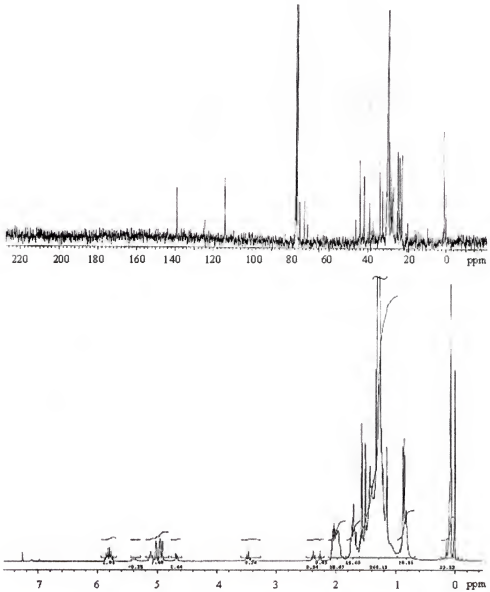

Figure 2.5 ^{13}C and ^{1}H NMR spectra of the product mixture of the reaction of ketone 33 with $Ti(CH_3)_2Cl_2$.

Another trial of this reaction was made, using the tertiary alcohol (**32**) and one equivalent of $Ti(CH_3)_2Cl_2$, to determine if experimental error, such as water or air

contamination, led to the failure of the first attempt with the ketone (**33**). Unfortunately, similar results were obtained.

On further investigation of this reaction, the results are not surprising. Ziegler-Natta catalysts used for the polymerization of olefins are made by combining a transition metal compound from groups IVB to VIIIB of the periodic table with an organometallic compound, usually derived from a group IA to IIIA metal. The best known of these catalyst systems are derived from $TiCl_4$ or $TiCl_3$ and an aluminum trialkyl cocatalyst, but $Zn(CH_3)_2$ is also an effective cocatalyst.[111] Therefore, by using such a system for the methylation of ketones and alcohols bearing terminal olefins, one could expect to obtain oligomers or polymers produced through the reaction of the olefins with the catalyst system. Another method for the direct methylation of ketones and alcohols, involving their reaction with excess trimethylaluminum,[112] was rejected based on fears of similar reactivity with the terminal olefins and the harsh reaction conditions required.

2.2.4 Fourth Attempt: Successful Preparation of Monomer (22) by a Carboxylic Acid Reduction/Tosylation/Tosylate Reduction Reaction Sequence Method.

Reexamination of the second attempt above (Figure 2.3) led to the modification of the first step so that only one functional group that required transformation was present on the intermediates instead of two. This method, outlined in Figure 2.6, led to the first successful synthesis of a symmetrical geminal dimethyl diene (monomer **22a**; where n = 3). The reaction sequence was carried out several times because additional monomer was required for our collaboration with Medtronic on the telechelic diol work discussed in Chapter 4, as well as for the synthesis of the monomer analogues (**22b** and **22c**) with n = 6 and 9 for the EIB copolymer model study discussed in Chapter 3. Several modifications to the procedure were explored along the way to improve the overall yield, but ultimately

the original procedure was employed essentially unaltered. In the procedural description below, typical yields are given, and the best yields obtained for each step are shown in parentheses.

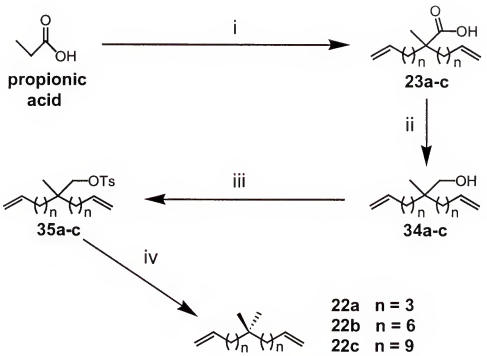

Figure 2.6 Successful reaction sequence (carboxylic acid reduction/tosylation/ tosylate reduction). Reagents and reaction conditions: i) 3 eq. of LDA, 2 eq. of alkenyl bromide (25), THF solvent, -30 °C; ii) 1.0 M $LiAlH_4$ in diethyl ether; iii) 2 eq. of TosCl and 3 eq. of pyridine, chloroform solvent, 0 °C; iv) 1.0 M $LiAlH_4$ in diethyl ether.

The first step in this reaction sequence involves the sequential addition of two equivalents of alkenyl bromide (**25**) to propionic acid, using lithium diisopropyl amide (LDA) as the enolate-forming base. The product of this reaction, upon acid workup, is the carboxylic acid (**23**), which has only one functional group to be modified. This results in higher yields and greatly simplifies the isolation of products in the reactions that follow, relative to the diester manipulations in Figure 2.3. The yield of the partially purified (see *Experimental Section* in Chapter 5) carboxylic acid intermediate (**23**) was usually about

50% (70% in best trial). The carboxylic acid (**23**) was then reduced to the alcohol (**34**) with $LiAlH_4$ in diethyl ether. After distillation, isolated yields of about 70-90% were typically obtained for the second step (93% in best trial).

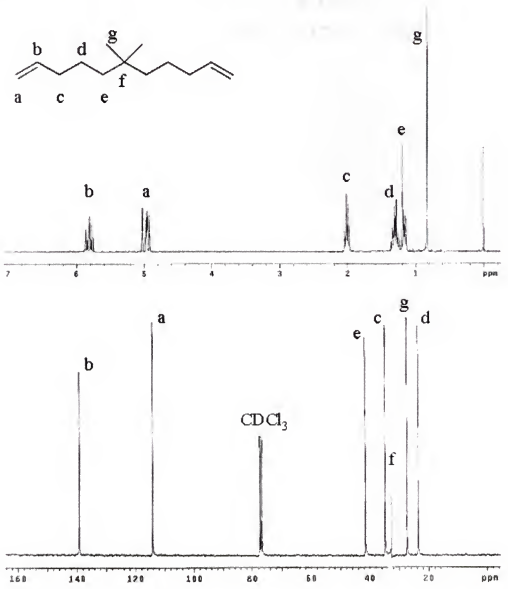

Figure 2.7 ^{1}H and ^{13}C NMR spectra of monomer 22a.

Conversion of the alcohol functionality into a good leaving group was accomplished by reacting **34** with two equivalents of toluenesulfonyl chloride in the presence of three equivalents of pyridine, in chloroform solvent, to give the tosylate (**35**).

Attempts to purify a small portion of the tosylate (**35a**) by distillation resulted in decomposition, so a yield of purified product was not calculated for this step (see *Experimental Section* in Chapter 5). However, purification at this stage of the reaction sequence is not crucial, and the crude tosylate can be utilized in the final step, without undesired consequences.

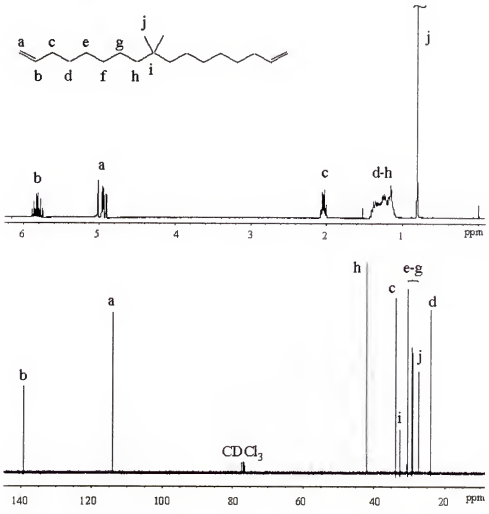

Figure 2.8 ^{1}H and ^{13}C NMR spectra of monomer 22b.

The final step of the monomer synthesis is the reduction of the tosylate group in **35** to give the symmetrical geminal dimethyl substituted diene (**22**). This was accomplished by the slow addition of $LiAlH_4$ to the tosylate (**35**) in diethyl ether. Pure monomer (**22**)

was obtained by column chromatography, and typical isolated yields of 50-65% were calculated for the last two steps (65% in best trial). The overall yields for all four steps were 27%, 10%, and 26% for the monomers **22a, b** and **c** respectively.

Figures 2.7, 2.8, and 2.9 show the ^{1}H and ^{13}C NMR spectra of the analogous series of symmetrical gem-dimethyl diene monomers **22a, b,** and **c** respectively. These results, along with GC analyses, indicate that the monomers are highly pure and symmetrical. However, upon close examination of the ^{1}H NMR spectrum of monomer **22c** (where n = 9) shown in Figure 2.9, resonances are observed at 5.4 ppm and 1.8 ppm that indicate the presence of about 5% internal olefin in this monomer. The isomer is also observed in the GC of monomer **22c**, and it is likely the result of a small amount of isomerization of the terminal olefin to next internal carbon atom of the chain (the β position). This is supported by the two doublets in the ^{1}H NMR spectrum at 1.8 ppm, which correspond to the terminal methyl groups in the cis and trans isomers of an internal olefin at the β position. A GC chromatogram of the 11-bromo-1-undecene (**25c**) that was used in the first step of the synthesis of monomer **22c** indicates that the olefin isomer is present in this starting material as purchased from Aldrich, and that it is not produced during the synthesis of the monomer. The absence of any internal olefin in monomers **22a** and **22b** further supports the assertion that the isomer was not a side-product of monomer synthesis.

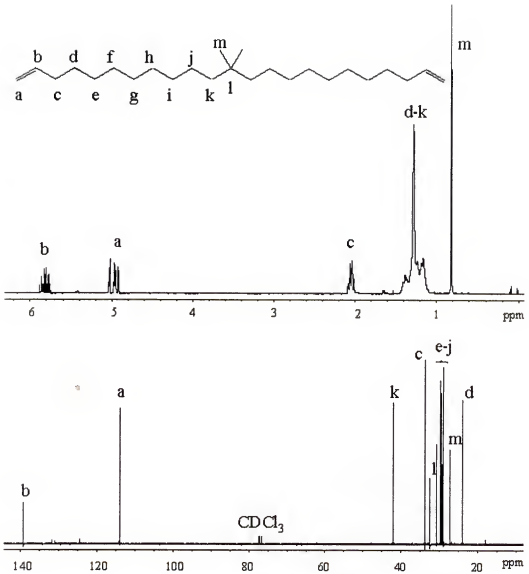

Figure 2.9 ^{1}H and ^{13}C NMR spectra of monomer 22c.

As a final preparation for ADMET polymerization with Schrock's molybdenum catalyst (**1**) the monomers (**22a-c**) were distilled over calcium hydride and degassed using three freeze-pump-thaw cycles. They were stored in an argon atmosphere dry box prior to polymerization.

2.3 Synthesis of Carboxylic Acid and Methyl Ester Bearing α,ω-Diene Monomers

The impetus for the synthesis of the carboxylic acid and methyl ester bearing α,ω-diene monomers, **23c** and **24c** respectively, came partly from the ease of preparing these novel ADMET monomers and partly from the observation that the fully hydrogenated ADMET polymers that they can be used to generate are of academic and industrial interest as model ethylene/methacrylic acid and ethylene/methyl methacrylate copolymers. These monomers were prepared readily due to the symmetrical gem-dimethyl diene monomer (**22**) synthetic work that was previously completed. As discussed in Chapter 1, most any functional group that can be incorporated into an α,ω-diene monomer can subsequently be incorporated into an ADMET polymer. Therefore, practically all of the α,ω-diene intermediates in the reaction schemes outlined in Section 2.2 could serve as monomers for ADMET polymerization. These two monomers (**23c** and **24c**) were selected for ADMET polymerization based on their utility for modeling commercial polymers.

The carboxylic acid monomer (**23c**; where n = 9) was prepared as outlined in Section 2.2.4 above, and was purified by column chromatography followed by two successive cold crystallizations from hexanes. The product was a white solid that melted at 43.5-45.5 °C, and was pure by GC, except for the 5% internal olefin isomer discussed in Section 2.2.4. The ^{1}H and ^{13}C NMR spectra of the carboxylic acid bearing monomer (**23c**) are shown in Figure 2.10. Prior to ADMET polymerization with Grubbs ruthenium benzylidene catalyst (**2**), monomer **23c** was melted and stirred under vacuum at 60 °C.

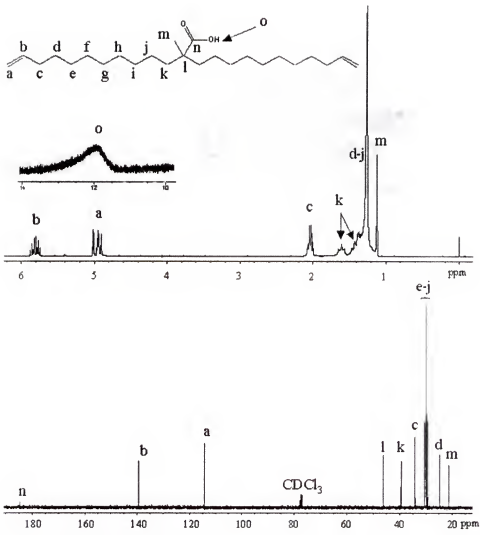

Figure 2.10 ^{1}H and ^{13}C NMR spectra of monomer 23c.

As outlined in Figure 2.11, the methyl ester bearing monomer (**24c**) was synthesized by the esterification of the carboxylic acid (**23c**). Pure **23c** (prepared as described above) was dissolved in acetone, to which potassium carbonate was then added, followed by methyl iodide. After distilling off excess methyl iodide and acetone, an extraction with pentane yielded pure **24c** (by GC), except for the 5% internal olefin isomer discussed in Section 2.2.4, with an isolated yield of 97%. Figure 2.12 shows the ^{1}H and ^{13}C NMR spectra of the methyl ester bearing monomer (**24c**). The monomer (**24c**)

was dried prior to ADMET polymerization with Grubbs ruthenium benzylidene catalyst (**2**) by stirring it with calcium hydride under vacuum overnight, and then filtering it through a 0.2 μm syringe filter in an argon atmosphere dry box.

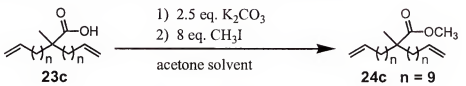

Figure 2.11 Synthesis of the ester functional monomer 24c.

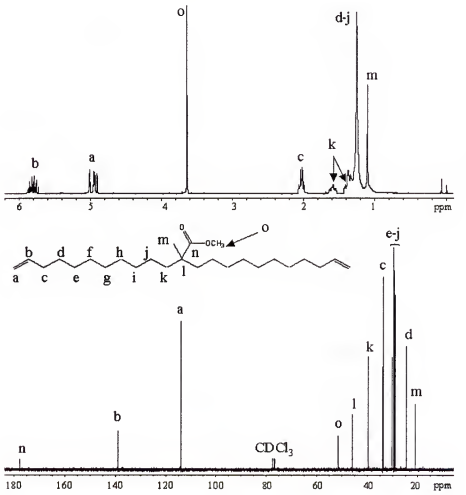

Figure 2.12 ^{1}H and ^{13}C NMR spectra of monomer 24c.

2.4 Conclusion

After several unsuccessful or aborted attempts, a successful route to the analogous series of symmetrical gem-dimethyl substituted α,ω-diene monomers (**22a-c**) was found. The use of these monomers for the production of ethylene/isobutylene (EIB) model copolymers (or gem-dimethyl branched polyethylene models) and amorphous telechelic hydrocarbon diols is discussed in Chapters 3 and 4 respectively.

Rigorous purification of the carboxylic acid intermediate (**23c**), made via the successful route to monomer **22**, yielded a monomer that could be used in the production of an ethylene/methacrylic acid (EMAA) model copolymer. Subsequent esterification of **23c** produced its methyl ester analog (**24c**), which could be used to make an ethylene/methyl methacrylate (EMMA) model copolymer. Both of these ethylene/functional monomer (EFM) model copolymers, made with monomers **23c** and **24c** using ADMET chemistry, are described in Chapter 3. The experimental procedures used for the synthesis and characterization of the monomers discussed in this Chapter are detailed in Chapter 5.

CHAPTER 3
SYNTHESIS, CHARACTERIZATION, AND THERMAL BEHAVIOR OF ADMET ETHYLENE-BASED MODEL COPOLYMERS

3.1 Introduction

For more than fifty years now, synthetic chemists have sought to make 1,1-disubstituted and functionalized polyethylenes via transition metal catalyzed polymerization. Such catalytic routes offer the promise of microstructural control that has not been achieved with the current free radical techniques, and could significantly broaden the utility and range of properties of these polymers. Unfortunately, the use of available metal complexes has been precluded by their susceptibility to poisoning by heteroatoms[113] and their relative inactivity toward 1,1-disubstituted α-olefins. However, recent research by the Brookhart[114] and Grubbs[115] groups suggests that nickel-based catalysts might lead to chain polymerization chemistry that inexpensively generates commercial scale functionalized polyethylene. Although some progress has been made in the copolymerization of 1,1-disubstituted α-olefins with ethylene using metallocene catalysts,[116,117] the commercialization of these processes has yet to be realized.

Due to the nature of the chain-growth polymerization mechanism and differing reactivity ratios of ethylene/comonomer pairs, the preparation of copolymers with precisely the same comonomer compositions and sequence distributions is rarely possible. Irregularities in the polymer microstructure result from random branching, due to chain transfer reactions or inconsistent placement of pendant groups from random incorporation of the comonomer. Many studies have been aimed at delineating the effect

of these irregularities in chain produced polyethylene random copolymers.[118] The consensus is that the melting point is depressed with increasing frequency and steric bulk of the imperfections (branches or polar pendant groups). Also, it is well-known that the sequence distributions of the comonomers are a major contributing factor to material properties. Therefore, model copolymers with more precise microstructures would be highly valuable for the strict comparison of different types of comonomers in ethylene-based copolymers.

With this in mind, we have exploited step polymerization techniques, the ADMET reaction, to synthesize model versions of ethylene copolymers with precisely placed pendant groups on the polymer backbone. Some of these ethylene-based model copolymers were discussed in Section 1.6.1, and these examples show that it is possible to incorporate virtually any functional group of interest in the backbone of polyethylene. Essentially, if the symmetric α,ω-diene with central pendant functionality can be synthesized, then a functional polyethylene with precise placement of the pendant group can be made. This has been possible due, largely, to the advent of well-defined metathesis catalysts (**1**, **2**, and **3**), some of which are tolerant of the presence of such functional groups as alcohols, ketones, esters, etc. Over the past few years, these catalysts have permitted the creation of polymer structures never before possible, by both ADMET [3,49] and ROMP[3] techniques.

The ADMET polymerization of a α,ω-diene monomer is straightforward polycondensation chemistry, similar to that required for the formation of polyester and nylon. The use of step growth polycondensation, rather than a chain growth technique, has made the precise control of polymer microstructure possible by eliminating chain

transfer reactions and the random incorporation of an α-olefin comonomer. The ADMET reaction operates by essentially one mechanism, with no side reactions (except for olefin isomerization when catalyst **3** is used; see Section 1.5.1), using a well-defined metathesis catalyst dissolved in bulk symmetric α,ω-diene monomer. The only variable in the repeating structure is the cis/trans distribution of the olefinic linkages. Upon hydrogenation, this variable is removed and the desired ethylene-based model copolymer with perfectly defined *mer* sequences is formed. The only difference in chain structure between ADMET produced ethylene-based model copolymers and a perfect copolymer model is that the pendant functionality is separated by an even number of carbon atoms in the ADMET polymers instead of an odd number.

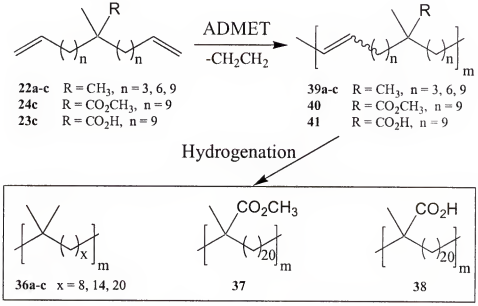

Figure 3.1 Synthetic scheme for the ADMET-made EIB, EMMA, and EMAA model copolymers (**36a-c**, **37**, and **38**, respectively).

This chapter describes the extension of our previous work to include ADMET-made models of ethylene/isobutylene (EIB) (**36a-c**), ethylene/methyl methacrylate (EMMA) (**37**) and ethylene/methacrylic acid (EMAA) (**38**) copolymers. Shown in Figure

3.1, these polymers with precisely placed substituents provide additional models for evaluation of the effect of functionality and regular branch placement on polyethylene. All, but one, of these ADMET ethylene-based model copolymers crystallize, and the details of their synthesis, characterization, and thermal behavior will be discussed in the sections that follow.

3.2 ADMET Models of Ethylene/Isobutlyene (EIB) Copolymers

3.2.1 Background for EIB Copolymers

Some observers have suggested that the lack of stereoregularity of the pendant groups in our previously studied ADMET ethylene-based model copolymers may affect their crystallinity and melting temperatures. Just as the type, frequency, and regioregularity (distribution) of branches can alter the properties of polyethylene, the stereoregularity (tacticity) of the side chains of α-olefin homopolymers greatly affects their properties. For example, isotactic polypropylene is highly crystalline, while atactic polypropylene is completely amorphous. The concepts of regioregularity and stereoregularity, as they relate to polymer microstructure, are illustrated in Figure 3.2.

While we believe that the pendant groups in our methyl branched and functionalized polyethylenes (see Section 1.6.1) are sufficiently far apart that tacticity should not be a concern, we desired to address this issue with greater certainty. However, since we can not produce stereoregular versions of our previous monosubstituted ethylene-based model copolymers using ADMET; and no other method currently exists, we chose to study gem-dimethyl branched polyethylene models (**36a-c**). Due to the symmetry of their gem-dimethyl branch points, tacticity will not be an issue for the regularly spaced gem-dimethyl polymer series. Indeed, these polymers represent the first *completely* regular branched polyethylene model polymers. It is expected that by studying

the crystallization and thermal behavior of these polymers, the effect of 'tacticity' in our regioregular polymers can be better understood.

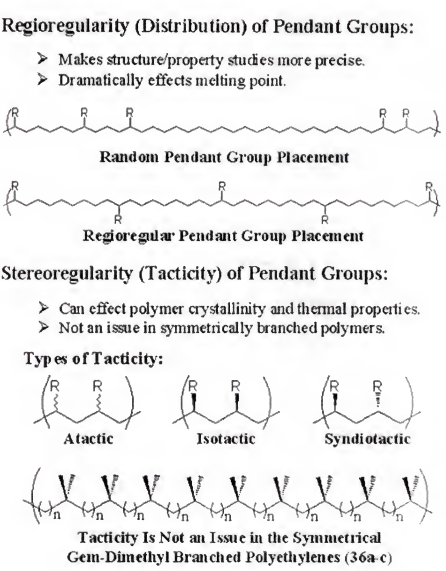

Figure 3.2 The concepts of regioregularity and stereoregularity in polymers.

Additionally, the synthesis of these gem-dimethyl branched polyethylenes (**36a-c**) will introduce a new route to the elusive ethylene/isobutylene (EIB) copolymer. The copolymerization of ethylene and isobutylene has not been industrially viable due to the vastly differing reactivities of the comonomers. In fact, the *Encyclopedia of Polymer Science and Engineering* boldly states that "…1,1-disubstituted α-olefins neither homo-

nor copolymerize with other monoolefins" using insertion or coordination polymerization conditions.[116] Contrary to this discouraging statement, there are a few reports of the coordinative copolymerization of isobutylene and ethylene in the literature. Using bis(indenyl)ethylidenezirconium dichloride activated with methylaluminoxane (MAO), Kaminsky and coworkers were able to make EIB copolymers with modest incorporation of isobutylene (up to 2.8 mole %). Even with very large molar ratios of isobutylene to ethylene (4000:1), higher isobutylene contents could not be achieved.[116] They also obtained lower molecular weight for the copolymer and decreased catalysts activity relative to ethylene homopolymerization using the same system. In 1998, Shaffer and coworkers produced highly alternating ethylene/isobutylene copolymers with up to 45 mole percent isobutylene content, using a titanium based metallocene catalyst system.[116] Despite low catalyst activity, they obtained EIB copolymers with number average molecular weights that ranged from 9,000 to 49,000 grams per mole, and isobutylene contents that ranged from 24 to 45 mole percent. All of the EIB copolymers were amorphous, with glass transition temperatures (T_g) between –25 and –37 °C. In another recent report, Grubbs and coworkers synthesized an alternating EIB model copolymer using Schrock's catalyst (**1**) for the ROMP of 3,3-dimethylcyclobutene, followed by diimide hydrogenation.[106] The resulting polymer was completely regioregular (>98%), despite the asymmetry of the monomer. They reasoned that the high regioselectivity of the reaction was due to the steric directing effect of the bulky gem-dimethyl substituent on the cyclobutene as it approaches the propagating alkylidenes. Polymers with number average molecular weights of 11,700 and 27600 grams per mole (PDI = 1.5-1.6) were obtained, but thermal analyses were not reported.

The following two sections will describe the synthesis and characterization, and the thermal behavior of a series of three ADMET EIB model copolymers (**36a-c**). The results of the thermal analyses of these EIB model copolymers will be compared to the ethylene/propylene model copolymers previously studied in the Wagener group (see Section 1.6.1), to determine if the stereoregularity (tacticity) of the pendant groups is an important issue in these studies. The results will also show that one of these polymers (**36a**) does not crystallize; a property that was used advantageously to produce the completely amorphous telechelic hydrocarbon diols described in Chapter 4.

3.2.2 Synthesis and Characterization of the EIB Model Copolymers

Shown in Figure 3.1 is the synthetic scheme for the production of a series of three EIB model copolymers (**36a-c**) from the symmetrical gem-dimethyl diene monomers (**22a-c**) using ADMET polycondensation chemistry. The monomers (**22a-c**) were polymerized in the bulk (no solvent) using Schrock's molybdenum alkylidene catalyst (**1**). This is an equilibrium polycondensation reaction, driven by the removal of ethylene under reduced pressure, which produces the unsaturated polymers (**39a-c**) with precise microstructures. The only variable in the structure of the repeat units is the cis/trans orientation of the internal olefins, which is removed upon quantitative hydrogenation.

A description of the synthesis of the first unsaturated polymer in the series (**39a**, where n = 3) will be given here as a representative example. The details of these experiments are provided in Chapter 5. The ADMET polymerization of the first monomer (**22a**) in the series was carried out using Schrock's catalyst (**1**) in bulk monomer. The addition was performed in an argon atmosphere dry box, using a 380:1 monomer to catalyst ratio. The reaction vessel was sealed, removed from the dry box, and then immediately placed on a vacuum line. Intermittent vacuum (opening the valve

slightly for 1 second) was applied at room temperature, with slow stirring, until the mixture became viscous. Full vacuum was then applied and, after several hours, the temperature was increased to about 45-50 °C. When the growing polymer grew too viscous to stir, the temperature was increased to 60 °C and the mixture was stirred slowly for two more days. The reaction is deemed complete when no more bubbles from ethylene evolution are observed, which is usually after a total of about five days.

The unsaturated polymer (**39a**), obtained after precipitation from toluene into cold methanol and vacuum drying, was a rubbery, tacky, faintly yellow material. It was soluble in chloroform, toluene, and THF. The GPC analysis indicated that the polymer has a high number average molecular weight (55,200 g/mol) and a polydispersity index (PDI = 1.7). The ^{1}H and ^{13}C NMR spectra of the unsaturated polymer (**39a**) are shown in Figure 3.3. The ^{1}H NMR spectrum shows the expected broad methylene carbon resonances in the aliphatic region (1.2 ppm) of the spectrum, along with a resonance at 0.82 ppm for the dimethyl branches and a broad multiplet at 1.9 for the allylic methylenes. Also noteworthy is the loss of the terminal alkene resonances of the diene monomer (**22a**) (see Figure 2.7), and the appearance of two new resonances for the cis and trans internal olefins of the unsaturated polymer (**39a**). The ^{13}C NMR spectrum also confirms loss of the terminal alkene resonances, and the appearance of two new resonances (cis: 130.01 ppm, and trans: 130.45 ppm) corresponding to the polymer's internal olefins. The small resonance at 28.08 ppm corresponds to the allylic methylene carbon that is next to the cis alkenes. These results indicate the clean conversion of the diene monomer (**22a**) to the unsaturated regularly spaced geminal dimethyl branched polymer (**39a**).

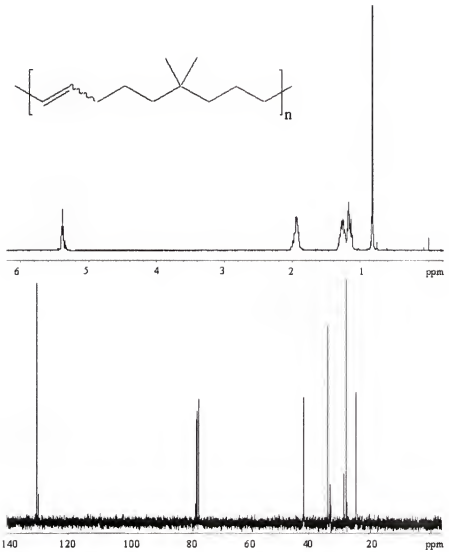

Figure 3.3 ^{1}H (top) and ^{13}C (bottom) NMR spectra for the unsaturated polymer (**39a**).

Similar procedures were followed to make the other two unsaturated polymers in the series, **39b** and **39c** where n = 6 and 9, respectively. The GPC analyses of these two polymers indicated number average molecular weights of 48,000 and 71,000 and PDI's of 1.8 and 1.6 for **39b** and **39c**, respectively. The ^{1}H and ^{13}C NMR spectra of **39b** and **39c** again indicate the precise microstructures that are obtained using ADMET polymerization (see *Appendix A*).

The quantitative hydrogenation of the unsaturated polymers (**39a-c**) is necessary for the strict comparison of these EIB model copolymers to their counterparts made by chain-growth polymerization methods. Two types of hydrogenation catalysts were used in this study, a heterogeneous catalyst and a homogeneous catalyst. The heterogeneous catalyst, palladium on activated carbon, was used to hydrogenate the first unsaturated polymer in the series (**39a**), while the homogeneous catalyst, Wilkinson's catalyst, was used for the other two (**39b** and **39c**).

Three attempts were required to completely saturate **39a** using the palladium on activated carbon system. The two attempts were carried out in a glass reactor at about 45-50 °C and 85-100 psi hydrogen pressure. These trials reduced the residual alkene content in the polymer to 10 and 3 percent, respectively. The third attempt was carried out in a Parr Instruments stainless steel reactor at 80-90 °C and 200 psi. This trial resulted in quantitative hydrogenation, as evidenced in the ^{1}H and ^{13}C NMR spectra and IR analysis. The NMR spectra (Figure 3.4) show the complete loss of olefinic resonances (compare to Figure 3.3), and confirm the highly regular structure of the EIB model copolymer (**36a**). The IR spectrum of the saturated polymer (**36a**) shows complete loss of the alkene C-H out-of-plane bending peak, which is present at 967 cm^{-1} in the unsaturated polymer (**39a**). Figure 3.5 shows the IR spectra of **36b** and **39b**, which are representative of the series of polymers. The IR spectra of **36a** and **36c** are given in *Appendix B*.

Due to the difficulties encountered in the hydrogenation of **39a** with the heterogeneous catalyst, the remaining two unsaturated polymers in the series (**39b** and **39c**) were hydrogenated using Wilkinson's homogeneous catalyst ($ClRh(PPh_3)_3$). These

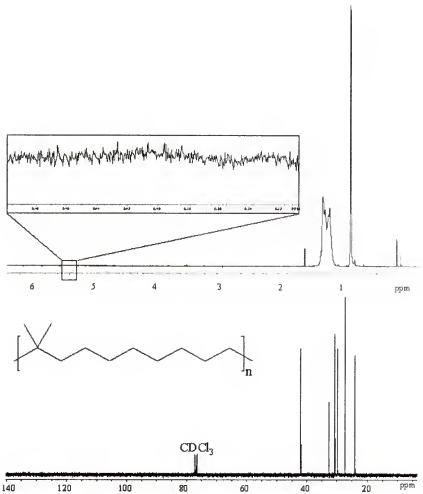

Figure 3.4 ^{1}H (top) and ^{13}C (bottom) NMR spectra for the EIB model copolymer (**36a**).

reactions were carried out in a Parr Instruments stainless steel reactor at 90 °C and 900 psi hydrogen pressure. Reactions in which this catalyst was used resulted in quantitative hydrogenation (by NMR and IR) after the first attempt. However, this homogeneous catalyst was more difficult to remove from the polymer than the heterogeneous catalyst, especially for **36b**. For **36b**, several column chromatography and precipitation cleaning cycles were required, and the polymer was still slightly brownish afterward. Other researchers in our group have found that this catalyst can be effectively removed from more highly crystalline polymers by simple precipitation. This is supported by the more easy removal of the catalyst from **36c**, which is somewhat more crystalline than **36b**.

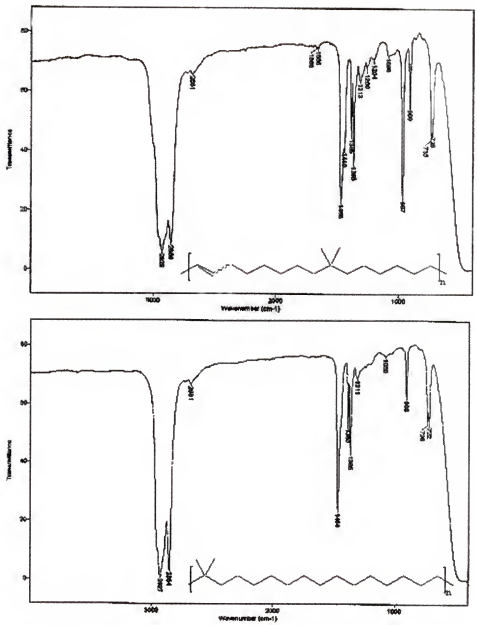

Figure 3.5 IR spectra for the unsaturated polymer (**39a**) (top) and the EIB model copolymer (**36a**) (bottom).

The ^{1}H and ^{13}C NMR spectra and the IR spectra of **36b** and **36c** are provided in *Appendices A and B*, respectively. The GPC analyses of the saturated EIB model copolymers (**36a-c**) indicate number average molecular weights of 56000, 49000, and 76000 grams per mole and PDI's of 2.0, 1.5, and 1.8 for **36a**, **36b**, and **36c**, respectively. These results, together with the NMR and IR data, show that high molecular weight

polymers with precise microstructures have been produced. This series of three polymers represents the first set of highly precise models for EIB copolymers that have controlled 'isobutylene' contents and distributions throughout the polymer chain.

3.2.3 Thermal Behavior of the EIB Model Copolymers

The thermal behavior of the EIB model copolymers (**36a-c**) was examined using Differential Scanning Calorimetry (DSC) at a scanning rate of 10 °C per minute. The first polymer in the series to be studied, **36a**, did not exhibit a melting transition (T_m). This is not very surprising, considering that the methyl branched analogue (**6a**, Figure 1.6) had a very low melting transition (-14 °C), and the dimethyl branch in **36a** is a larger 'defect' in the polyethylene chain. Also, Shaffer's metallocene-made random EIB copolymer (see Section 3.2.1) with about the same isobutylene content (24% *vs.* 22.2% in **36a**) was completely amorphous (no T_m).[116] The glass transition temperature (T_g) of **36a** is -47 °C (see Figure 3.6). This value is 10 °C lower than the T_g of Shaffer's corresponding random EIB copolymer (-37 °C), but is similar to the T_g of the methyl branched ADMET polymer, **6a** (-44 °C). The small peak that appears immediately after the T_g in Figure 3.6 cannot be explained at this time. It was present in each of two heating scans performed on this polymer sample.

The DSC traces of EIB model copolymers **36b** and **36c** (Figures 3.7 and 3.8) show that both of these gem-dimethyl branched polymers are semicrystalline. Polymer **36b**, with dimethyl branches on every 15th carbon atom of the chain, has a sharp melting endotherm with a peak at 32 °C. Polymer **36c**, with dimethyl branches on every 21st carbon atom of the chain, has a relatively broad melting endotherm with a peak at 45 °C and a low temperature shoulder at 37 °C. The breadth of this endotherm and the shoulder

are possibly due to the melting of secondary crystal regions that form over time at room temperature, after the sample has been cooled from the melt. Polymer **36c** also has a broad and somewhat ill-defined glass transition. An attempt was made to clarify this transition by rapidly quenching the sample from 120 °C into liquid nitrogen, and scanning from –100 °C to 80 °C. However, this resulted in a DSC trace that resembled the one shown in Figure 3.9, where the 'cold crystallization' phenomenon obscures the glass transition.

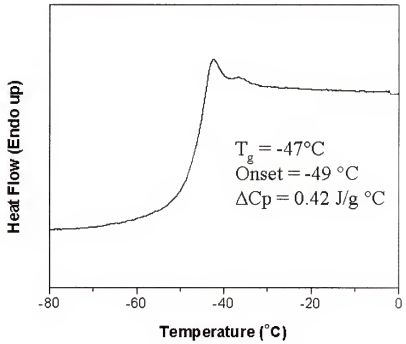

Figure 3.6 DSC trace for the EIB model copolymer (**36a**).

The rather broad hysteresis between the melting and crystallization transitions, and the discrepancies between the enthalpies (ΔH) of melting and crystallization suggest that these polymers crystallize fairly slowly. This is supported by the finding that the samples undergo a 'cold crystallization' during the heating cycles of subsequent scans. This

phenomenon, first theoretically treated by Wunderlich,[119] was also observed in the ADMET model ethylene/vinyl acetate copolymers (**8a-d**) studied previously.[74]

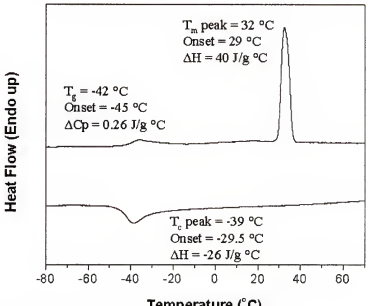

Figure 3.7 DSC trace for the EIB model copolymer (**36b**).

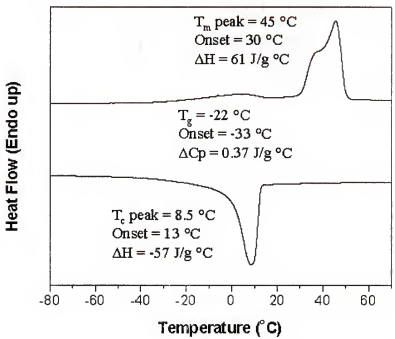

Figure 3.8 DSC Trace for the EIB Model Copolymer (**36c**).

The 'cold crystallization' is seen in the DSC thermogram as a rise and a dip, above and below the baseline, between the glass and melting transitions (see Figure 3.9). This occurs, because the sample cools too rapidly from the melt to fully crystallize during the cooling scan. Then, as the temperature passes through the T_g on the next heating scan, further crystallization ensues before the sample melts. When the samples are annealed at room temperature for a day, the 'cold crystallization' is no longer present and the thermal traces look similar to the first scans shown in Figures 3.7 and 3.8. Cooling the samples at a slower rate should diminish this 'cold crystallization' effect.

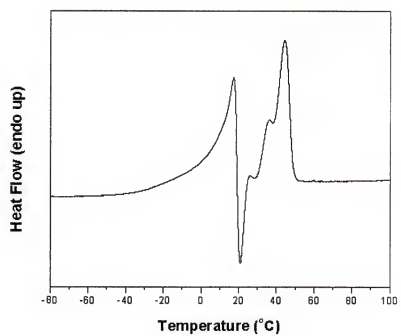

Figure 3.9 DSC trace showing the 'cold crystallization' phenomenon that was observed on the second scan of the EIB model copolymer (**36c**).

Table 3.1 lists the melting and glass transition temperatures of the EIB model copolymer series, along with the analogous methyl branched polyethylene series for comparison. The gem-dimethyl branched polymers, **36b** and **36c**, melt 7 and 17 °C lower than their methyl branched counterparts (**6c** and **6e**), respectively. This is in accord with

the previous finding that the melting points within an analogous series of ADMET functionalized polyethylenes tend to decrease with increasing steric bulk of the pendant groups (see Section 1.6.1). Also, the melting point of **36c** lies between those of the analogous methyl branched (**6e**) and acetate functionalized (35 °C) ADMET polyethylenes. Since the steric requirements of the gem-dimethyl pendant group also lies between those of the methyl and acetate pendant groups, it is reasonable to conclude that this is the major cause of the observed differences in melting points among these three polymers. Due to the symmetry of the gem-dimethyl substituents, these results suggest that the steric bulk, frequency, and distribution of the pendant groups are far more important than the stereoregularity (tacticity) when the pendant groups are spaced nine carbon atoms or more apart, as they are in all of the ADMET model polyethylenes studied to date.

Table 3.1 Thermal transitions of the ADMET gem-dimethyl branched and methyl branched model polyethylenes.

Branches per 1000 carbon atoms	Gem-dimethyl polymer	T_m (°C)	T_g (°C)	Methyl Polymer	T_m (°C)	T_g (°C)
111	36a	none	-47	6a	-14	-44
67	36b	32	-42	6c	39	-
48	36c	45	-22	6e	62	-43

3.3 ADMET Model of Ethylene/Methyl Methacrylate (EMMA) Copolymers

3.3.1 Background for EMMA Copolymers

Ethylene/methyl methacrylate (EMMA) copolymers are produced commercially by Sumitomo Chemical Company, Ltd., under the trade name Acryft. These copolymers are manufactured by a high-pressure radical polymerization process that is similar to that used to produce low-density polyethylene (LDPE).[120] This process results in random

incorporation of the acrylate copolymer, and introduces both short- and long-chain alkyl branches to the copolymer backbone via chain transfer and intramolecular 'backbiting' reactions.

Recently, there has been renewed interest in producing ethylene/polar monomer copolymers using transition metal-based catalysts. This is due to development of the new highly active late transition metal catalysts based on palladium and nickel, which were recently reported by Brookhart and Grubbs.[114,121,122] Brookhart's palladium-based catalysts have been used in the copolymerization of ethylene with acrylates and other polar monomers. While high molecular weights and variable degrees of comonomer incorporation were obtained, these copolymers were amorphous, highly branched materials. Also, most of the ester groups were located at the ends of the branches, rather than directly pendant to the polyethylene backbone.[114,121] The copolymerization of ethylene with acrylates using Grubbs' nickel-based catalysts has yet to be demonstrated, but they have been shown to tolerate the presence of ethyl acetate and other functional additives in ethylene homopolymerizations.[122]

Due to the random distribution of pendant functional groups and variable degrees of alkyl branching present in all of the above copolymers, the true relationship between their comonomer content and thermal behavior cannot be determined. Nevertheless, studies of this nature have been reported, in which both commercially available and specially designed, periodic (regioregular) copolymers were examined. Matsuo and coworkers studied three commercially available random EMMA copolymers with 3, 6.5, and 14.6 mole percent methyl methacrylate (MMA), and found that their melting points decreased with increasing MMA content (T_m = 100, 85, and 64 °C, respectively).[120]

Yokota and coworkers prepared two periodic EMMA copolymers, one alternating copolymer and one ethylene-ethylene-(MMA) copolymer, using unsaturated precursor polymers made from methyl 2-methyl-2,4-pentadienoate and 1,3-butadiene/MMA, respectively.[123] The unsaturated precursor polymers were quantitatively hydrogenated with platinum black, palladium on activated carbon, or *p*-toluenesulfonylhydrazide. The alternating EMMA copolymer was completely amorphous in the absence of annealing, but the ethylene-ethylene-(MMA) copolymer was semicrystalline and had a surprisingly high melting temperature (90 °C). The author indicates that both of these periodic EMMA copolymers were atactic, though evidence for this was not provided for the ethylene-ethylene-(MMA) copolymer.

The following two sections describe the synthesis and characterization, and the thermal behavior of an EMMA model copolymer made via ADMET polymerization. In Section 3.3.3, the thermal behavior of the ADMET-made copolymer is compared to that of the random and periodic EMMA copolymers mentioned above. A comparison of the EMMA model copolymer and all of the other ADMET ethylene-based model copolymers will be made in Section 3.5.

3.3.2 Synthesis and Characterization of the EMMA Model Copolymer

The synthetic scheme for the production of the EMMA model copolymer (**37**) using ADMET polycondensation chemistry is shown in Figure 3.1. The procedure for the ADMET polymerization of the ester functionalized α,ω-diene monomer (**24c**) is similar to the one described for the EIB model copolymer (**36a**) in Section 3.2.2, with a few exceptions. Grubbs' ruthenium benzylidene catalyst (**2**) was used instead of Schrock's catalyst (**1**), due to its superior ability to tolerate polar functional groups. The reaction

was started at about 35 °C, because catalyst **2** is slower than catalyst **1** and the monomer (**24c**) has a sufficiently high boiling point. After an hour of intermittent vacuum, the vacuum valve was left slightly open to allow the slow, continuous removal of ethylene without undue splattering of the reaction components. The temperature was gradually increased to about 60 °C over five days, and the reaction was deemed complete on the sixth day.

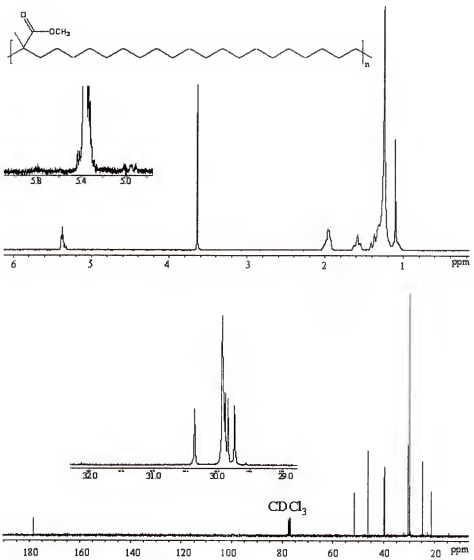

Figure 3.10 ^{1}H (top) and ^{13}C (bottom) NMR spectra for the EMMA model copolymer (**37**).

The ^{1}H and ^{13}C NMR spectra of the unsaturated polymer (**40**) are provided in *Appendix A*. They indicate the highly precise microstructure of this ADMET polymer, and that reasonably high molecular weight has been obtained. Only trace resonances for the terminal olefin end-groups are visible in the ^{1}H NMR spectrum at about 5 and 5.8 ppm. The GPC analysis of this unsaturated polymer indicates a number average molecular weight of 26,000 grams per mole and a PDI of 1.9.

Quantitative hydrogenation of the unsaturated polymer (**40**) to give the EMMA model copolymer (**37**) was accomplished using Wilkinson's catalyst. The conditions of the homogeneous hydrogenation were similar to those used in the production of the EIB model copolymers **39b** and **39c**, except that a mixture of toluene and ethyl acetate was used as the solvent system. A clear, colorless, highly viscous liquid was obtained after a purification sequence consisting of column chromatography, precipitation, column chromatography again, and vacuum drying at 60 °C.

The GPC analysis of the saturated polymer (**37**) indicates a number average molecular weight of 27,000 grams per mole and a PDI of 2.0. The highly precise microstructure of the EMMA model copolymer (**37**) is evident from the ^{1}H and ^{13}C NMR spectra shown in Figure 3.10. The complete disappearance of the olefin resonances in the NMR spectra and the alkene C-H out-of-plane bending peak at 967 cm^{-1} in the IR spectrum (see Figure 3.11) indicate that the hydrogenation was quantitative. However, minor resonances in the methylene region of the ^{13}C NMR spectrum suggest that the repeat units are not completely uniform. This is to be expected, due to the small quantity (< 5%) of internal olefin isomer present in the monomer (**24c**) (see Section 2.3). The result is a few repeat units (< 5%) in the polymer structure that have slightly less than 20

methylene units between the pendant groups. The effect of these very minor imperfections on the thermal behavior of the polymer should be negligible.

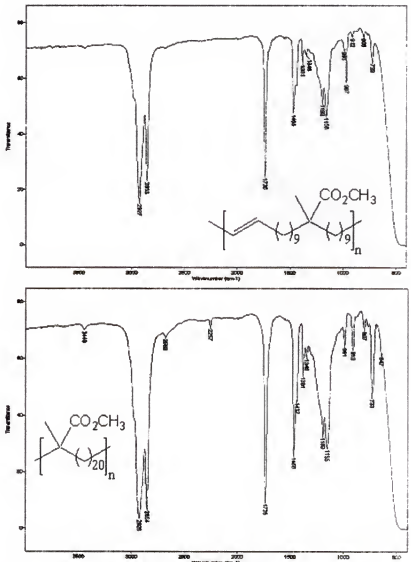

Figure 3.11 IR spectra for the unsaturated polymer (**40**) (top) and the EMMA model copolymer (**37**) (bottom).

3.3.3 Thermal Behavior of the EMMA Model Copolymer

The thermal behavior of the EMMA model copolymer (**37**) was examined using Differential Scanning Calorimetry (DSC) at a scanning rate of 10 °C per minute. The DSC trace is shown in Figure 3.12. The melting transition peak occurs at 7 °C for this

polymer, which has 48 pendant groups per 1000 carbon atoms (equivalent MMA content is 9.5 mole percent). The melting transition endotherm is fairly sharp, but it exhibits a long gradual pre-melting. This is mirrored in the crystallization curve on the cooling scan. It is interesting that this sample lacks the broad hysteresis between the melting and crystallization transitions that was observed for the analogous EIB model copolymer (**36c**). Also, two subsequent DSC scans of the EMMA model copolymer did not show the 'cold crystallization' phenomenon that was observed for the EIB model copolymers. These results suggest that the EMMA model copolymer crystallizes faster than the corresponding EIB model copolymer. This is despite the larger size of the pendant group in **37**, which significantly lowers the melting point relative to the EIB model copolymer, **36c** (by 38 °C).

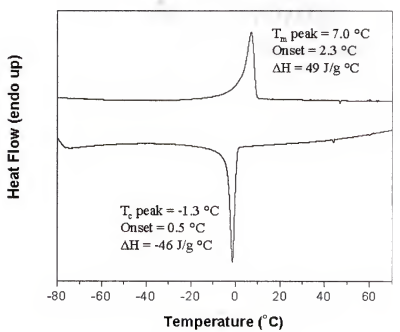

Figure 3.12 DSC trace for the EMMA model copolymer (**37**).

Table 3.2 lists the melting points as a function of MMA content for Yakota's periodic EMMA copolymers, Matsuo's random EMMA copolymers, and the ADMET-

made EMMA model copolymer (**37**). There are two striking observations that can be made from a comparison of these melting point data. First, the ADMET-made polymer melts at a significantly lower temperature than the random EMMA copolymers with similar 'MMA' contents. Such behavior has been observed for all of the ADMET ethylene-based model copolymers studied to date. The ADMET-made copolymers consistently melt at lower temperatures than the corresponding commercially available random copolymers. Second, and perhaps most striking, is the anomalously high melting point of Yakota's ethylene-ethylene-MMA periodic copolymer (90 °C). It is very surprising that this polymer crystallizes at all, and even more so that its melting point is so high, when the alternating MMA and ADMET-made copolymers are amorphous and low temperature melting, respectively. Clearly, there is something special about the ethylene-ethylene-MMA copolymer that makes it melt at such a high temperature, but the cause is unclear.

Table 3.2 Melting transitions of the ADMET EMMA model copolymer (37), Yakota's periodic EMMA copolymers, and Matsuo's and Macknight's random EMMA copolymers.

EMMA Copolymer Type	% MMA	T_m (°C)
Periodic copolymers		
Yakota's	50	none
	33.3	90
ADMET-made (37)	9.5	7
Random copolymers		
Matsuo's	14.6	64
	6.5	85
Macknight's	3.5	94
Matsuo's	3.0	100

Yakota's alternating EMMA and ethylene-ethylene-MMA copolymers exhibit glass transition temperatures at 5 and –6 °C, respectively. However, a glass transition was not

observed for the ADMET-made EMMA model copolymer (**37**) in the temperature range studied (-80 to 100 °C), even when the sample was quenched rapidly from the melt into liquid nitrogen.

The above results further demonstrate the utility of ADMET for the modeling of ethylene-based copolymers. More EMMA model copolymers with different methylene spacer lengths would provide a better understanding of the relationship between the commoner content and the thermal behavior of this commercially relevant copolymer. The melting point of the EMMA model copolymer (**37**) will be compared to those of the other ADMET ethylene-based model copolymers in Section 3.5.

3.4 ADMET Model of Ethylene/Methacrylic Acid (EMAA) Copolymers

3.4.1 Background for EMAA Copolymers

Rees and coworkers first synthesized ethylene/methacrylic acid (EMAA) copolymers in 1964, and thereby introduced the world to ionic polymers (ionomers).[124] Currently, EMAA copolymers a produced commercially by DuPont under the trade-name Surlyn, and they have a variety of uses that range from bowling pins and hockey helmets to food packaging and dog chew toys. Like the EMMA copolymers discussed in Section 3.3, these copolymers are produced by a high-pressure radical polymerization process. Therefore, the comonomer is randomly distributed throughout the polymer backbone, and variable degrees of alkyl branching are present as a result of chain transfer and 'backbiting' reactions. Additionally, a small amount of ester groups are incorporated into commercial EMAA copolymers during their polymerization. These factors make precise structure-property relationship studies difficult, and once again provide an opportunity to

demonstrate the unique utility of ADMET polymers for the precision modeling of commercially relevant ethylene-based copolymers.

Several studies, conducted with both the carboxylic acid and partially neutralized (ionomer) forms of commercial EMAA copolymers, have shown a nearly linear dependence of the percent crystallinity on MAA content, and a decrease in the melting temperature with increasing MAA content.[124-126] Random copolymers having greater than 13.3 mole percent MAA were completely amorphous.[124] Also, Yakota and coworkers have prepared two periodic EMAA copolymers with acid groups on every 4th and 6th carbon atom of the polyethylene backbone, respectively, by hydrolyzing their periodic EMMA copolymers (see Sections 3.3.1 and 3.3.3).[127] Both of these periodic EMAA polymers had high glass transition temperatures (T_g = 132 and 99, respectively) and were completely amorphous (no T_m).[128]

The following two sections describe the synthesis and characterization, and the thermal behavior of an EMAA model copolymer made via ADMET polymerization. In Section 3.4.3, the thermal behavior of the ADMET-made copolymer is compared to that of the random EMAA copolymers mentioned above, and the ADMET-made EMMA copolymer described in Section 3.3. A comparison of the EMAA model copolymer and all of the other ADMET ethylene-based model copolymers will be made in Section 3.5.

3.4.2 Synthesis and Characterization of the EMAA Model Copolymer

The synthetic scheme for the production of the EMAA model copolymer (**38**) using ADMET polycondensation chemistry is shown in Figure 3.1. Two attempts were required to make the unsaturated polymer (**41**), both using Grubbs' ruthenium benzylidene catalyst (**2**). The procedure for the first ADMET polymerization of the carboxylic acid

functionalized α,ω-diene monomer (**23c**) is similar to the one described for the EMMA model copolymer (**37**) in Section 3.3.2, with a few exceptions. The reaction was started at about 45 °C, because the monomer (**23c**) is solid below 43 °C. A monomer to catalyst ratio of 250:1 was used. The catalyst was slow to dissolve in this monomer, so only mild bubbling was observed as intermittent vacuum was applied. After thirty minutes of intermittent vacuum, the vacuum valve was left slightly open to allow the slow, continuous removal of ethylene without undue splattering of the reaction components. Within an hour after initiating the reaction, most of the catalyst had dissolved and the mixture was bubbling vigorously. The temperature was gradually increased to about 55 °C over five days, but the mixture had ceased to bubble after the third day. The ^{1}H NMR spectrum of the unsaturated polymer (**41**) made in this first attempt is shown in Figure 3.13. It is readily apparent that the polymerization did not proceed to high molecular weight, due to the presence of residual terminal olefin resonances at about 5 and 5.8 ppm in the spectrum. An integration of the olefin peaks indicates an average of only six repeat units in the polymer chains.

A second attempt to produce the unsaturated polymer (**41**) was made, with the goal of increasing its molecular weight. This time an initial monomer to catalyst ratio of only 440:1 was used, but more catalyst was added periodically during the reaction. More catalyst (**2**) was added on the second, fourth, and sixth days, bringing the total monomer to catalyst ratio to about 150:1. The temperature was increased from 50 to 65 °C over the first three days, and the reaction flask was removed from the vacuum line on the seventh day.

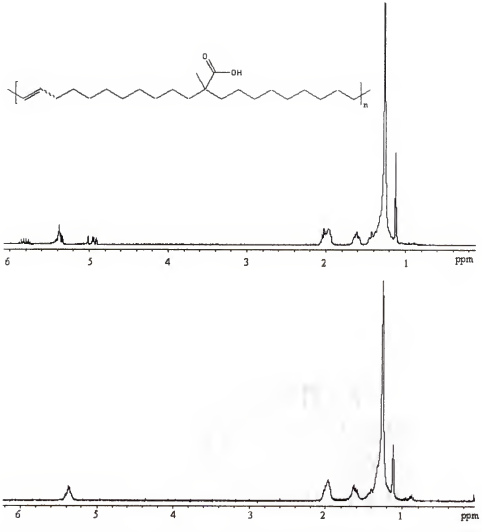

Figure 3.13 ^{1}H NMR spectra for the first (top) and second (bottom) attempts to make the unsaturated polymer (**41**).

The ^{1}H NMR spectrum of the unsaturated polymer (**41**) made in the second attempt is shown in Figure 3.13. This time there are no resonances due to the terminal olefin end-groups visible in the spectrum, which indicates that a high molecular weight polymer has likely been obtained. Attempts to obtain a ^{13}C NMR spectrum, in both deuterated chloroform and DMSO, were unsuccessful due to the low solubility of the polymer in these solutions. A GPC analysis of this polymer indicated a number average weight of only about 4000 grams per mole, but this number is unlikely to be reliable due to the

polymer's low solubility in the solvent (THF). Apparently, only the soluble, low molecular weight fractions were present in the GPC sample.

An analysis of the IR spectra of the unsaturated polymers (**41**) made in each of the two attempts provides additional evidence for the high molecular weight of the polymer made in the second attempt. The IR spectra are shown together in Figure 3.14, along with the spectrum of the monomer (**23c**) for comparison. The monomer exhibits two peaks, one at 1822 cm^{-1} and one at 3078 cm^{-1}, that are due to its terminal olefins. The polymer made in the first attempt also has two peaks at these positions, due to its high concentration of end-groups. However, these peaks are not visible in the IR spectrum of the polymer made in the second attempt, which further suggests that the molecular weight of this polymer is reasonably high.

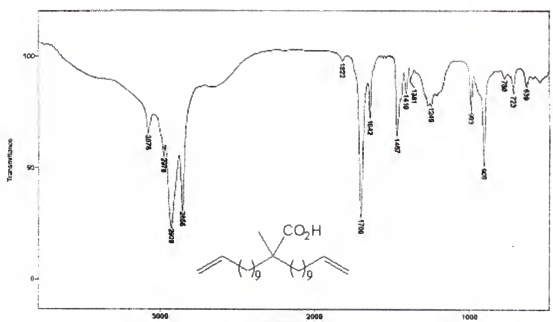

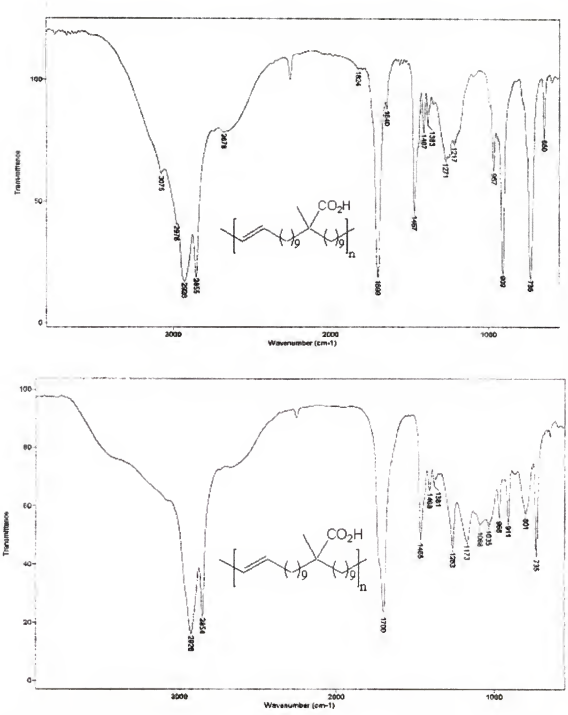

Figure 3.14 IR spectra for the monomer (**23c**) (previous page), and the first (top) and second (bottom) attempts to make the unsaturated polymer (**41**).

Quantitative hydrogenation of the unsaturated polymer (**41**) to give the EMAA model copolymer (**38**) was accomplished using Wilkinson's catalyst. The conditions of the homogeneous hydrogenation were similar to those used in the production of the

EMMA model copolymer (**37**), where toluene and ethyl acetate was used as the solvent system. However, this polymer (**38**) precipitated during the course of the hydrogenation. A black, very tacky material was obtained that was insoluble in common organic solvents, including chloroform, toluene, ethyl acetate, methanol, ethanol, THF, and DMSO. Mixtures of *p*-xylene and 1-butanol successfully dissolved most of the material at reflux, but some black particles remained insoluble. The remaining material eventually dissolved when a small amount of sodium hydroxide was added to the mixture. A grayish precipitate formed after the solution was slowly added to acidic methanol (1 M HCl) and stirred for about an hour. The precipitate became a translucent, slightly black, tacky, viscous material after drying at 70 °C under vacuum.

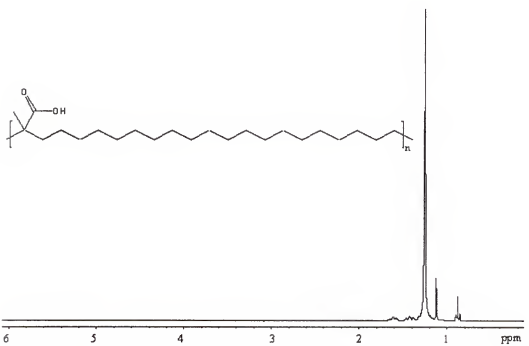

Figure 3.15 ^{1}H NMR spectrum for the EMAA model copolymer (**38**).

The ^{1}H NMR spectrum of the saturated EMAA model copolymer (**38**) is shown in Figure 3.15. No olefinic resonances are observed, indicating that the hydrogenation was a

success. However, there is a triplet at 0.88 ppm that is likely due to the methyl end-groups of low molecular weight oligomers. These are present, due to the extremely low solubility of the polymer in deuterated chloroform, which prevents the observation of the higher molecular weight fraction of the sample. In fact, the polymer phase separates and is seen as a top layer in the NMR tube. For the same reason, a GPC analysis of the polymer in THF also indicates an erroneously low number average molecular weight of about 4100 grams per mole. However, due to the lack of observable end-groups in the ^{1}H and IR spectra of the unsaturated polymer (**41**), the molecular weight of the EMAA model copolymer (**38**) should be sufficiently high (M_n > 15,000 grams per mole) to allow a meaningful comparison of its thermal behavior with that of commercial EMAA copolymers.

The IR spectrum of the EMAA model copolymer (**38**) is provided in *Appendix B*. This spectrum closely resembles that of a commercial EMAA copolymer with 6.5 mole percent MAA content, which was reported by Coleman and coworkers.[126] The only significant difference is that their IR spectrum contains a peak at 1735 cm^{-1}, due to a small quantity of ester groups that are typically incorporated during polymerization. Additionally, the disappearance of the alkene C-H out-of-plane bending peak at 968 cm^{-1} in the IR spectrum of **38** indicates that the hydrogenation of the unsaturated polymer (**41**) was quantitative.

3.4.3 Thermal Behavior of the EMAA Model Copolymer

The thermal behavior of the EMAA model copolymer (**38**) was examined using Differential Scanning Calorimetry (DSC) at a scanning rate of 10 °C per minute. The DSC trace is shown in Figure 3.16. The peak of the melting transition is at 13 °C for this

polymer, which has 48 pendant groups per 1000 carbon atoms (equivalent MAA content is 9.5 mole percent). Like the EMMA model copolymer (**37**) discussed in Section 3.3.3, the EMAA model copolymer (**38**) has a fairly sharp melting transition endotherm, but it exhibits slightly less pre-melting before the peak. The crystallization peak occurs at 4.5 °C in the cooling scan, and the enthalpy associated with this transition closely matches that of the enthalpy of melting (20.7 and 21.6 J/g, respectively). Like its ester analogue (**37**), the DSC trace of this carboxylic acid-functionalized polyethylene (**38**) lacks the broad hysteresis between the melting and crystallization transitions that was observed for the analogous gem-dimethyl substituted polyethylene (**36c**). Also, consecutive DSC scans of the EMAA model copolymer did not show the 'cold crystallization' phenomenon that was observed for the EIB model copolymers. These results suggest that, like the EMMA model copolymer, the EMAA model copolymer crystallizes faster than the corresponding EIB model copolymer. This is despite the larger size of the pendant groups in **37** and **38**, which significantly lowers their melting points relative to the EIB model copolymer (**36c**) (by 38 and 32 °C, respectively).

Table 3.3 lists the thermal transitions as a function of MAA content for Yakota's periodic EMAA copolymers, McKnight's and Coleman's random EMAA copolymers, and the ADMET-made EMAA model copolymer (**38**). Once again, it is immediately apparent that the ADMET-made polymer has a much lower melting point (> 40 °C) than the random EMAA copolymers with similar 'MAA' content. A possible explanation for this phenomenon is that the pendant groups in ADMET-made model ethylene-based copolymers are included in the polyethylene crystal phase, while the pendant groups are largely excluded in many random copolymers. X-ray scattering studies conducted on

methyl branched ADMET polyethylenes have revealed that the methyl groups are included in the crystal phase,[129] while DSC and X-ray studies conducted on random EMAA copolymers by MacKnight support the view that the methacrylic acid side groups are largely excluded.[125] The inclusion of more 'defects' in the crystal phase can be expected to lower the melting point significantly, whereas the exclusion of many of the 'defects' in random copolymers should bring the melting point closer to that of the parent polyethylene homopolymer.

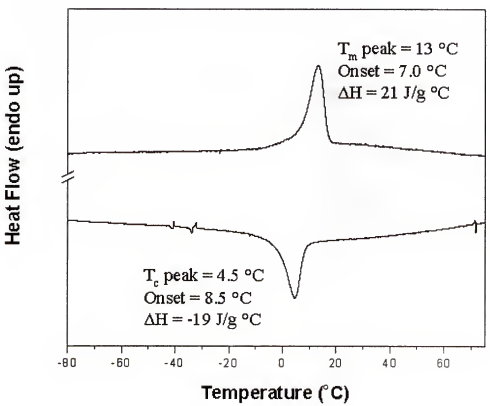

Figure 3.16 DSC trace for the EMAA model copolymer (**38**).

A comparison of the melting points between a random EMMA copolymer and an analogous random EMAA copolymer with those of the ADMET-made versions further illustrates this point. MacKnight found that the random copolymers (each with 3.5 mole

percent comonomer) melted at the same temperature,[130] despite the difference in the relative size of the ester and carboxylic acid pendant groups. The fact that the difference in size of these pendant groups has no effect on the melting temperature supports the exclusion model for these two random copolymers. The ADMET-made model EMMA and EMAA copolymers (each with 9.5 mole percent 'comonomer') have melting points that differ slightly (by 6 °C), which supports the inclusion model for these periodic copolymers. However, these models are not mutually exclusive, since other random copolymers with similar comonomer contents have somewhat different melting temperatures. It is likely that, in random copolymers, some of the pendant groups are included in the crystal phase, while the majority are excluded. Also, hydrogen bonding and other interactions among polar pendant groups can influence the crystallinity and melting point of a polymer, making the strict comparison of copolymers with diverse functional groups more complicated.

Table 3.3 Thermal transitions of the ADMET EMAA model copolymer (38), Yakota's periodic EMAA copolymers, and Coleman's and Macknight's random EMAA copolymers.

EMAA Copolymer Type	% MAA	T_m (°C)	T_g (°C)
Periodic copolymers			
Yakota's	50	none	132
	33.3	none	99
ADMET-made (37)	9.5	13	-
Random copolymers			
Coleman's	28.5	none	25-32
	20.4	none	25-32
	13.3	53	-
	6.5	87	-
Macknight's	3.5	95	25

Table 3.3 also lists the glass transition temperatures for some of the EMAA copolymers. While the random copolymers all exhibit glass transitions between 25 and 32 °C, those of Yokota's periodic EMAA copolymers are much higher (99 and 132 °C for 33.3 and 50 mole percent MAA, respectively). The periodic copolymers both have a relatively high MAA content, so their glass transition temperatures more closely resembles that of poly(methacrylic acid) (T_g = 228 °C).[128] However, like the EMMA model copolymer (**37**), the EMAA model copolymer (**38**) did not exhibit a glass transition temperature in the DSC trace in the temperature range studied (-80 to 100 °C).

This ADMET-made EMAA model copolymer (**38**) is yet another example of the utility of the ADMET reaction for the modeling of commercially relevant polymers. More EMAA model copolymers with different methylene spacer lengths would provide a better understanding of the relationship between the commoner content and the thermal behavior of the copolymer. Such polymers are also ideally suited for the modeling of EMAA ionomers and studying the effect of ionic group content on various physical properties, such as thermal transitions, crystallinity, ionic aggregation, melt rheology, and interpolymer complexation in polymer blends. In the next section, the melting point of the EMAA model copolymer (**38**) will be compared to those of the other ADMET ethylene-based model copolymers that have been studied thus far.

3.5 Melting Point Comparisons for ADMET Ethylene-Based Model Copolymers

The peak melting temperatures of an analogous series of ADMET ethylene-based model copolymers are listed in Table 3.4. The polymers are listed in order of increasing steric bulk of their pendant groups. The significant effect of varying the identity of the pendant group can immediately be seen from the width of the range of melting points,

which spans nearly 130 °C from ADMET linear polyethylene to the ADMET EMMA model copolymer. In accord with previous findings discussed in Section 1.6.1, the melting points of these polymers decrease with increasing steric bulk of their pendant groups.

Table 3.4 Peak melting temperatures for an analogous series of ADMET ethylene-based model copolymers.

ADMET Polymer	R	R'	T_m (°C)
5	H	H	134
6d	CH_3	H	62
36c	CH_3	CH_3	45
8b	$OC(O)CH_3$	H	35
38	CO_2H	CH_3	13
37	CO_2CH_3	CH_3	7

With a few logical assumptions, a comparison of the entire series of ADMET ethylene-based model copolymers produced to date can be made. By assuming that the melting point of an ADMET ethylene/methyl acrylate (EMA) model copolymer (**9**) with 20 methylene 'spacers' between pendant groups lies between the melting points of the analogous model copolymers with 18 and 22 methylene 'spacers' (**9a** and **9b** with T_m = 14 and 37 °C, respectively), it is apparent that the EMAA (**38**) and EMMA (**37**) model copolymers melt a lower temperatures than the EMA analogue. Since the ADMET ethylene/ethyl acrylate (EEA) model copolymer (**10**) melts only 1 °C lower than the analogous EMA model copolymer (**9a**), the EMAA (**38**) and EMMA (**37**) model copolymers should melt at lower temperatures than the EEA analogue as well. Lastly, by assuming that the melting point of an ADMET ethylene/styrene model copolymer with

20 methylene 'spacers' is not more than 19 °C higher than its analogue (**11**) with 18 methylene 'spacers' (T_m = -12 °C), we can conclude that the EMAA (**38**) and EMMA (**37**) model copolymers melt at higher temperatures than the ethylene/styrene analogue. This seems reasonable because none of the other model copolymers with 20 'spacers' melt more than 12 °C higher than their 18 'spacer' analogues. Using these arguments, the following list of comonomers can be made, for all of the ADMET ethylene-based model copolymers produced to date, in order of increasing steric bulk and decreasing melting point of the corresponding model copolymer: carbon monoxide, vinyl chloride, propylene, isobutylene, vinyl acetate, methyl acrylate, ethyl acrylate, methacrylic acid, methyl methacrylate, and styrene.

3.6 Conclusion

The synthesis, characterization, and thermal behavior of ADMET-made models of ethylene/isobutylene (EIB) (**36a-c**), ethylene/methyl methacrylate (EMMA) (**37**) and ethylene/methacrylic acid (EMAA) (**38**) copolymers have been described. These ethylene-based model copolymers, with sequence ordered pendant groups, were compared to their random copolymer counterparts made using chain-growth polymerization methods. The ADMET model copolymers exhibited sharper melting transitions relative to their random copolymer counterparts, but their melting points occurred at lower temperatures. Also, these new model copolymers were compared with the previously studied series of ADMET ethylene-based model copolymers, which were discussed in Section 1.6.1. In accord with the findings of the previous study, the melting points of these polymers decreased with increasing steric bulk of their pendant groups. Only one of these ADMET ethylene-based model copolymers failed to crystallize (**36a**),

and this property was used advantageously to produce the amorphous telechelic hydrocarbon diols that will be described in Chapter 4.

CHAPTER 4
COMPLETELY AMORPHOUS TELECHELIC HYDROCARBON DIOLS

4.1 Introduction

Telechelic polymers are macromolecules with one or more functional handles at their chain ends that can be used for further reaction. For many applications, such as block copolymer synthesis, it is crucial that the functionality (number of functional end groups per chain) be as close as possible to 2 in order to obtain high conversion. Many of the methods used to make telechelics are complicated by side reactions that lead to polymers with a functionality other than 2.[78,131]

Telechelic hydrocarbons bearing two terminal primary hydroxyl groups are highly desirable materials due to their potential for derivatization.[132] Such materials are most often used for the production of special types of elastomeric polyurethanes.[133,134] The unique properties of these polyurethane block copolymers stem from the microphase separation between their hard segment domains and soft segment domains. Through physical or chemical crosslinks, the hard segments impart strength and cohesion, while the soft segments impart flexibility, solubility, and processability to the material. The soft segments of many commercial polyurethanes are composed of hydroxyl telechelic polyethers, such as hydroxyl terminated polytetrahydrofuran. One such polyurethane, Biomer, is one of the materials used to make artificial hearts.[135] There has been considerable interest in extending the lifetime of these implantable devices for obvious reasons. A possible solution is to replace the polyether soft segments with purely

hydrocarbon "liquid rubber" soft segments, which lack the vulnerable carbon-oxygen ether linkages.

Hydroxyl telechelic polybutadiene and polyisoprene "liquid rubbers" have been prepared by living anionic techniques, but they lack the desired 2.0 functionality due to spontaneous, undesirable termination during their synthesis.[133,134] [132] However, perfectly bifunctional telechelic polybutadienes with various end-groups have been prepared using both ADMET[77,78] and ROMP[131,136-140] techniques. The hydroxyl telechelic polybutadienes were typically prepared using protecting group strategies, although a recent article by Grubbs and coworkers reported that a hydroxyl functional chain transfer agent (CTA) could be used directly in ROMP reactions with a ruthenium catalyst containing an N-heterocyclic ligand (similar to **3**).[140] While these telechelic "liquid rubbers" based on polybutadiene promise to be useful materials, their olefinic double bonds make them vulnerable to oxidation and limit their utility for biological applications.

Fully saturated "liquid rubbers", such as telechelic polyisobutylenes (PIBs), represent a viable solution to the problem of degradation. PIB is chemically and oxidatively inert, because it has no olefinic double bonds and contains only primary and secondary hydrogens.[141] It is a rubbery, highly hydrophobic material with a T_g at about –70 °C, which makes it ideally suited for use in polyurethane soft segments. Also, it is inert to enzymes due to its insolubility in aqueous media. Many attempts to make PIB-based bifunctional telechelics have met with limited success, since functionalities other than 2 are obtained as a result of chain transfer events during their radical or cationic methods of preparation.[132] However, the discovery of living cationic olefin

polymerization in the mid-1980s led to the development of a variety of telechelic PIBs with functionality at, or very near to, 2.[142] The hydroxyl telechelic PIBs were used for the preparation of unique hydrophobic polyurethanes, which are interesting for biomaterial applications.[132]

In this chapter, the synthesis and characterization of several perfectly difunctional, completely amorphous telechelic hydrocarbon diols, made using ADMET chemistry, will be described. These hydroxyl telechelics, shown in Figure 4.1, are based on the ADMET ethylene/isobutylene (EIB) model copolymer (**36a**) that was described in Chapter 3. The molecular structures of the three telechelic diols (**42a-c**) differ by the number of methylene 'spacers' at their chain ends, which is a direct result of the identity of the monofunctional reactant (MR) used to end-cap the polymer chains during the ADMET reaction. The term 'monofunctional reactant' refers to the number of metathesis active olefin groups, namely one, in the reagent used to cap the chain-ends. The MR's function in step-growth polycondensation reactions is similar to that of a chain transfer agent (CTA) in chain-growth polymerizations, such as ROMP. Essentially, it serves to limit the molecular weight of the polymer and cap the chain-ends with a desired functional group.

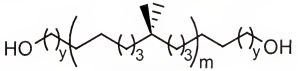

42a-c

where y = 1, 3, and 9, respectively

Figure 4.1 ADMET-made telechelic hydrocarbon diols (**42a-c**).

Due to structural similarities, the telechelic diols (**42a-c**) have all of the advantages of the PIB-based materials mentioned above. Although the current high cost of producing

the monomer (**22a**) renders this method too expensive for many high-volume commercial uses, these telechelic diols (**42a-c**) may find application in biomedical devices, for which long-life outweighs cost. This work was part of a collaborative research effort with Medtronic, Inc., and has resulted in a US patent application.

4.2 Synthesis of the Telechelic Diol with Short Chain-Ends (42a)

Our collaborators at Medtronic, Inc. challenged us to make a perfectly difunctional, completely amorphous telechelic hydrocarbon diol with a number average molecular weight between 1000 and 2000 grams per mole. The synthetic scheme shown in Figure 4.2 was developed to accomplish this task. It involves the ADMET polymerization of monomer (**22a**) in the presence of a diacetate MR (either **43a** or **43b**, where y = 1 and 3, respectively) to make the unsaturated diacetate telechelic polymer (**44a** or **44b**, respectively). This polymer is then quantitatively hydrogenated to give the saturated diacetate telechelic polymer (**45a** or **45b**, respectively). Finally, the acetate end-groups are hydrolyzed to give the desired telechelic diol (**42a** or **42b**, respectively).

Initially, the diacetate MR with only one methylene 'spacer' (y = 1) between its olefin and acetate groups (**43a**) was used, due to its commercial availability and its successful implementation as a CTA in ROMP reactions.[136] The telechelic diol made using this MR is termed "the telechelic diol with a short chain-end". Several attempts to make the unsaturated diacetate polymer (**44a**) are described below, culminating in the successful synthesis of the first perfectly bifunctional telechelic hydrocarbon diol (**42a**) in the fifth attempt.

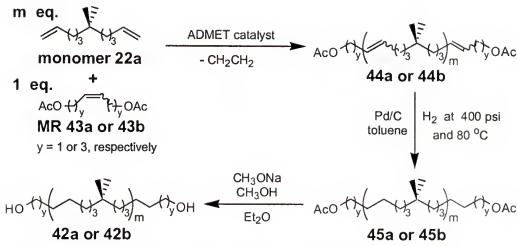

Figure 4.2 Synthetic scheme for the telechelic diols **42a** and **42b**.

4.2.1 The First and Second Attempts

For the first attempt, a polymerization method was used that is very similar to the one that produced polymer **39a** (see Section 3.2.2), with only a few exceptions. This method uses typical ADMET conditions with a simple apparatus that includes a Schlenk flask, equipped with a magnetic stir bar, that is connected to a high vacuum line. The vacuum line facilitates the removal of the ethylene byproduct of the ADMET reaction and drives the reaction equilibrium forward. One difference from the procedure used to make **39a** is that a monomer (**22a**) to MR (**43a**) to catalyst (**3**) ratio of 7:1:0.05 was used to limit the molecular weight to about 1100 to 1200 grams per mole, and to end-cap the oligomer with acetate functionality at both ends. Another difference was that the ruthenium catalyst with an N-heterocyclic ligand (catalyst **3**) was employed, instead of Schrock's catalyst (**1**), to ensure the longevity of the catalyst in the presence of the diacetate MR (**43a**).

The reaction was carried out at 40-45 °C over a 24 hour period, at which time no bubbling was observed. A ^{1}H NMR analysis (Figure 4.3) showed a large amount of unreacted monomer (**22a**) or chains with terminal olefin end-groups; note the olefinic

proton resonances at about 5.0 and 5.8 ppm. It was also noticed that some of the MR was removed from the reaction by the applied vacuum, since it had condensed in the valve adapter above the reaction flask. This would increase the monomer to MR ratio during the reaction and consequently increase the molecular weight of the polymer.

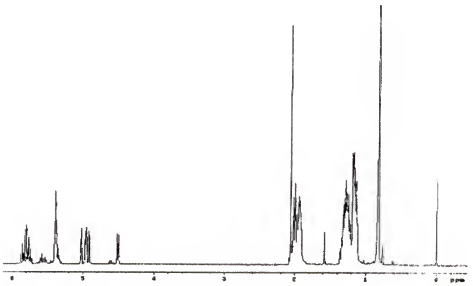

Figure 4.3 ^{1}H NMR spectrum for the first attempt to make the unsaturated telechelic diacetate (**44a**).

For the above reasons, the second attempt was begun at room temperature and was allowed to run for 55 hours with gradual increases in temperature up to 45 °C. While this attempt proved much better, the ^{1}H NMR spectrum still showed some terminal olefins present, indicating that the polymer was not perfectly end-capped with acetate groups. Also, integration of the end-group vs. repeat unit olefin peaks indicated a molecular weight that was larger than the target molecular weight (3400 g/mol instead of 1200 g/mol). Again, this can be attributed to the removal of the MR from the reaction mixture by vacuum.

Three solutions to this problem were envisioned: 1) a larger, less volatile MR could be used with the existing polymerization method; 2) the reaction could be carried out in refluxing solvent under constant argon flow to drive off the ethylene byproduct without removing the smaller MR (**43a**); and 3) the monomer could be polymerized to high molecular weight under vacuum and then depolymerized with the MR under argon. Option 2 was chosen for the next two attempts for several reasons. The Wagener group has had previous success at producing oligomers in refluxing solvent under constant argon flow. Also, the shorter MR (**43a**) was already in hand, and option 2 seemed simpler and more direct than the polymerization-depolymerization method in option 3.

4.2.2 The Third and Fourth Attempts

The third and fourth attempts utilized the same apparatus and the argon flow method (option 2 above) of removing the ethylene by product. The apparatus is shown in Figure 4.4, and is designed to ensure the thorough mixing of reactants and to keep the reactants in the flask through the use of a condenser and refluxing solvent. In the third attempt, methylene chloride was used as the solvent, limiting the reaction temperature to its boiling point (about 40 °C). After three days, the reaction mixture had turned dark brown, indicating that the catalyst had likely decomposed. However, it was allowed to run for two more days, after which the ^{1}H NMR spectrum shown in Figure 4.5 was taken. It can be readily seen, from the terminal olefin resonances at about 5.0 and 5.8 ppm, that the reaction was not nearly complete.

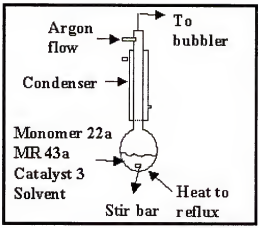

Figure 4.4 Reaction apparatus used in the third and forth attempts to make the unsaturated telechelic diacetate (**44a**).

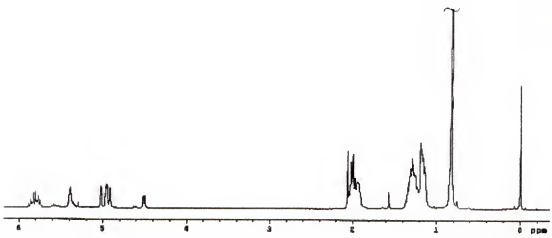

Figure 4.5 ^{1}H NMR spectrum for the third attempt to make the unsaturated telechelic diacetate (**44a**).

At about the same time that this attempt was made, kinetic experiments designed to evaluate catalyst **3** in ADMET reactions had revealed that the catalyst was somewhat sluggish at lower temperatures (see Section 1.5.1). However, it became very highly active at about 60 °C. In light of this, a fourth attempt was made using conditions that were similar to the third attempt, except that deuterated chloroform was used as the solvent. This solvent was chosen for two reasons: 1) it boils at 61 °C, so it keeps the reaction temperature at a good temperature for the catalyst (**3**); and 2) aliquots of the reaction

mixture can be conveniently taken and analyzed by NMR spectroscopy to determine the extent of reaction.

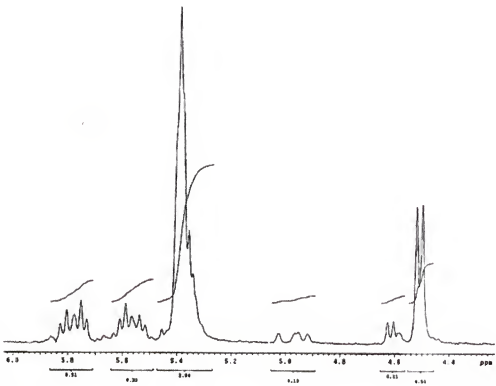

Figure 4.6 Olefin region of the ^{1}H NMR spectrum for the fourth attempt to make the unsaturated telechelic diacetate (**44a**).

After thirteen days, eight aliquots, and three added portions of catalyst **3** during the course of the reaction, terminal olefins were still present in the ^{1}H NMR spectrum and it became obvious that this method was not a viable route. At the time that this attempt was made, it was believed that the most likely causes for the failure of this method were the inability of the argon flow to efficiently remove the ethylene byproduct and the dilution of the reactants in solvent. It was reasoned that these factors might decrease the rate of productive metathesis, and contribute to the premature decomposition of the catalyst. While this method may be useful for producing oligomers, it is not useful for making perfectly difunctional telechelics. The olefin region of the ^{1}H NMR spectrum of the last

aliquot (aliquot 8) is shown in Figure 4.6. While integration of the acetate end-group vs. repeat unit olefin peaks indicated a molecular weight that was right on the target molecular weight, about 5% terminal olefin still remained after thirteen days and three additional infusions of catalyst **3**.

4.2.3 The Fifth Attempt: Success!

For the fifth attempt to make the unsaturated telechelic diacetate polymer (**44a**), the polymerization-depolymerization method was chosen (option 3 in Section 4.2.1). The synthetic method and the apparatus that was used are shown schematically in Figure 4.7. It was anticipated that the polymerization to high molecular weight under vacuum would ensure the removal of the ethylene byproduct and greatly reduce the number of terminal olefins present. Then, the unsaturated polymer (**39a**) could be depolymerized and end-capped with the MR (**43a**) under argon atmosphere, with the amount of MR added controlling the molecular weight of the telechelic product.

The polymerization step was carried out in the same way that was used to make polymer **39a** (see Section 3.2.2), except that catalyst (**3**) was used instead of Schrock's molybdenum catalyst (**1**). The temperature was gradually brought to 60 °C and the reaction was run for about 46 hours, at which time no more bubbling was observed and the mixture was highly viscous. A solution of the MR (**43a**) in about 4-5 mL of toluene was then added to the polymer and catalyst in an argon atmosphere drybox, and the mixture was stirred at 60 °C for three days. The toluene was added to decrease the viscosity of the mixture so that it could be stirred. Also, since only a few drops of **43a** were used, it would have been difficult to ensure that all of it ended up evenly dispersed

in the reaction mixture, and not on the side of the flask, had the added solvent not been used.

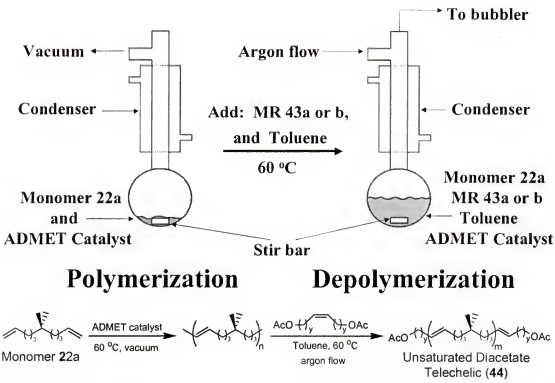

Figure 4.7 The polymerization-depolymerization method and apparatus.

Unfortunately, the added solvent may have contributed to the premature decomposition of the catalyst during the depolymerization reaction. Also, it was realized at this time that the MR (**43a**) can form a six-membered ring chelate with the ruthenium catalyst (**3**) in one of the reaction intermediates (see Figure 4.8), which may impede the progress of the reaction. This chelation effect has also been observed in ROMP reactions.[136,138] As a result, not all of the MR was consumed in the reaction and the molecular weight exceeded the target slightly (about 1600 grams per mole by ^{1}H NMR vs. the target of about 1200). The ^{1}H NMR spectrum of the unsaturated telechelic diacetate polymer (**44a**) is shown in Figure 4.9. A small amount of residual MR can be seen at 4.68 ppm, as well as three resonances (2.07, 4.58, and 5.86 ppm) that correspond

to half of the MR ($H_2C=CCH_2OAc$), which indicates that the reaction had not gone to completion. However, the absence of terminal olefin resonances at about 5.0 and 5.8 ppm in the ^1H NMR spectrum indicates that the polymer is 'perfectly' bifunctional within detection limits.

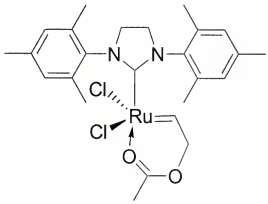

Figure 4.8 Chelation of catalyst **3** when MR **43a** is used.

While this represented a significant accomplishment, by producing the first 'perfectly' bifunctional unsaturated telechelic diacetate polymer (**44a**), it was believed that the molecular weight control of this method could be further improved by running the depolymerization reaction with less added solvent and with a longer MR (**43b** with y = 3). It will be demonstrated in Section 4.3 that these modifications prolong the active life of the catalyst and increase the rate of reaction, since the longer MR is less likely to form an *eight* membered cyclic ring with the ruthenium catalyst.

The hydrogenation of the unsaturated telechelic diacetate (**44a**) to the fully saturated telechelic diacetate (**45a**) was accomplished using a Parr high-pressure reactor and palladium on activated carbon as the heterogeneous catalyst. After the unsaturated material (**44a**) was dissolved in toluene, the catalyst was added and the mixture was stirred at 100 rpm. The reactor was charged to 400 psi with hydrogen, and heated to 80

°C. After five days, the reaction was complete. The catalyst was removed by filtration and the solvent was removed by heating the sample under vacuum. Figure 4.10 shows the ^{1}H NMR spectrum of the saturated telechelic diacetate (**45a**), in which no olefinic resonances can be observed. The ^{1}H NMR spectrum also indicates a number average molecular weight of 2100 grams per mole. A possible reason for the success of this heterogeneous hydrogenation procedure for the telechelic polymers, while it was not successful for the ADMET EIB model copolymers discussed in Section 3.2.2, is the higher solubility of the low molecular weight telechelic polymers.

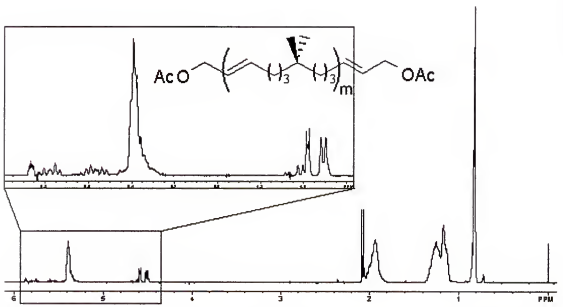

Figure 4.9 ^{1}H NMR spectrum for the fifth attempt to make the unsaturated telechelic diacetate (**44a**).

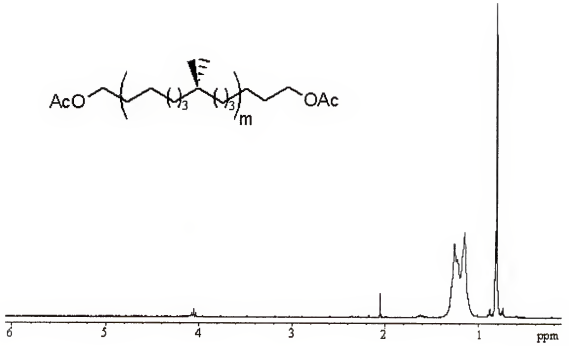

Figure 4.10 ^{1}H NMR spectrum for the saturated telechelic diacetate (**45**a).

The final step to prove the synthetic scheme in Figure 4.2 was the hydrolysis of the acetoxy end-groups to hydroxyl end-groups. This was accomplished by dissolving the saturated telechelic diacetate (**45**a) in diethyl ether, chilling the solution in an ice bath, then adding 0.7 M sodium methoxide in methanol and stirring for 24 hours. After simple extraction steps, the ^{1}H NMR and ^{13}C NMR spectra of the telechelic diol (**42**a), shown in Figure 4.11, were obtained. The complete disappearance of the acetoxy end-group resonances at 2.05 ppm and 4.05 ppm, and the appearance of a new hydroxyl end group resonance at 3.64 ppm in the ^{1}H NMR spectrum indicate that the reaction was quantitative. Analysis of the integrals in the ^{1}H NMR spectrum indicated that the telechelic diol (**42a**) had a number average molecular weight of about 2400 grams per mole. The progressive increase in molecular weight from compounds **44a** through **42a** is most likely the result of fractionation during the product isolation steps.

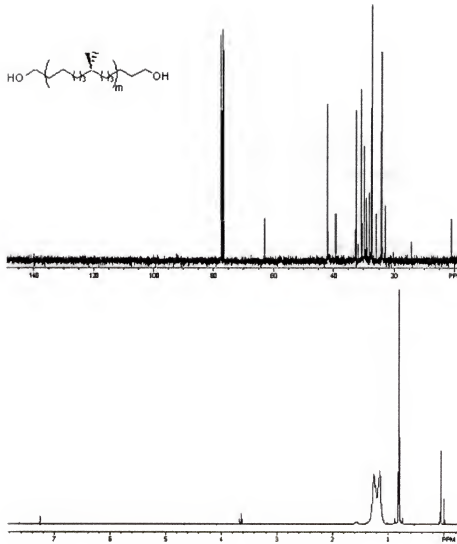

Figure 4.11 ^{13}C (top) and ^{1}H (bottom) NMR spectra for the telechelic diol (**42a**).

4.3 Synthesis of Telechelic Diols with Medium Length Chain-Ends (42b)

In the hope of achieving better molecular weight control, a MR with three methylene 'spacers' between its olefin and acetate groups (**43b**) was made by the dimerization of acetic acid 4-pentenyl ester using the Grubbs benzylidene metathesis catalyst (**2**). The telechelic polymers made from this MR are termed "telechelics with medium length chain-ends". It is important to note that the ruthenium catalyst with an N-heterocyclic ligand (**3**) did not work in this reaction, as a number of isomers were

observed due to migration of the olefinic double bond (see Section 1.5.1). This was the first time that this isomerization side-reaction was observed in the Wagener group. The cause of this isomerization when catalyst **3** is used is still unknown. However, the reaction is fairly well-controlled when catalyst **2** is used at 50 ºC, with only the cis/trans isomers of the desired product plus one constitutional isomer observed by GC and ^{13}C NMR spectroscopy (see *Appendix A* for the NMR spectra). The constitutional isomer is likely the result of olefin migration to the adjacent carbon atom, after the dimerization has taken place. This would give rise to the extra peak in the GC results and the two additional sets of cis/trans olefin resonances observed in the ^{13}C NMR spectrum (there are two sets because the constitutional isomer is not symmetrical). When catalyst **3** is used, we have found that olefin migration occurs both before and after dimerization (this is true during polymerization reactions as well), so many isomeric products are formed. However, the constitutional isomer formed when the catalyst **2** is used does not appear to adversely affect the polymerization reaction. It should be noted, though, that due to the olefin migration in this reaction and in the polymerization and depolymerization reactions that use catalyst **3**, the number of methylene 'spacers' in the end-groups and between gem-dimethyl pendant groups are not consistent throughout the telechelic polymer's chains. This is evidenced by the "extra" peaks that can be found in the ^{1}H and ^{13}C NMR spectra of the telechelic polymers (**44b**, **45b**, and **42b**), shown in Figures 4.12-4.14 below.

The use of the longer MR (**43b**, where y = 3) and more careful product isolation resulted in much improved control of the number average molecular weight of the telechelic diol (**42b**). When the polymerization-depolymerization method (described in

Section 4.2.3) was used with this MR (**43b**) to make the unsaturated diacetate polymer (**44b**) in two separate reactions, the average numbers of repeat units (determined by ^{1}H NMR) were 8.7 and 7.3, respectively. These were very close to their targets, which were averages of 8.2 and 7.0 repeat units, respectively, based on the monomer to CTA molar ratios. These average numbers of repeat units correspond to number average molecular weights of 1550 and 1340 grams per mole, respectively, for the two polymers (**44b**). The GPC results for the first of these two polymers indicate a number average molecular weight of 2700 grams per mole and a PDI of 1.7. However, the NMR molecular weight determination is taken to be more accurate, because polystyrene standards, which differ structurally from the telechelic polymers, were used to determine the GPC molecular weights.

The ^{1}H NMR spectrum (see Figure 4.12) indicates that the unsaturated telechelic diacetate (**44b**) is perfectly bifunctional, due to the disappearance of the terminal olefin resonances at about 5.0 and 5.8 ppm. An IR spectrum of **44b** (see *Appendix B*) supports this finding, due to the lack of terminal olefin peaks at about 1825 and 3075 cm^{-1}. The ^{13}C NMR spectrum (see Figure 4.12) is complicated by the isomerization of olefins caused by catalyst **3** in the polymerization-depolymerization step and by catalyst **2** in the production of the MR (**43b**). Many unexpected peaks are seen as a result of this olefin isomerization. However, upon hydrogenation, the polymer structure will only vary by a few methylene units between some of the gem-dimethyl groups, which is not likely to adversely affect the material properties of the final telechelic diol (**42b**).

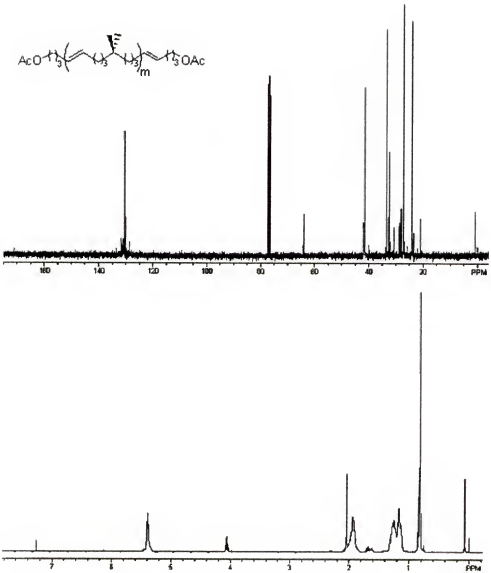

Figure 4.12 ^{13}C (top) and ^{1}H (bottom) NMR spectra for the unsaturated telechelic diacetate (**44b**) made by the polymerization-depolymerization method.

The unsaturated diacetate polymer (**44b**) was hydrogenated using the heterogeneous method that was described in Section 4.2.3. The crude polymer (**44b**) was dissolved in toluene, placed in a Parr reactor, and the palladium on activated carbon catalyst was added. This time, the high-pressure reactor was charged to 500 psi with hydrogen, because the reactors appeared to leak over time in all previous reactions and

this higher pressure would allow more time between recharges. However, it was later found by a ^{1}H NMR analysis of the reaction solvent that the reactors were not leaking, but that the toluene solvent was hydrogenated to some extent under the reaction conditions employed. This does not appear to happen at 50 °C or less, so the reaction may work better at a lower temperature or with a different solvent, such as hexanes. Regardless, the telechelic polymer (**45b**) obtained, after reacting for about 5 days followed by column chromatography purification, was completely hydrogenated. This was evidenced by the disappearance of the olefinic resonances at 5.4 ppm in the ^{1}H NMR spectrum (see Figure 4.13) and the alkene C-H out-of-plane bending peak at 969 cm^{-1} in the IR spectrum (see *Appendix B*). It should be noted that the broad peak at 3468 cm^{-1} in the IR spectrum is due to water that accumulated in the sample as a result of months spent in the humid Florida atmosphere before the sample was analyzed.

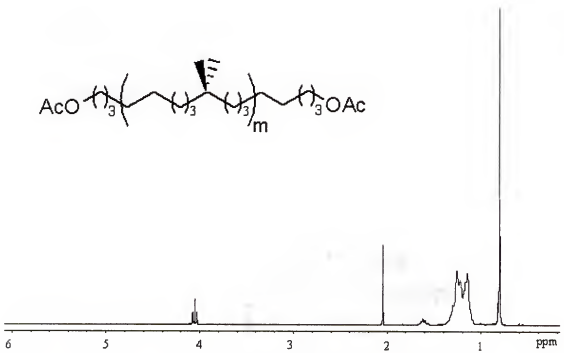

Figure 4.13 ^{1}H NMR spectrum for the saturated telechelic diacetate (**45b**).

The ^{1}H NMR spectrum indicates a number average molecular weight of 1600 grams per mole (8.9 repeat units on average) for the saturated telechelic diacetate (**45b**) from the first trial, while the GPC analysis indicates 2900 grams per mole and a PDI of 1.7. For the second trial, a number average molecular weight of 1300 grams per mole (6.9 repeat units on average) was determined by a ^{1}H NMR analysis.

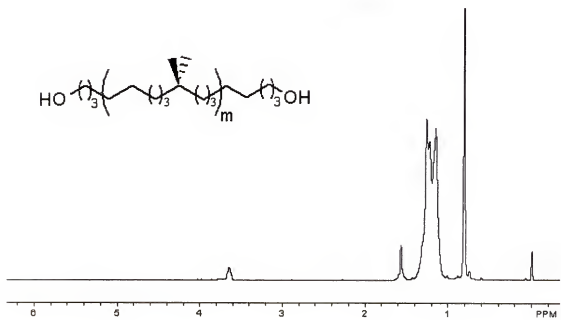

Figure 4.14 ^{1}H NMR spectrum for the telechelic diol (**42b**).

The final step in the reaction sequence remained unchanged from the one described in Section 4.2.3, except for the extraction steps. The saturated telechelic diacetate (**45b**) was hydrolyzed with 0.7 M sodium methoxide in methanol and diethyl ether to give the telechelic diol (**42b**). The extraction procedure was improved, so fractionation was not observed this time. The ^{1}H NMR spectrum (see Figure 4.14) indicates that the hydrolysis reaction was quantitative, due to the complete disappearance of the acetate end-group resonances at about 2.0 and 4.0 ppm and the appearance of a new hydroxyl end-group resonance at about 3.6 ppm. This is also supported by the disappearance of the acetate

C=O stretching peak at about 1745 cm^{-1} in the IR spectrum (see *Appendix B*). For the first trial, the number average molecular weight was about 1500 grams per mole (8.7 repeat units on average) by ^1H NMR, and 2600 grams per mole (PDI = 1.8) by GPC. For the second trial, the number average molecular weight was about 1200 grams per mole (6.9 repeat units on average) by ^1H NMR.

The quantitative ADMET reaction and excellent molecular weight control obtained with this MR (**43b**) using the polymerization-depolymerization method, inspired an attempt to make the unsaturated telechelic diacetate (**44b**) using the direct ADMET polymerization method. This was originally attempted with the shorter MR (**43a**, where y = 1), but the method failed to produce a perfectly difunctional telechelic diacetate polymer (**44a**) (see Section 4.2.1). This time, a perfectly difunctional telechelic diacetate polymer (**44b**) was obtained with the longer MR (**43b**) using the direct polymerization method, but the molecular weight could not be controlled. It had a number average molecular weight of 10,400 grams per mole by ^1H NMR, instead of the expected 1300 grams per mole (67 instead of 7 repeat units on average). The GPC determined number average molecular weight was about 11,100 grams per mole with a PDI of 1.9.

This method was able to produce a perfectly bifunctional telechelic, because the longer MR (**43b**) does not chelate the ruthenium catalyst (**3**) as the shorter MR (**43a**) did. This increased the rate of reaction, allowing a perfectly difunctional telechelic to be made before the catalyst decomposed. The target molecular weight was overshot because, during the polymerization, some of the MR (**43b**) is temporarily converted back to its monomer (CH_2=$CH(CH_2)_3OCOCH_3$), which is volatile enough to be removed by the

reduced pressure conditions. With less MR present to cap the chain-ends of the polymer, the number average molecular weight was increased.

The thermal behavior of the telechelic polymers **44b**, **45b**, and **42b**, made in the first trial, and the unsaturated telechelic diacetate **44b**, made using the direct polymerization method, were analyzed by DSC at a scanning rate of 10 °C per minute. The DSC traces are shown in Figure 4.15. All of these telechelic polymers were completely amorphous (no T_m) and exhibited glass transition temperatures (T_g's) between –80 and –50 °C. While the difference between the T_g's of the unsaturated and saturated telechelic diacetates (**44b** and **45b**) with similar M_n's is very small (T_g = -73 and –70 °C, respectively), they are both about 15 °C lower than the corresponding telechelic diol (**42b**). This suggests that the effect of the olefins in the telechelic backbone is negligible, while the effect of changing the end-group from an acetate to a hydroxyl group is significant in these low molecular weight oligomers. The relative increase in T_g for the telechelic diol (**42b**) is likely due to hydrogen bonding between the hydroxyl end-groups. The T_g of the higher molecular weight unsaturated diacetate telechelic, made by the direct polymerization method, is –54 °C. This value is closer to the T_g of the corresponding high molecular weight ADMET EIB model copolymer (**36a**), which is at –47 °C, than it is to the lower molecular weight unsaturated telechelic diacetate (-73 °C). This demonstrates that the T_g increases with the length of the polymer chains for low molecular weight oligomers.

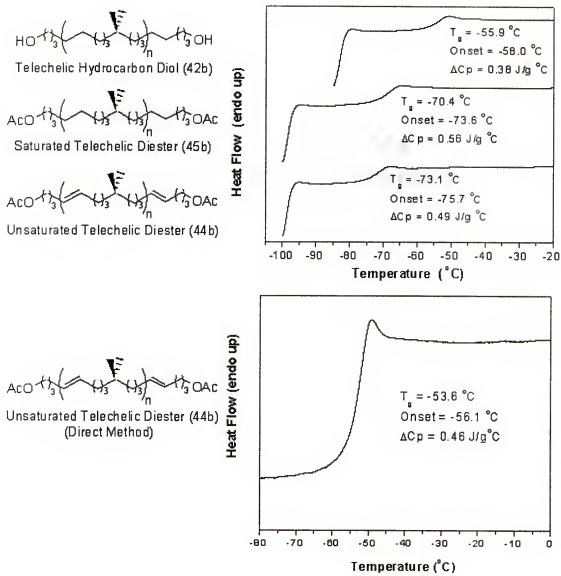

Figure 4.15 DSC traces for the telechelics (**42b**, **44b**, and **45b**) made using the polymerization-depolymerization method (top) and the unsaturated telechelic diacetate (**44b**) made using the direct method (bottom).

The successful synthesis and characterization of the perfectly difunctional, completely amorphous telechelic hydrocarbon diol (**42b**) proved that ADMET polymerization is a viable method for the production of this long-sought, useful material. However, it was believed that this method could be further improved upon by using an even longer MR (**43c**) with a different alcohol precursor end-group. It was also deemed

important to determine if a telechelic diol could be made without the undesired olefin isomerization side-reaction, by using catalyst **2**. These experiment are described in the next section.

4.4 Synthesis of Telechelic Diols with Long Chain-Ends (42c)

It was theorized that the molecular weight control of the direct polymerization method could be improved by using a longer, less volatile MR than **43b**. By choosing a very high boiling MR, such as 1-benzoxy-10-undecene ($C_6H_5CH_2O(CH_2)_9CH{=}CH_2$), the MR would also probably not need to be dimerized before using it in the direct polymerization. The unsaturated telechelic di(benzyl ether) made using this MR (**46**) could be deprotected to the alcohol in the hydrogenation step, by a process called hydrogenolysis, using the palladium on activated carbon catalyst. The advantages are: 1) the elimination of the depolymerization step; 2) the combination of the last two steps of the previous method (formerly hydrogenation then hydrolysis) into one step; and 3) the possibility of not needing to dimerize the MR (**46**) before its use. The new synthetic scheme is shown in Figure 4.16. While the previous polymerization-depolymerization method outlined in Section 4.3 worked very well, the proposed changes would streamline the large-scale production of the telechelic diol (**42**).

The MR (**46**) was made via Williamson ether synthesis. Sodium hydride was used to form the alkoxide of 10-undecene-1-ol, which was then reacted with benzyl bromide. After aqueous workup and extraction with diethyl ether, the crude product was distilled over calcium hydride at reduced pressure. Because its boiling point was sufficiently high (140-141.5 °C at 0.1 mmHg), **46** could be used in the direct polymerization method without dimerizing it first.

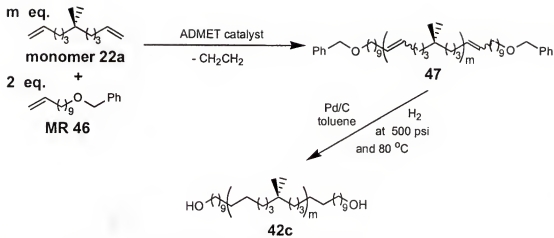

Figure 4.16 Synthetic scheme for the telechelic diol **42c**.

For the strict comparison of this method with the ones that were described in Sections 4.2 and 4.3, catalyst **3** was used in the first direct polymerization of monomer **22a** with the benzyl ether MR (**46**). A monomer to MR ratio of 6.8:2 was used, so the target number average molecular weight of the unsaturated telechelic di(benzyl ether) was 1530 grams per mole. The polymerization was started at 30 °C, using intermittent vacuum to remove the ethylene until the bubbling slowed enough to apply full vacuum. The reaction temperature was gradually increased to 50 °C over the five day reaction period. Bubbling (ethylene evolution) had ceased by the fourth day.

The ^{1}H and ^{13}C NMR spectra of the unsaturated telechelic di(benzyl ether) (**47**) are shown in Figure 4.17, and they indicate that it is perfectly bifunctional with the limits of detection. The ^{1}H NMR spectrum indicated a number average molecular weight of 1220 grams per mole (4.8 average number of repeat units), which was considerable less than the target of 1530 grams per mole (6.8 repeat units). The most plausible explanation for this is that the monomer (**22a**) was now more volatile than the MR (**46**), so some of it was removed under vacuum. As was anticipated, the ^{13}C NMR spectrum was complicated by many peaks, due to the olefin isomerization side-reaction caused by catalyst **3**.

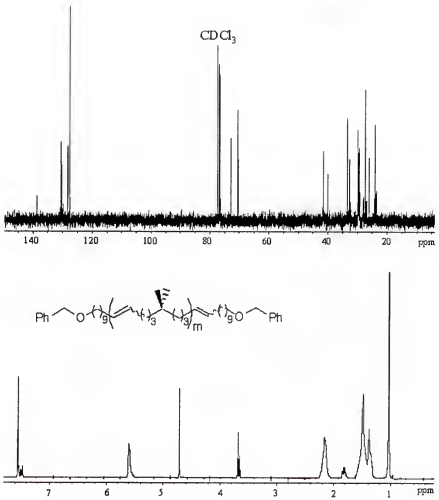

Figure 4.17 ^{13}C (top) and ^{1}H (bottom) NMR spectra for the unsaturated telechelic di(benzyl ether) (**47**) made with catalyst **3**.

The hydrogenation and hydrogenolysis of the unsaturated telechelic di(benzyl ether) (**47**) were carried out simultaneously using palladium on activated carbon and reaction conditions that were similar to those described in Section 4.2.3. Both reactions were quantitative, as evidenced by the disappearance of the olefin and benzyl ether resonances, and the appearance of hydroxyl resonances in the ^{1}H and ^{13}C NMR spectra of the telechelic diol (**42c**), shown in Figure 4.18. The ^{1}H NMR spectrum indicates a number average molecular weight of 1050 grams per mole (4.8 average number of repeat units), which is consistent with its precursor telechelic polymer (**47**). The GPC analysis of this

telechelic diol (**42c**) gave a number average molecular weight of 2000 grams per mole and a PDI of 1.6. The GPC results for all of the telechelics discussed in this chapter tend to overestimate the number average molecular weight by about 1000 grams per mole relative to the ^{1}H NMR results. However, these results are still useful for determining an approximate molecular weight and for providing information about the molecular weight distribution.

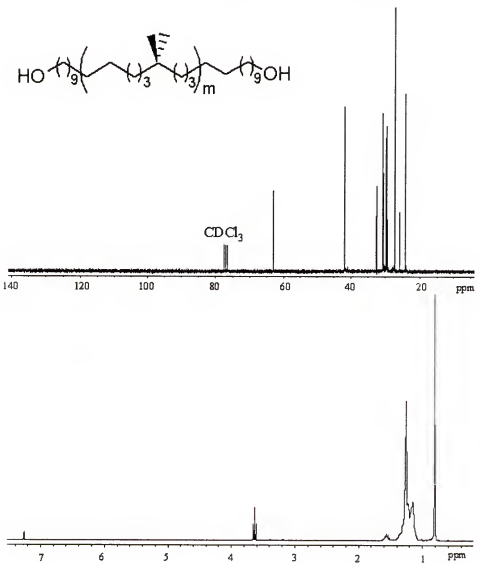

Figure 4.18: ^{13}C (top) and ^{1}H (bottom) NMR spectra for the telechelic diol (**42c**) made using catalyst **3**.

With the goal of demonstrating that a telechelic diol can be made with *precisely* spaced gem-dimethyl pendant groups along its backbone, catalyst **2** was used in a second trial of the reaction sequence shown in Figure 4.16. This catalyst (**2**) routinely produces polymers with precise microstructures, in the absence of significant olefin isomerization. Similar reaction conditions were used, in the direct polymerization, to those described in the previous trial, with only a few exceptions. This time, a monomer (**22a**) to MR (**46**) ratio of 7.8:2 was used. Also, in the hope of limiting the loss of monomer and thereby improving the molecular weight control, the reaction was initiated at room temperature and the ethylene was removed by an argon flow for the first day. Vacuum was applied on the second day and the temperature was gradually increased to 50 °C over the four day reaction period. By the third day the reaction had ceased to bubble (evolve ethylene), and was likely complete.

The resulting unsaturated telechelic di(benzyl ether) (**47**) was perfectly bifunctional within the detection limits of the ^{1}H NMR spectrum, shown in Figure 4.19. The ^{1}H NMR spectrum also indicated a number average molecular weight of 1650 grams per mole (7.6 average number of repeat units), which was very close to the target of 1680 grams per mole (7.8 repeat units). The GPC analysis of this telechelic polymer gave a number average molecular weight of 2500 grams per mole and a PDI of 1.7. Significantly, no olefin isomerization was observed in the ^{13}C NMR spectrum, as only the expected resonances from the repeat units and the end-groups are visible.

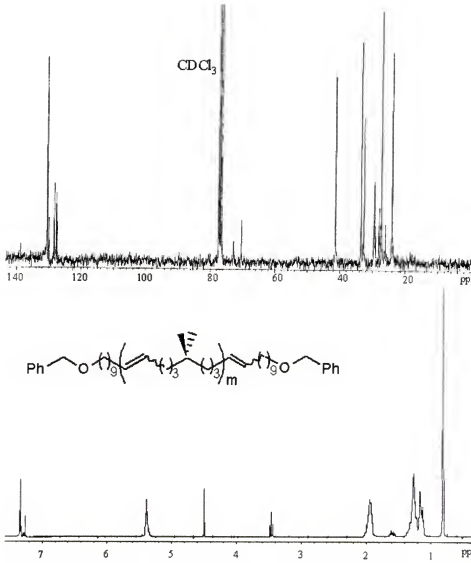

Figure 4.19 ^{13}C (top) and ^{1}H (bottom) NMR spectra for the unsaturated telechelic di(benzyl ether) (**47**) made with catalyst **2**.

The simultaneous hydrogenation and hydrogenolysis reactions were carried out in the same manner as the first trial, with similar results. The ^{1}H and ^{13}C NMR spectra of the telechelic diol (**42c**) are shown in Figure 4.20. Both of the reactions were quantitative within NMR detection limits. This is supported by the IR data for the telechelic polymers (**47** and **42c**), which are provided in *Appendix B*. The alkene C-H out-of-plane bending peak at 967 cm^{-1} is absent in the IR spectrum of **42c**, as are the aromatic peaks at 697,

1496, 3029, 3065, and 3095 cm^{-1}. The ^1H NMR spectrum indicates a number average molecular weight of 1840 grams per mole (9.9 average number of repeat units), which is somewhat higher than expected based on the molecular weight of the precursor telechelic polymer (**47**). The GPC analysis gave a number average molecular weight of 2700 grams per mole (PDI = 1.7), which is also higher than that of the precursor (**47**). Fractionation

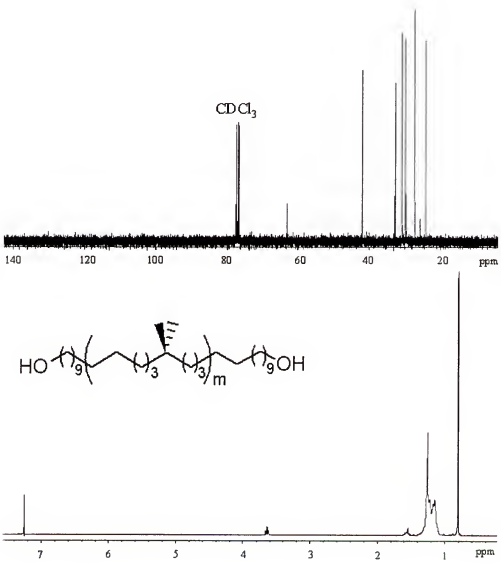

Figure 4.20 ^{13}C (top) and ^1H (bottom) NMR spectra for the telechelic diol (**42c**) made using catalyst **2**.

during the product isolation steps is the most likely cause of this increase in molecular weight. In spite of this fractionation, this method appears to be the best overall for producing a perfectly difunctional telechelic diol (**42**). It has excellent control of the molecular weight and microstructure of the polymer in the ADMET polymerization step, and requires the fewest number of steps to obtain the telechelic diol (**42**).

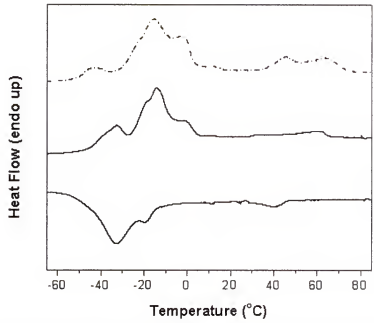

Figure 4.21 DSC traces for the telechelic diols (**42c's**) made using catalyst **3** (dashed line) and catalyst **2** (solid line).

However, a DSC analysis of both of the telechelic diols described in this section (**42c's** made with catalysts **3** and **2**) reveals an unfortunate consequence of the greater length of the MR (**46**) used to make them. The DSC traces, taken at a scanning rate of 10 °C per minute, are shown in Figure 4.21. The surprising result is that both of these telechelic diols exhibit a melting transition that begins just after the glass transition temperature, which occurs at about –45 to –50 °C. The melting transitions are very broad, spanning nearly 110 °C, and are multi-modal (exhibiting many shoulders and peaks). The most plausible explanation for this behavior is the melting of many discrete, low

molecular weight oligomers (where n = 0, 1, 2…) with long methylene sequences at their chain ends and very few gem-dimethyl pendant groups to disrupt their crystallization.

This anomalous melting behavior could be avoided by using a benzyl ether MR with fewer methylene 'spacers' between the ether oxygen and the terminal olefin. Since the volatility of the MR is inversely proportional to the number of methylene 'spacers', the appropriate length of the MR would have to be found that balances the molecular weight control (when the direct polymerization method is used) with the suppression of crystallization. Using the simple synthetic method shown in Figure 4.16, the improved MR should produce a completely amorphous telechelic hydrocarbon diol that is similar to the **42b** that was made via the more complicated polymerization-depolymerization, hydrogenation, hydrolysis reaction sequence.

4.5 Conclusion

Several methods have been investigated for the production of perfectly bifunctional, completely amorphous telechelic hydrocarbon diols using ADMET chemistry. Three monofunctional reactants (MR's), each with a different number of methylene 'spacers' between its olefin and alcohol precursor functional group, were used to end-cap the polymer chains. All three MR's could be used to make difunctional telechelic diols, but the use of the shortest MR (**43a**) led to relatively poor molecular weight control and the use of the longest MR (**46**) led to a semicrystalline material. The best results were obtained when the medium length MR (**43b**), with three methylene 'spacers', was used in combination with the polymerization-depolymerization production method. The resulting telechelic diol (**42b**) was perfectly bifunctional within NMR and IR spectroscopy detection limits, and it was completely amorphous with a T_g at –56 °C.

Additionally, a simple two-step procedure was developed that was more efficient than the successful polymerization-depolymerization method. It involved the direct ADMET polymerization of the gem-dimethyl diene monomer (**22a**) in the presence of a MR with a benzyl ether protecting group, followed by a one-pot hydrogenation-deprotection step. However, this method was only tested with the longest MR (**46**), which yielded the semicrystalline material. An improvement, involving the use of a benzyl ether MR with fewer than nine methylene 'spacers', was suggested that might lead to a perfectly difunctional, *completely amorphous* telechelic hydrocarbon diol using this simple procedure. This work was part of a collaborative research effort with Medtronic, Inc., and has resulted in a US patent application.

CHAPTER 5
EXPERIMENTAL

5.1 Instrumentation and Analysis

The ^{1}H NMR (300 MHz) and ^{13}C NMR (75 MHz) spectra were recorded on a Varian Associates Gemini 300 or VXR-300 superconducting spectrometer system. Chemical shifts for ^{1}H NMR were referenced to TMS and those for ^{13}C NMR were referenced to residual signals from $CDCl_3$ solvent. Reaction conversions and purity of products were monitored by chromatography. Gas chromatography was performed on a Shimadzu GC-17A gas chromatograph equipped with a Hewlett Packard HP-5 cross-linked 5% phenyl methyl siloxane column (length = 25m, film thickness = 0.33μm, ID = 0.2mm) and a flame ionization detector. Thin layer chromatography (TLC) was performed on Whatman™ aluminum backed, 250 μm silica gel coated plates, using mixtures of hexanes and ethyl acetate as the mobile phase. TLC plates were stained with phosphomolybdic acid (10%) in ethanol to see UV inactive products and impurities. High resolution mass spectra (HRMS) were obtained on a Finnegan 4500 gas chromatograph/mass spectrometer using the electron ionization (EI) mode. GPC data were obtained using a Waters Associates 6000A liquid chromatograph apparatus equipped with a HP refractive index detector. HPLC grade THF was used as the mobile phase, and a column bank consisting of two PLgel 5 μm MIXED-C columns (300mm length each) was used as the stationary phase. Polymer samples were prepared in HPLC grade THF (~5% w/w) and passed through a 45 μm syringe filter prior to injection. A

constant flow rate of 1.0 mL per minute at 35 °C was maintained, and the instrument was calibrated using polystyrene standards from Polymer Laboratories. Elemental analyses were performed by Atlantic Microlabs Inc., Norcross, GA.

Differential scanning calorimetry (DSC) analyses were performed using a Perkin-Elmer DSC 7 at a heating rate of 10 °C per minute. Thermal calibrations were made using indium and n-octane as the standards. All samples were prepared in hermetically sealed pans. Sample sizes were typically 2-4 mg for melting transition measurements and 12-15 mg for glass transition measurements, though some of the samples were used to obtain both of these measurements. The samples were analyzed from –100 to 100 °C and multiple heating and cooling cycles were obtained for each to verify the results.

5.2 Materials

The olefin metathesis catalysts **1**, **2**, and **3** were synthesized following literature procedures.[18,36,143,144] 5-Bromo-1-pentene (**25a**), 8-bromo-1-octene (**25b**), and 11-bromo-1-undecene (**25c**) were purchased from Aldrich and distilled from CaH_2 (38-40 °C at 93 mmHg, 117-119 °C at 88 mmHg, and 116-117 °C at 10 mmHg, respectively). Propionic acid was purchased from Aldrich and distilled from anhydrous Na_2SO_4 (71-72 °C at 65 mmHg), then redistilled from a few crystals of $KMnO_4$ prior to use. Diethyl ether (Et_2O) and tetrahydrofuran (THF) were distilled from Na/K alloy using benzophenone as the indicator. Chloroform ($CHCl_3$) was distilled from P_2O_5, and hexamethylphosphoramide (HMPA) was distilled from CaH_2 prior to their use. 1,4-bisacetoxy-2-butene (MR 43a) was purchase from Aldrich and distilled from CaH_2 (63 °C at 0.1 mmHg) and acetic acid 4-pentenyl ester was purchased from TCI and distilled from CaH_2 (66-68 °C at 53 mmHg). All other reagents were used as received.

5.3 Synthesis of α,ω-Diene Monomers

5.3.1 Gem-Dimethyl and Carboxylic Acid Monomer Syntheses

This section describes the synthesis of a series of three symmetrical gem-dimethyl α,ω-diene monomers in four steps. Sample procedures are given for the first monomer in the series (22a). The procedure for the first step is taken from the most recent synthesis of the monomer (22a), which has a higher yield than the original synthesis (70% vs. 50%). The procedures for the last three steps are drawn from the original synthesis, so the overall yield for the four steps is based on the original synthesis procedures (with a 50% first step yield). The product of step 1 for the third monomer in the series is also the carboxylic acid monomer (23c).

5.3.1.1 Step 1: dialkenylation of propionic acid (carboxylic acid monomer synthesis)

Synthesis of 6-methyl-1,10-undecadiene-6-carboxylic acid (23a). A 131 mL (262 mmol) sample of a 2.0 M solution of lithium diisopropylamide (LDA) in THF (from Aldrich, cat. # 49,458-5) was placed in a flame dried, argon purged 1000 mL 3-neck round bottom flask equipped with a magnetic stir bar, 125 mL addition funnel, 250 mL addition funnel, and a condenser. The solution was cooled to –35 °C, and 9.48g (128 mmol) of propionic acid was added via syringe to the 125 mL addition funnel, followed by about 10 mL of THF. The propionic acid solution was added dropwise over about 50 minutes, and then the addition funnel was washed with THF. The reaction smoked considerably at the early stages of the addition, and white salts formed. Approximately 25 mL of HMPA (about 1.1 equivalent to propionic acid) was added by syringe, and the mixture turned from a pale yellow to orange (salts still present). The mixture was allowed to warm to 10 °C over about 1 hour, followed by heating to 50 °C for 1.5 hours. The

mixture was a reddish-orange with salts present. The mixture was slowly chilled to –35 °C and 20.3g (136 mmol) of 5-bromo-1-pentene was added to the 125 mL addition funnel via syringe. This was slowly dripped into the reaction mixture over 15 minutes. The mixture cleared after about 1 mL was added (colorless solution), then gradually turned yellowish with white salts. The mixture was slowly brought to 50 °C (salts dissolved and solution became yellowish during heating) and was left to stir for 2.5 hours. After 2.5 hours, excessive salts had formed, so THF was slowly added by cannula until the salts had dissolved and the mixture became a yellowish color again (about 200 mL of THF was added). The solution was again chilled to –35 °C, and 65.5 mL (161 mmol) the 2.0 M LDA solution was added to the reaction mixture dropwise from the 250 mL addition funnel over 40 minutes. The reaction mixture was allowed to warm to room temperature (solution turned more yellow), followed by heating to 50 °C for 1.5 hours (solution turned orange). The mixture was chilled to –35 °C, and 21.4g (144 mmol) of 5-bromo-1-pentene was slowly added from the 125 mL addition funnel over 25 minutes, and was then rinsed down with THF. The color lightened to yellow after the first few drops. The mixture was allowed to warm to room temperature, followed by heating to 50 °C for 12 hours.

After 12 hours, the mixture was allowed to cool to room temperature and then it was slowly poured over about 500 mL of ice in a 1000 mL beaker with stirring. HCl (3 M) was added with stirring until all salts had dissolved. After concentration on a rotary evaporator, the quenched reaction mixture was extracted three times with diethyl ether. The combined organic layers were washed three times with 3 M HCl, and then dried over anhydrous magnesium sulfate, gravity filtered, and evaporated under reduced pressure.

The percent yield was calculated to be about 70% based on the mass of the crude product (34.0g) and a GC analysis (55% 23a in crude). The product was not purified before taking it on to the next step. However, in the original synthesis of 23a, the monoalkenylated intermediate was recovered by column chromatography using a 5:1 mixture of methylene chloride and ethyl acetate as the mobile phase. Partially purified portions of 23a were also obtained in this manner. The recovered monoalkenylated product could then be used to make more of the desired dialkenylated product (23a).

The following spectral properties were observed: ^{1}H NMR ($CDCl_3$): δ 1.14 (s, 3H), 1.30-1.51 (m, 4H), 1.63 (dt, 4H), 2.04 (q, 4H), 4.93-5.04 (m, 4H), 5.72-5.83 (m, 2H), 11.95 (s, broad, 1H); ^{13}C NMR: δ 21.07, 23.75, 34.10, 38.46, 45.61, 114.67, 138.46, 184.38; EI/HRMS: $[M + 1]^+$ calcd. for $C_{13}H_{22}O_2$: 211.1698; found: 211.1698. Elemental analysis calcd. for $C_{13}H_{22}O_2$: 74.23 C, 10.55 H; found: 73.97 C, 10.59 H.

Synthesis of 9-methyl-1,16-heptadecadiene-9-carboxylic acid (23b). Synthesized as above. Crude yield of 23b after partial purification by column chromatography: 54%.

Synthesis of 12-methyl-1,22-trieicosadiene-12-carboxylic acid (23c). Synthesized as above. Crude yield of 23c after partial purification by column chromatography: 44%. The purest column fractions were recrystallized twice from hexanes and 2.3g were isolated. A melting point of 43.5 to 45.5 °C was determined for 23c. Half of the pure crystals were used to make the EMAA model copolymer (38) and half were used to synthesize the methyl ester monomer (24c). The crude acid was used for the next step.

The following spectral properties were observed: ^{1}H NMR ($CDCl_3$): δ 1.12 (s, 3H), 1.17-1.46 (m, 30H), 1.61 (t, 2H), 2.04 (q, 4H), 4.91-5.02 (m, 4H), 5.74-5.86 (m, 2H),

11.89 (s, broad, 1H); ^{13}C NMR: δ 21.24, 24.68, 29.17, 29.37, 29.71, 29.80, 30.38, 34.05, 39.32, 45.98, 114.32, 139.45, 184.67; EI/HRMS: $[M + 1]^+$ calcd. for $C_{25}H_{46}O_2$: 378.3498; found: 378.3525. Elemental analysis calcd. for $C_{25}H_{46}O_2$: 79.29 C, 12.25 H; found: 79.11 C, 12.31 H.

5.3.1.2 Step 2: carboxylic acid reduction to the alcohol

Synthesis of 6-hydroxymethyl-6-methyl-1,10-undecadiene (34a). To an argon purged 1000 mL 3-neck flask equipped with a stir bar and condenser, were added 200 mL of dry Et_2O and 12.0 g of the semi-purified carboxylic acid mixture (about 82% dialkenylated and 18% monoalkenylated by GC analysis) from the original synthesis of 23a. Prior to addition, the carboxylic acid mixture had been left under vacuum for 12 hours to partially dry it. The solution was stirred for 5 minutes and cooled in an ice bath, before 140 mL of 1.0 M lithium aluminum hydride (LAH) in Et_2O (from Aldrich, cat. # 21,279-2) was added slowly, in three portions, via syringe (LAH powder suspended in ether can be substituted here with similar results). Gas evolution was observed upon addition of LAH. The reaction mixture was allowed to warm to room temperature and stirred for 20 hours.

The mixture was very slowly poured onto ice in a 1400 mL beaker. Vigorous evolution of gas was observed. HCl (3 M) was added slowly until the salts dissolved. The aqueous layer was extracted three times with Et_2O. The combined ether layers were washed with two portions of 3 M HCl, once with saturated sodium bicarbonate, and once with de-ionized water. The organic layer was then dried over magnesium sulfate, gravity filtered, and evaporated under reduced pressure.

The crude product was a strong smelling, viscous, clear oil, obtained in 94.3% yield. The crude product was distilled at a pressure of 0.1 mmHg. The monoalkenylated alcohol boiled at 41-43 °C, and alcohol 34a boiled at 84-85 °C. An isolated yield of 72.3% was obtained for 34a.

The following spectral properties were observed: ^{1}H NMR ($CDCl_3$): δ 0.84 (s, 3H), 1.19-1.35 (m, 9H), 2.03 (q, 4H), 3.35 (d, 2H), 4.93-5.05 (m, 4H), 5.75-5.86 (m, 2H); ^{13}C NMR ($CDCl_3$): δ 21.83, 22.81, 34.57, 35.84, 37.21, 69.64, 114.43, 138.90; EI/HRMS: $[M]^+$ calcd. for $C_{13}H_{24}O$: 196.1827, found: 196.1829. Elemental analysis calcd. for $C_{13}H_{24}O$: 79.52 C, 12.33 H; found: 79.40 C, 12.36 H.

Synthesis of 9-hydroxymethyl-9-methyl-1,16-heptadecadiene (34b). Synthesized as above. The crude alcohol (34b) was distilled with a boiling point of 114-117 °C at 0.02 mmHg. Isolated yield of 34b: 84%. The following spectral properties were observed: ^{1}H NMR ($CDCl_3$): δ 0.82 (s, 3H), 1.20-1.40 (m, 20H), 2.04 (q, 4H), 3.33 (s, 2H), 4.91-5.02 (m, 4H), 5.75-5.86 (m, 2H); ^{13}C NMR ($CDCl_3$): δ 21.88, 23.37, 28.95, 29.17, 30.46, 33.80, 36.39, 37.24, 68.83, 114.11, 139.15; EI/HRMS: $[M]^+$ calcd. for $C_{19}H_{36}O$: 280.2766, found: 280.2774. Elemental analysis calcd. for $C_{19}H_{36}O$: 81.35 C, 12.94 H; found: 81.35 C, 13.13 H.

Synthesis of 12-hydroxymethyl-12-methyl-1,22-tricicosadiene (34c). Synthesized as above. The crude alcohol (34c) was distilled with a boiling point of 153-155 °C at 0.02 mmHg. Isolated yield of 34c: 93%. The following spectral properties were observed: ^{1}H NMR ($CDCl_3$): δ 0.82 (s, 3H), 1.20-1.37 (m, 32H), 2.04 (q, 4H), 3.33 (s, 2H), 4.91-5.01 (m, 4H), 5.74-5.88 (m, 2H); ^{13}C NMR ($CDCl_3$): δ 21.88, 23.38, 28.91, 29.12, 29.48, 29.60, 29.64, 30.60, 33.79, 36.40, 37.21, 69.83, 114.06, 139.17.

5.3.1.3 Step 3: tosylation of the alcohol

Synthesis of 6-methyl-6-(*p*-toluenesulfonyl)methyl-1,10-undecadiene (35a). To a flame dried, argon purged 500 mL 3-neck flask equipped with a stir bar, were added 100 mL of dry $CHCl_3$ via cannula, and 7.72g (39.3 mmol) of the alcohol 34a from the previous step. After cooling the solution in an ice bath and stirring for 15 minutes, about 9 mL (125 mmol) of dry pyridine was added via syringe. The reaction mixture was stirred for 30 minutes, and then toluenesulfonyl chloride was added in four 4g portions (about 84 mmol total) over a 30 minute period. The reaction mixture was allowed to warm to room temperature and stir for 48 hours.

The reaction mixture was poured over ice in a 1000 mL beaker, and 3 M HCl (about 200 mL) was added slowly, with stirring. The mixture was extracted three times with $CHCl_3$. The combined organic layers were washed twice with saturated potassium carbonate and twice with distilled water. The $CHCl_3$ layer was dried over magnesium sulfate, gravity filtered, and evaporated under reduced pressure. A yield of 21.8g of crude product was obtained, but ^1H and ^{13}C NMR showed the presence of toluenesulfonic acid impurity. No residual alcohol (34a) was observed in the NMR spectra after the reaction. An attempt to distill a small portion of the product mixture resulted in decomposition. The crude product was used for the next step.

The following spectral properties were observed: ^1H NMR ($CDCl_3$): δ 0.82 (s, 3H), 1.12-1.23 (m, 8H), 1.94 (q, 4H), 2.45 (s, 3H), 3.69 (s, 2H), 4.90-4.99 (m, 4H), 5.66-5.79 (m, 2H), 7.34 (d, 2H), 7.78 (d, 2H); ^{13}C NMR ($CDCl_3$): δ 21.73, 22.42, 34.24, 35.70, 36.33, 75.98, 114.60, 127.89, 129.77, 132.75, 138.51, 144.64.

Synthesis of 9-methyl-9-(*p*-toluenesulfonyl)methyl-1,16-heptadecadiene (35b). Synthesized as above. The crude product (35b) was used in the next step. The following spectral properties were observed: ^{1}H NMR ($CDCl_3$): δ 0.80 (s, 3H), 1.06-1.37 (m, 20H), 1.03 (q, 4H), 2.45 (s, 3H), 3.68 (s, 2H), 4.92-5.02 (m, 4H), 5.76-5.85 (m, 2H), 7.34 (d, 2H), 7.78 (d, 2H); ^{13}C NMR ($CDCl_3$): δ 21.76, 23.02, 28.86, 29.03, 30.15, 33.77, 36.22, 36.33, 76.16, 114.16, 127.88, 129.70, 132.88, 139.05, 144.53.

Synthesis of 12-methyl-12-(*p*-toluenesulfonyl)methyl-1,22-trieicosadiene (35c). Synthesized as above. The crude product (35c) was used in the next step. The following spectral properties were observed: ^{1}H NMR ($CDCl_3$): δ 0.80 (s, 3H), 1.06-1.37 (m, 20H), 1.03 (q, 4H), 2.45 (s, 3H), 3.68 (s, 2H), 4.92-5.02 (m, 4H), 5.76-5.85 (m, 2H), 7.34 (d, 2H), 7.78 (d, 2H); ^{13}C NMR ($CDCl_3$): δ 21.80, 23.08, 28.95, 29.14, 29.51, 29.58, 30.33, 33.82, 36.25, 36.35, 76.24, 114.09, 127.91, 129.72, 132.95, 139.19, 144.50.

5.3.1.4 Step 4: reduction of the tosylate

Synthesis of 6,6-dimethyl-1,10-undecadiene (22a). To a flame dried, argon purged 500 mL 3-neck flask equipped with a condenser, addition funnel, and stir bar, were added 80 mL of dry Et_2O and 20.7g of the crude tosylate (35a) from the previous step. The solution was chilled in an ice bath, and 175 mL of 1.0 M lithium aluminum hydride in Et_2O was slowly added from the addition funnel. The reaction mixture immediately turned cloudy white. The mixture was allowed to warm to room temperature, and stirred for 20 hours.

The reaction mixture was very slowly poured over ice in a 1600 mL beaker, with stirring. Distilled water was added until frothing ceased. Then, 3 M HCl was added until the white salts had completely dissolved. The mixture was concentrated on a rotary

evaporator and the aqueous layer was extracted three times with pentane. The combined organic layers were washed twice with saturated potassium carbonate, twice with 3 M HCl, and once with 100 mL of distilled water. The colorless crude product was purified by flash column chromatography using silica gel 60 as the stationary phase and hexanes as the mobile phase. A sample of 4.68g of pure 22a was obtained. The two-step yield (steps 3 and 4) was 66%, and the overall yield for all four steps was 27%. Prior to polymerization, monomer 22a was distilled from CaH_2 at 15.0 mm Hg into a 50 mL Schlenk flask, subjected to three freeze-pump-thaw cycles, and stored under argon atmosphere. The boiling point at 15.0 mm Hg was 80-81.5 °C.

The following spectral properties were observed: ^{1}H NMR ($CDCl_3$): δ 0.83 (s, 6H), 1.13-1.21 (dt, 4H), 1.25-1.35 (m, 4H), 2.01 (q, 4H), 4.91-5.04 (m, 4H), 5.75-5.88 (m, 2H); ^{13}C NMR ($CDCl_3$): δ 23.45, 27.25, 32.57, 34.70, 41.43, 114.16, 139.19; EI/HRMS: $[M]^+$ calcd. for $C_{13}H_{24}$: 180.1878, found: 180.1877. Elemental analysis calcd. for $C_{13}H_{24}$: 86.58 C, 13.42 H; found: 85.99 C, 13.26 H.

Synthesis of 9,9-dimethyl-1,16-heptadecadiene (22b). Synthesized as above. The crude product (22b) was columned as above, dried over CaH_2 at 0.02 mmHg for12 hours, and filtered through a 0.45 μm syringe filter into a Schlenk flask in an argon atmosphere dry box. Two-step isolated yield of 22b: 23%; overall four-step yield: 10%. The following spectral properties were observed: ^{1}H NMR ($CDCl_3$): δ 0.81 (s, 6H), 1.15-1.40 (m, 20H), 2.04 (q, 4H), 4.90-5.03 (m, 4H), 5.75-5.88 (m, 2H); ^{13}C NMR ($CDCl_3$): δ 23.99, 27.29, 29.01, 29.24, 30.54 32.58, 33.86, 42.00, 114.10, 139.24; EI/HRMS: $[M]^+$ calcd. for $C_{19}H_{36}$: 264.2817, found: 264.2827. Elemental analysis calcd. for $C_{19}H_{36}$: 86.27 C, 13.73 H; found: 86.51 C, 13.77 H.

Synthesis of 12,12-dimethyl-1,22-trieicosadiene (22c). Synthesized as above. The columned monomer (22c) was distilled with a boiling point of 125-127 °C at 0.01 mmHg. Two-step isolated yield of 22c: 64%; overall four-step yield: 26%. The following spectral properties were observed: ^{1}H NMR ($CDCl_3$): δ 0.81 (s, 6H), 1.15-1.40 (m, 32H), 2.04 (q, 4H), 4.90-5.03 (m, 4H), 5.74-5.88 (m, 2H); ^{13}C NMR ($CDCl_3$): δ 24.05, 27.32, 28.99, 29.20, 29.56, 29.69, 29.76, 30.71, 32.59, 33.86, 42.03, 114.10, 139.21; EI/HRMS: $[M]^+$ calcd. for $C_{25}H_{48}$: 348.3756, found: 348.3759. Elemental analysis calcd. for $C_{25}H_{48}$: 86.11 C, 13.89 H; found: 86.05 C, 14.05 H.

5.3.2 Ester Monomer Synthesis

Synthesis of 12-methyl-1,22-trieicosadiene-12-methyl ester (24c). A 1.20g sample of carboxylic acid 23c was dissolved in 25 mL of acetone in a 100 mL round bottom flask equipped with a stir bar. A 1.16g sample of K_2CO_3 was added and the mixture was stirred for 10 min. A 1.6 mL sample of CH_3I was added via syringe with the hood sash down low. A pre-assembled simple distillation apparatus was attached to the reaction flask and the mixture was stirred for 6 hours. After distilling off the CH_3I and most of the acetone, the crude product was concentrated on a rotory evaporator. The product was dissolved in pentane and washed twice with 3M HCl and twice with distilled water. The pentane layer was dried over magnesium sulfate, gravity filtered, and evaporated under reduced pressure. The ester monomer (24c) thus obtained was >99% pure by GC and the isolated yield was 97%. Prior to polymerization, 24c was dried over CaH_2 at 0.02 mmHg for12 hours, and filtered through a 0.2 μm syringe filter into a Schlenk flask in an argon atmosphere dry box.

The following spectral properties were observed: ^{1}H NMR ($CDCl_3$): δ 1.11 (s, 3H), 1.25-1.41 (m, 30H), 1.55-1.63 (dt, 2H), 2.03 (q, 4H), 3.64 (s, 3H), 4.91-5.02 (m, 4H), 5.74-5.87 (m, 2H); ^{13}C NMR ($CDCl_3$): δ 21.14, 24.51, 28.91, 29.10, 29.44, 29.51, 30.09, 33.78, 39.44, 45.94, 51.38, 114.07, 139.15, 178.12; EI/HRMS: $[M]^+$ calcd. for $C_{26}H_{48}O_2$: 392.3654, found: 392.3648. Elemental analysis calcd. for $C_{26}H_{48}O_2$: 79.52 C, 12.33 H; found: 79.30 C, 12.45 H.

5.4 Synthesis of ADMET Ethylene-Based Model Copolymers

5.4.1 Synthesis of the EIB Model Copolymers (36a-c)

5.4.1.1 Synthesis of the unsaturated gem-dimethyl substituted polymers (39a-c)

Synthesis of 39a. In an argon atmosphere dry box, 0.76g (4.2 mmol) of the dry, degassed monomer 22a was placed in a 50 mL round bottom flask equipped with a Teflon™ magnetic stir bar. A 8.6mg sample (0.011 mmol, 380:1 monomer to catalyst ratio) of Schrock's molybdenum alkylidene catalyst (1) was added, and an adapter with a Teflon™ vacuum valve was attached to the flask, to allow the direct attachment of the reaction flask to a vacuum line. The mixture immediately began to bubble, so the reaction vessel was quickly removed from the glove box and attached to a vacuum line. The vessel was warmed in a 40 °C oil bath and intermittent vacuum (open valve for ~1 sec periodically) was applied until the mixture became viscous enough to leave open to vacuum ($<10^{-1}$ mmHg) after about 5 hours. The mixture quickly became more viscous and turned from a pale yellow to purple. After 24 hours the mixture was exposed to high vacuum ($<10^{-3}$ mmHg), and the temperature was increased to 50 °C. After another 24 hours, the temperature was increased to 60 °C, and the mixture was very slowly stirred for another 48 hours (a total reaction time of 4 days). After cooling to room temperature

the reaction was quenched by exposure to air. The unsaturated polymer was dissolved in 30 mL of toluene and precipitated in vigorously stirred, ice-cold methanol. The rubbery, tacky precipitate was collected by filtration, and transferred to a 50 mL round bottom flask. It was then dried at 60 °C under vacuum for five days.

The following spectral properties were observed: ^{1}H NMR ($CDCl_3$): δ 0.82 (s, 6H), 1.12-1.17 (m, 4H), 1.19-1.32 (m, 4H), 1.90-1.99 (m, 4H), 5.32-5.45 (m, 2H); ^{13}C NMR ($CDCl_3$): δ 24.20, 27.33, 28.12, 32.62, 33.56, 41.57, 130.01 (cis alkene), 130.45 (trans alkene). GPC data: M_n = 55,200; PDI (M_w/M_n) = 1.7.

Synthesis of 39b. Synthesized as above, with the following exceptions: a monomer to catalyst ratio of 440:1 was used and the reaction time was 5 days. The following spectral properties were observed: ^{1}H NMR ($CDCl_3$): δ 0.81 (s, 6H), 1.14-1.30 (m, 20H), 1.95-2.03 (m, 4H), 5.32-5.45 (m, 2H); ^{13}C NMR ($CDCl_3$): δ 24.01, 27.24 (cis), 27.28, 29.29, 29.40 (cis), 29.74, 29.83 (cis), 30.56, 32.58, 32.66, 42.04, 129.89 (cis alkene), 130.35 (trans alkene). Elemental analysis calculated for the repeat unit ($C_{17}H_{32}$): 86.35 C, 13.65 H; found: 86.27 C, 13.82 H. GPC data: M_n = 48,400; PDI (M_w/M_n) = 1.8.

Synthesis of 39c. Synthesized as above, with the following exceptions: a monomer to catalyst ratio of 480:1 was used and the reaction time was 5 days. The following spectral properties were observed: ^{1}H NMR ($CDCl_3$): δ 0.81 (s, 6H), 1.14-1.32 (m, 32H), 1.95-2.04 (m, 4H), 5.32-5.45 (m, 2H); ^{13}C NMR ($CDCl_3$): δ 24.04, 27.22 (cis), 27.30, 29.21, 29.34 (cis), 29.57, 29.60 (cis), 29.68, 29.71, 29.76, 29.79 (cis), 30.71, 32.58. 32.63, 42.04, 129.89 (cis alkene), 130.35 (trans alkene). Elemental analysis calculated for the repeat unit ($C_{23}H_{44}$): 86.16 C, 13.84 H; found: 85.68 C, 13.97 H. GPC data: M_n = 70,800; PDI (M_w/M_n) = 1.6.

5.4.1.2 Synthesis of the saturated gem-dimethyl substituted polymers (36a-c)

Synthesis of 36a. A solution of 0.537g of the unsaturated polymer 39a in 35 mL of toluene was added to a 250 mL high-pressure flask equipped with a stir bar and a gas valve with a pressure gauge. A 265mg sample of 10% palladium on activated carbon was added. The hydrogenation vessel was charged with 85 psi of hydrogen, and the mixture was stirred vigorously at room temperature for 48 hours. After 48 hours, the temperature was increased to 43 °C and the pressure was increased to 100 psi, and the mixture was stirred for 4 more days. The reaction mixture was run through a short column of silica gel 60, using toluene as the solvent. After concentrating the polymer solution to 30 ml, it was precipitated in ice-cold methanol, with vigorous stirring. A tacky, rubbery, white solid was obtained upon vacuum filtration. The polymer was dried under vacuum at 70 °C for 24 hours. An NMR analysis indicated 10% residual olefin.

In a second hydrogenation attempt, the above procedure was repeated with the partially reduced (10% olefin) product from the first attempt. An NMR analysis indicated 3% residual olefin. In the third hydrogenation attempt, 220mg of the partially reduced (3%) product from the second attempt was dissolve in 20 mL of toluene and placed in a Parr Instruments high-pressure stainless steel reactor. A 200mg sample of 10% palladium on activated carbon and a magnetic stir bar were added. The reactor was charged with 200 psi of hydrogen and heated to 75 °C for 6 days. The polymer 36a was precipitated as above and dried by heating to 60 °C under vacuum for 5 days. No residual olefin was detected by NMR and IR spectroscopy.

The following spectral properties were observed: ^{1}H NMR ($CDCl_3$): δ 0.81 (s, 6H) and 1.15-1.26 (m, 16H); ^{13}C NMR ($CDCl_3$): δ 24.51, 27.78, 30.29, 31.20, 33.04, and

42.49. Elemental analysis calculated for the repeat unit $(C_{11}H_{22})_n$: 85.62 C, 14.38 H; found: 85.65 C, 14.39 H. GPC data: M_n = 55,700; PDI (M_w/M_n) = 2.0.

Synthesis of 36b. A solution of 430mg of the unsaturated polymer 39b in 125 mL of toluene was added to a Parr Instruments high-pressure stainless steel reactor with a stir bar. A 60mg sample of Wilkinson's catalyst ($Rh(PPh_3)_3Cl$) was added, the reactor was purged with hydrogen, and then charged to 900 psi with hydrogen and heated to 90 °C. After 3 days the reactor was allowed to cool, the pressure was released, and the sides of the reactor's glass insert were rinsed with toluene. The reactor was then recharged to 900 psi, heated to 90 °C, and the reaction was continued for 2 more days. The crude product 36b was columned 2 times through silica gel 60 with toluene as the solvent, precipitated in cold methanol, columned 3 more times, and precipitated in cold methanol again. After drying at 60 °C for 5 days, the product was a faint brownish, rubbery, slightly tacky, material. No residual olefin was detected by NMR and IR spectroscopy.

The following spectral properties were observed: ^1H NMR ($CDCl_3$): δ 0.81 (s, 6H) and 1.15-1.26 (m, 28H); ^{13}C NMR ($CDCl_3$): δ 24.04, 27.32, 29.75, 29.77, 29.79, 30.72, 32.58, and 42.02. Elemental analysis calculated for the repeat unit $(C_{17}H_{34})$: 85.62 C, 14.38 H; found: 84.30 C, 14.37 H. GPC data: M_n = 48,700; PDI (M_w/M_n) = 1.8.

Synthesis of 36c. Synthesized as above for 36b, with the following exceptions: a 573mg sample of 39c and 40mg of Wilkinson's catalyst ($Rh(PPh_3)_3Cl$) were used. The crude product 36c was columned once through silica gel 60 with toluene as the solvent and then precipitated in cold methanol. After drying at 60 °C under vacuum for 6 days, the product was a faint brownish, translucent, hard, rubbery material. No residual olefin was detected by NMR and IR spectroscopy.

The following spectral properties were observed: ^{1}H NMR ($CDCl_3$): δ 0.81 (s, 6H) and 1.15-1.26 (m, 40H); ^{13}C NMR ($CDCl_3$): δ 24.04, 27.32, 29.74 (broad peak), 30.72, 32.58, and 42.02. Elemental analysis calculated for the repeat unit ($C_{23}H_{46}$): 85.62 C, 14.38 H; found: 85.48 C, 14.50 H. GPC data: M_n = 76,400; PDI (M_w/M_n) = 1.5.

5.4.2 Synthesis of the EMMA Model Copolymer (37)

5.4.2.1 Synthesis of the unsaturated ester-functionalized polymer (40)

Synthesis of 40. In an argon atmosphere dry box, 570mg (1.45 mmol) of the dry, degassed monomer 24c was placed in a 50 mL round bottom flask equipped with a Teflon™ magnetic stir bar. A 6.1mg sample (0.0074 mmol, 200:1 monomer to catalyst ratio) of Grubbs' ruthenium benzylidene catalyst (2) was added, and an adapter with a Teflon™ vacuum valve was attached to the flask. The mixture began to bubble slightly, so the reaction vessel was quickly removed from the glove box and attached to a vacuum line. The vessel was warmed in a 35 °C oil bath and intermittent vacuum (open valve for ~1 sec periodically) was applied until the mixture became viscous enough to leave open to vacuum (<10^{-2} mmHg) after about 1 hour. The mixture became more viscous and turned from purple to reddish-orange after 1 day. On the second day the temperature was increased to 45 °C and on the sixth day it was increased to 60 °C. The reaction was removed from the vacuum line on the seventh day. Very faint traces of terminal olefin were detected by NMR and IR spectroscopy.

The following spectral properties were observed: ^{1}H NMR ($CDCl_3$): δ 1.10 (s, 3H), 1.24-1.41 (m, 30H), 1.59 (dt, 2H), 1.96 (t, 4H), 3.64 (s, 3H), and 5.29-5.44 (m, 2H); ^{13}C NMR ($CDCl_3$): δ 21.14, 24.56, 27.21 (cis), 29.18, 29.32 (cis), 29.50 (broad peak), 29.54 (cis), 29.58, 29.66, 29.77 (cis), 30.14, 32.61, 39.52, 45.97, 51.42, 129.86 (cis alkene),

130.32 (trans alkene), and 178.18. Elemental analysis calculated for the repeat unit ($C_{24}H_{44}O_2$): 79.05 C, 12.17 H; found: 78.71 C, 12.22 H. GPC data: M_n = 26,100; PDI (M_w/M_n) = 1.9.

5.4.2.2 Synthesis of the saturated ester-functionalized polymer (37)

Synthesis of 37. Synthesized as above for 36b, with the following exceptions: a 513mg sample of unsaturated polymer (40), 50mg of Wilkinson's catalyst ($Rh(PPh_3)_3Cl$), and a toluene-ethyl acetate (75:25) solvent mixture were used. The crude product 37 was columned once through silica gel 60 with toluene-ethyl acetate (75:25) as the solvent system, precipitated in cold methanol, and then columned again. After concentrating the product on a rotory evaporator, it was dried at 60 °C under vacuum for 5 days. The product (37) was a clear, colorless, tacky, viscous, liquid material. No residual olefin was detected by NMR and IR spectroscopy.

The following spectral properties were observed: ^{1}H NMR ($CDCl_3$): δ 1.10 (s, 3H), 1.24-1.31 (m, 36H), 1.37 (dt, 2H), 1.59 (dt, 2H), 3.64 (s, 3H); ^{13}C NMR ($CDCl_3$): δ 21.14, 24.55, 29.51, 29.61, 29.66, 29.68, 29.71 (broad peak), 30.13, 39.48, 45.97, 51.40, and 178.18. Elemental analysis calculated for the repeat unit ($C_{24}H_{46}O_2$): 78.61 C, 12.65 H; found: 78.53 C, 12.77 H. GPC data: M_n = 27,200; PDI (M_w/M_n) = 2.0.

5.4.3 Synthesis of the EMAA Model Copolymer (38)

5.4.3.1 Synthesis of the unsaturated carboxylic acid-functionalized polymer (41)

Synthesis of 41. A 408mg (1.08 mmol) sample of monomer 23c was placed in a nitrogen-purged, flame dried 50 mL 3-neck round bottom flask equipped with a Teflon™ magnetic stir bar and a valve adapter. The monomer (23c) was dried under vacuum, with stirring, at 55 °C for 18 hours. A 2.0mg sample (0.0024 mmol, 440:1 monomer to

catalyst ratio) of Grubbs' ruthenium benzylidene catalyst (2) was added under a nitrogen purge. The catalyst did not completely dissolve immediately. The vessel was warmed in a 55 °C oil bath and intermittent vacuum (open valve for ~1 sec periodically) was applied until the mixture became viscous enough to leave open to vacuum ($<10^{-2}$ mmHg) after about 1 hour. The catalyst dissolved completely within 30 minutes. The mixture became more viscous and turned from pink to orange after 1 day. On the second day the temperature was increased to 60 °C and 2.0mg of catalyst 2 was added. On the fourth day the temperature was increased to 65 °C and 1.0mg of catalyst 2 was added. On the sixth day 1.0mg of catalyst 2 was added (for a total monomer to catalyst ratio of 150:1), and the mixture bubbled only slightly. The reaction was removed from the vacuum line on the seventh day. No terminal olefin was detected by NMR and IR spectroscopy.

The following spectral properties were observed: ^{1}H NMR ($CDCl_3$): δ 1.12 (s, 3H), 1.24-1.45 (m, 30H), 1.59-1.64 (m, 2H), 1.96-2.07 (m, 4H), 5.24-5.45 (m, 2H), and 11.68 (s, broad, 1H). Elemental analysis calculated for the repeat unit ($C_{23}H_{42}O_2$): 78.79 C, 12.08 H; found: 78.49 C, 12.17 H. GPC data: M_n = 4100; PDI (M_w/M_n) = 1.7 (Note: the high molecular weight fraction was likely filtered from the GPC sample, see discussion in Section 3.4.2).

5.4.3.2 Synthesis of the saturated carboxylic acid-functionalized polymer (38)

Synthesis of 38. Synthesized as above for 36b, with the following exceptions: a 302mg sample of unsaturated polymer (41), 20mg of Wilkinson's catalyst ($Rh(PPh_3)_3Cl$), and a toluene-ethyl acetate (75:25) solvent mixture were used. The crude product (38) precipitated from the reaction mixture as a black residue. The polymer (38) was insoluble in chloroform, toluene, ethyl acetate, methanol, ethanol, THF, and DMSO. Most of the

polymer dissolved in a refluxing mixture of *p*-xylene and 1-butanol (75:25 v/v), but some black particles remained insoluble. The remaining material eventually dissolved when a about 0.3g of sodium hydroxide was added to the mixture. A grayish precipitate formed after the solution was slowly added to acidic methanol (1 M of HCl) and stirred for about 1 hour. The product (38) became a translucent, slightly black, tacky, viscous material after drying at 70 °C under vacuum for 5 days. No residual olefin was detected by ^{1}H NMR and IR spectroscopy.

The following spectral properties were observed: ^{1}H NMR ($CDCl_3$): δ 1.12 (s, 3H), 1.19-1.37 (m, 36H), 1.42 (t, 2H), 1.62 (t, 2H), 11.62 (s, broad, 1H). GPC data: M_n = 4100; PDI (M_w/M_n) = 1.8 (Note: the high molecular weight fraction was likely filtered from the GPC sample, see discussion in Section 3.4.2).

5.5 Synthesis of Telechelic Hydrocarbon Diols

5.5.1 Synthesis of the Monofunctional Reactants (43b and 46)

5.5.1.1 Synthesis of monofunctional reactant 43b

Synthesis of 1,8-bisacetoxy-4-octene (43b). In an argon atmosphere dry box, 108 mg (0.131 mmol) of Grubbs' ruthenium benzylidene catalyst (2) was added to a 3-neck 100 mL round bottom flask equipped with one dry ice/isopropanol-cooled condenser and one water-cooled condenser, each with a hose connector with a valve, and a magnetic stir bar. The apparatus was removed from the dry box and attached to a Schlenk line through the dry ice/isopropanol-cooled condenser. The flask was opened to argon after purging the hose. An oil bubbler was attached to the water-cooled condenser. A 21.66g (0.1690 mol) sample of acetic acid 4-pentenyl ester was added to the flask by syringe, and the flask was placed in a 47 °C oil bath. A small amount of bubbling was observed in the

purple solution. The valve connected to the oil bubbler was opened to allow argon and ethylene byproduct to flow out continuously. After 30 minutes, the dry ice/isopropanol bath was filled, the bubbler valve was closed, and the pressure was reduced to 70 mmHg. The solution bubbled vigorously as it degassed, and then slowed to a moderate rate. After 90 minutes at reduced pressure the bubbling had ceased and the solution was a purplish-brown. The reaction vessel was opened to air and left stirring overnight at 48 °C. The crude product was 95% dimer by GC (65% was 1,8-Bisacetoxy-4-octene and 30% was 1,8-Bisacetoxy-3-octene), and was now a black solution. The product was distilled over CaH_2 at 0.3 mmHg (bp 111-113 °C) and stored in a Schlenk flask. The isolated yield was 63%. The ^1H and ^{13}C NMR spectra and GC analysis indicate that 13% of the isolated product is the constitutional isomer 1,8-bisacetoxy-3-octene (cis and trans).

The following spectral properties were observed: ^1H NMR ($CDCl_3$): δ 1.39-1.47 (m, 0.5H, isomer), 1.60-1.76 (m, 4H), 1.98-2.14 (m, 9H), 2.26-2.41 (m, 0.5H, isomer), 4.06 (dt, 4H), 5.34-5.55 (m, 2H); ^{13}C NMR ($CDCl_3$): δ 20.96, 23.48 (cis), 28.30 (trans), 28.41 (cis), 28.76 (trans), 63.87 (cis/trans), 129.29 (cis alkene), 129.79 (trans alkene), and small constitutional isomer peaks at: δ 25.56, 25.79, 26.78, 27.96, 28.17, 31.88, 32.08, 63.98, 64.35, 124.85 (cis alkene 1), 125.70 (trans alkene 1), 132.02 (cis alkene 2), and 132.66 (trans alkene 2); EI/HRMS: $[M]^+$ calcd. for $C_{12}H_{20}O_4$: 228.1362, found: 228.1330. Elemental analysis calcd. for $C_{12}H_{20}O_4$: 63.12 C, 8.84 H; found: 62.76 C, 8.88 H.

5.5.1.2 Synthesis of monofunctional reactant 46

Synthesis of benzyl 1-undec-10-enyl ether (46). A 4.7g sample of sodium hydride (60% dispersion in mineral oil) was added to a flame dried, argon filled 3-neck 250 mL round bottom flask equipped with a condenser, addition funnel, and stir bar. About 60

mL of dry THF was added and the mixture was stirred for 10 minutes. A 11.8 mL sample of ω-undecylenyl alcohol (from Aldrich) was placed in the addition funnel with about 8 mL of THF, and it was slowly added to the reaction flask. The mixture bubbled slightly as the alcohol was added. After 1.5 hours, 14 mL of benzyl bromide (from Aldrich) was placed in the addition funnel, and added slowly to the reaction flask. The mixture began to reflux gently after several minutes, and it was left stirring overnight. The reaction was quenched by slowly pouring the mixture over ice water with vigorous stirring. After 1 hour, the product was extracted with Et_2O and the organic layer was washed three times with 3 M HCl, dried over magnesium sulfate, and concentrated on a rotory evaporator. The product was distilled twice over CaH_2 at 0.08 mmHg (bp 127-130 °C) and stored in a Schlenk flask. The isolated yield was 41%.

The following spectral properties were observed: ^{1}H NMR ($CDCl_3$): δ 1.27-1.36 (m, 12H), 1.59 (p, 2H), 2.03 (q, 2H), 3.46 (t, 2H), 4.50 (s, 2H), 4.88-5.02 (m, 2H), 5.74-5.88 (m, 1H), and 7.24-7.35 (m, 5H); ^{13}C NMR ($CDCl_3$): δ 26.66, 29.40, 29.59, 29.91, 29.94, 30.01, 30.25, 34.29, 70.96, 73.30, 114.54, 127.88, 128.03, 128.74, 139.13, and 139.65; EI/HRMS: $[M]^+$ calcd. for $C_{18}H_{28}O$: 260.2140, found: 260.2142. Elemental analysis calcd. for $C_{18}H_{28}O$: 83.01 C, 10.84 H; found: 83.19 C, 10.99 H.

5.5.2 Synthesis of the Telechelic Diols (42a-c)

5.5.2.1 Synthesis of 42a by the ADMET polymerization-depolymerization method

Synthesis of the unsaturated telechelic diacetate (44a). In an argon atmosphere dry box, 29mg (0.17 mmol) of the dry, degassed MR 43a was placed in a 50 mL round bottom Schlenk flask equipped with a Teflon™ magnetic stir bar, followed by 4 mL of dry, degassed toluene. In a separate 50 mL Schlenk flask (the reaction vessel) equipped

with a stir bar, 211mg (1.168 mmol) of monomer 22a was added, followed by 3.0 mg (380:1 monomer to catalyst ratio) of the second-generation Grubbs' catalyst (3). The reaction vessel was removed from the dry box and immediately attached to a Schlenk line, where the side arm was flame dried under vacuum. The vessel was warmed in a 43 °C oil bath and intermittent vacuum (open valve for ~1 sec periodically) was applied until the mixture became viscous enough to leave open to vacuum ($<10^{-2}$ mmHg) after about 6.5 hours. The mixture had turned from pink to orangish-brown. After another 15 hours, the mixture was very viscous and difficult to stir, and the temperature was increased to 60 °C (still an occasional bubble). After another 22 hours, no bubbles were observed, so the reaction vessel was sealed and taken into the dry box where the MR (43a) in toluene solution was added to the reaction vessel. The reaction vessel was removed from the dry box and attached to a Schlenk line. The side arm was flame dried under vacuum and backfilled three times with argon. The reaction vessel was opened to the argon line and placed in a 60 °C oil bath. The polymer dissolved in the toluene solution and stirred easily. The yellow solution gradually turned light brown over 72 hours, at which time the solvent was removed by heating under vacuum. No terminal olefin was detected by NMR spectroscopy.

The following spectral properties were observed: ^{1}H NMR ($CDCl_3$): δ 0.83 (s), 1.17-1.27 (m), 1.93-2.02 (m), 2.09 (s), 4.51 (d, end-group), 5.26-5.47 (m), 5.52-5.64 (m, end-group), 5.73-5.87 (m, end-group). The ^{1}H NMR spectrum also shows resonances due to residual MR (actually $H_2C{=}CCH_2OAc$) at δ 2.07, 4.59, 4.57, and 5.86. The ^{13}C NMR has many peaks due to an olefin isomerization side-reaction, so they will not be listed. ^{1}H NMR determined M_n = 1800. GPC data: M_n = 1900; PDI (M_w/M_n) = 1.6

Synthesis of the saturated telechelic diacetate (45a). A 153 mg sample of 44a was dissolved in 150 mL of toluene, and placed a Parr Instruments high-pressure reactor. A 107 mg sample of 10% palladium on activated carbon was added, the reactor was charged with 400 psi of hydrogen, and the mixture was stirred at 80 °C. After five days the mixture was allowed to cool to room temperature and the pressure was released. The reaction mixture was filtered through a short pad of silica gel using a mixture of toluene and ethyl acetate as the mobile phase (75:25 v/v). The solvents were removed by heating the sample to 60 °C under vacuum. No residual olefin was detected by NMR spectroscopy.

The following spectral properties were observed: ^{1}H NMR ($CDCl_3$): δ 0.83 (s), 1.15-1.28 (m), 1.62 (t, end-group), 2.05 (s, end-group), and 4.05 (t, end-group). The ^{13}C NMR has many peaks due to an olefin isomerization side-reaction, so they will not be listed. ^{1}H NMR determined M_n = 2100.

Synthesis of the telechelic diol (42a). A 95mg sample of 45a was dissolved in 10 mL of Et_2O in a 50 mL round bottomed flask, equipped with a condenser and magnetic stir bar. The solution was chilled in an ice bath and 5 mL of an ice-chilled 0.7 M solution of sodium methoxide in methanol was added by syringe. After the mixture had been allowed to stir for 24 hours, the solvents were removed using a rotary evaporator. A yellowish residue and white salts remained. About 10 mL of diethyl ether was added, followed by 10 mL of slightly acidic water. The crude product dissolved upon stirring. The organic layer was colorless, while the aqueous layer was yellow. The mixture was poured into a separatory funnel, along with one washing with slightly acidic water and two with ether. The separatory funnel was shaken and the aqueous layer was drained. The

aqueous layer was basic to litmus paper. The organic layer was washed twice with slightly acidic water, and the combined aqueous layers were still basic to litmus paper. The organic layer was labeled 'organic layer 1' and set aside. The aqueous layer was then made slightly acidic to litmus paper by adding dilute HCl, upon which the aqueous solution turned from yellow to colorless. The aqueous layer was extracted three times with 5 mL of ether, and the combined organic layers were labeled 'organic layer 2'. Both organic layers were concentrated in a rotary evaporator in separate flasks. The first organic layer yielded a colorless residue, while the second yielded a very small amount of colorless residue and a small amount of yellowish salt. Some fractionation of the polymer (42a) was, thus, observed. No residual acetate end-groups were detected by NMR spectroscopy.

The following spectral properties were observed: ^{1}H NMR ($CDCl_3$): δ 0.82 (s), 1.15-1.30 (m), 1.57 (t, end-group), and 3.64 (t, end-group). The ^{13}C NMR has many peaks due to an olefin isomerization side-reaction, so they will not be listed. ^{1}H NMR determined $M_n = 2400$.

5.5.2.2 Synthesis of 42b by the ADMET polymerization-depolymerization method

Synthesis of the unsaturated telechelic diacetate (44b). Synthesized as above for 44a, with the following exceptions: 1.014g (5.62 mmol) of monomer 22a, 11.8mg (400:1 monomer to catalyst ratio) of catalyst 3, 156mg (0.683 mmol, or 8.23:1 monomer to MR ratio) of MR 43b, and 1 mL of toluene were used. The monomer was polymerized for 2 days, and the polymer was depolymerized for 3 days. No terminal olefin was detected by NMR and IR spectroscopy.

The following spectral properties were observed: ^{1}H NMR ($CDCl_3$): δ 0.82 (s), 1.14-1.35 (m), 1.63-1.72 (m, end-group), 1.90-1.99 (m), 2.05 (s, end-group), 4.06 (t, end-group), and 5.34-5.49 (m). The ^{13}C NMR has many peaks due to an olefin isomerization side-reaction, so they will not be listed. ^{1}H NMR determined M_n = 1550. GPC data: M_n = 2700; PDI (M_w/M_n) = 1.7

Synthesis of the saturated telechelic diacetate (45b). Synthesized as above for 45a, with the following exceptions: 795mg of unsaturated telechelic diacetate 44b, 340mg of 10% palladium on activated carbon, and 100 mL of toluene were used. No residual olefin was detected by NMR and IR spectroscopy.

The following spectral properties were observed: ^{1}H NMR ($CDCl_3$): δ 0.81 (s), 1.15-1.30 (m), 1.62 (p, end-group), 2.05 (s, end-group), and 4.05 (t, end-group). The ^{13}C NMR has many peaks due to an olefin isomerization side-reaction, so they will not be listed. ^{1}H NMR determined M_n = 1600. GPC data: M_n = 2900; PDI (M_w/M_n) = 1.7

Synthesis of the telechelic diol (42b). Synthesized as above for 42a, with the following exceptions: 555mg of saturated telechelic diacetate 45b, 378mg of sodium methoxide in 10 mL of methanol (~0.7 M solution), and 25 mL of Et_2O were used. Also, the workup was modified as follows: it was calculated that 7 mL of 1.0 M HCl would neutralized the base in the mixture, so it was important for the yield not to exceed this amount (acid appears to make the product more soluble in water). The product was dissolved in 30 mL of Et_2O, 20 mL of distilled water and 5.5 mL of 1 M HCl, and placed in a separatory funnel. The aqueous layer was drained, extracted twice with 10 mL of Et_2O, and the extracts were combined with the first Et_2O layer. The combined Et_2O layers were washed twice with 1 mL of 1 M HCl in 15 mL of water, and twice with 15 mL of

water. The Et_2O layer was dried over magnesium sulfate, filtered, and concentrated in a rotory evaporator. The clear, colorless residue was dried at 50 °C under vacuum. No residual acetate end-groups were detected by NMR and IR spectroscopy.

The following spectral properties were observed: ^1H NMR ($CDCl_3$): δ 0.81 (s), 1.15-1.37 (m), 1.57 (p, end-group), and 3.64 (t, end-group). The ^{13}C NMR has many peaks due to an olefin isomerization side-reaction, so they will not be listed. ^1H NMR determined M_n = 1490. GPC data: M_n = 2600; PDI (M_w/M_n) = 1.8.

5.5.2.3 Synthesis of 44b by the direct ADMET polymerization method

Synthesis of the unsaturated telechelic diacetate (44b). In an argon atmosphere dry box, 670mg (3.72 mmol) of monomer 22a, 122mg of MR 43b (0.534 mmol, or 6.95:1 monomer to MR ratio), and 6.7mg of catalyst 3 (470:1 monomer to catalyst ratio) were placed in a 50 mL Schlenk flask equipped with a Teflon™ magnetic stir bar. The reaction vessel was quickly removed from the dry box and attached to a vacuum line. The vessel was warmed in a 43 °C oil bath and intermittent vacuum (open valve for ~1 sec periodically) was applied until the mixture became viscous enough to leave open to vacuum ($<10^{-2}$ mmHg) after about 10 hours. The mixture gradually became more viscous and turned from light pink to orange. On the third day the temperature was increased to 64 °C, and the reaction was removed from the Schlenk line on the fourth day. No terminal olefin was detected by NMR spectroscopy.

The following spectral properties were observed: ^1H NMR ($CDCl_3$): δ 0.82 (s), 1.14-1.35 (m), 1.63-1.72 (m, end-group), 1.90-1.99 (m), 2.05 (s, end-group), 4.06 (t, end-group), and 5.34-5.49 (m). The ^{13}C NMR has many peaks due to an olefin isomerization

side-reaction, so they will not be listed. ^{1}H NMR determined M_n = 10,400. GPC data: M_n = 11,200; PDI (M_w/M_n) = 1.9.

5.5.2.4 Synthesis of 47 by the direct ADMET polymerization method

Synthesis of the unsaturated telechelic di(benzyl ether) (47) with catalyst 3. Synthesized as above for 44b (direct method), with the following exceptions: 379mg (2.10 mmol) of monomer 22a, 5.0mg of catalyst 3 (360:1 monomer to catalyst ratio), 161mg of MR 46 (0.618 mmol, or 3.4:1 monomer to MR ratio) were used. The reaction was allowed to proceed for 4 days. No terminal olefin was detected by NMR spectroscopy.

The following spectral properties were observed: ^{1}H NMR ($CDCl_3$): δ 0.82 (s), 1.13-1.41 (m), 1.61 (p, end-group), 1.85-2.03 (m), 3.46 (t, end-group), 4.50 (s, end-group), 5.34-5.45 (m), and 7.26-7.34 (m, end-group). The ^{13}C NMR has many peaks due to an olefin isomerization side-reaction, so they will not be listed. ^{1}H NMR determined M_n = 1220.

Synthesis of the telechelic diol (42c) (catalyst 3 trial). Synthesized as above for 45a, with the following exceptions: 0.48g of unsaturated telechelic di(benzyl ether) 47 (made with catalyst 3), 0.20g of 10% palladium on activated carbon, and 100 mL of toluene were used. The reaction was allowed to proceed for 6 days, and the columned product was dried at 70 °C under vacuum for 5 days. No residual olefin or benzyl ether end-groups were detected by NMR spectroscopy.

The following spectral properties were observed: ^{1}H NMR ($CDCl_3$): δ 0.81 (s), 1.13-1.34 (m), 1.57 (p, end-group), and 3.64 (t, end-group). The ^{13}C NMR has many

peaks due to an olefin isomerization side-reaction, so they will not be listed. ^{1}H NMR determined M_n = 1050. GPC data: M_n = 2000; PDI (M_w/M_n) = 1.6.

Synthesis of the unsaturated telechelic di(benzyl ether) (47) with catalyst 2. Synthesized as above for 44b (direct method), with the following exceptions: 105mg (0.582 mmol) of monomer 22a, 2.4mg of catalyst 2 (250:1 monomer to catalyst ratio), 39mg of MR 46 (0.149 mmol, or 3.9:1 monomer to MR ratio) were used. The reaction was left at room temperature for the first day, 45 °C for the second day, and 50 °C for the last 2 days. No terminal olefin was detected by NMR and IR spectroscopy.

The following spectral properties were observed: ^{1}H NMR ($CDCl_3$): δ 0.82 (s), 1.13-1.41 (m), 1.61 (p, end-group), 1.85-2.03 (m), 3.46 (t, end-group), 4.50 (s, end-group), 5.34-5.45 (m), and 7.26-7.34 (m, end-group); ^{13}C NMR ($CDCl_3$): δ 24.17, 26.19, 27.30, 28.09, 29.18, 29.49, 29.77, 32.58, 33.52, 41.54, 70.51, 72.83, 127.41, 127.58, 128.30, 129.98, 130.43, and 138.67. ^{1}H NMR determined M_n = 1650. GPC data: M_n = 2500; PDI (M_w/M_n) = 1.7.

Synthesis of the telechelic diol (42c) (catalyst 2 trial). Synthesized as above for 45a, with the following exceptions: 140mg of unsaturated telechelic di(benzyl ether) 47 (made with catalyst 2), 60mg of 10% palladium on activated carbon, and 50 mL of toluene were used. The reaction was allowed to proceed for 3 days, and the columned product was dried at 70 °C under vacuum for 5 days. No residual olefin or benzyl ether end-groups were detected by NMR and IR spectroscopy.

The following spectral properties were observed: ^{1}H NMR ($CDCl_3$): δ 0.81 (s), 1.13-1.34 (m), 1.57 (p, end-group), and 3.64 (t, end-group); ^{13}C NMR ($CDCl_3$): δ 24.03, 25.74, 27.30, 29.44, 29.60, 29.62, 29.67, 29.69, 29.71, 29.74, 29.76, 29.80, 30.72, 32.58,

32.82, 42.03, and 63.11. ^{1}H NMR determined M_n = 1840. GPC data: M_n = 2700; PDI (M_w/M_n) = 1.7.

APPENDIX A
ADDITIONAL ^{1}H AND ^{13}C NMR SPECTRA

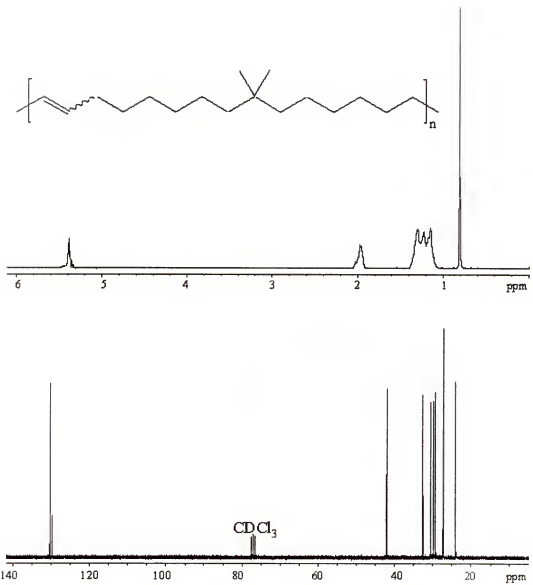

A1: ^{1}H (top) and ^{13}C (bottom) NMR spectra for the unsaturated polymer (**39b**).

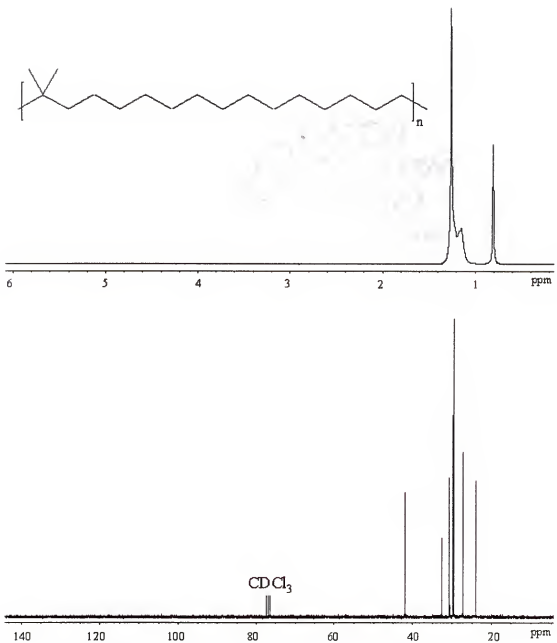

A2: ^{1}H (top) and ^{13}C (bottom) NMR spectra for the EIB model copolymer (**36b**).

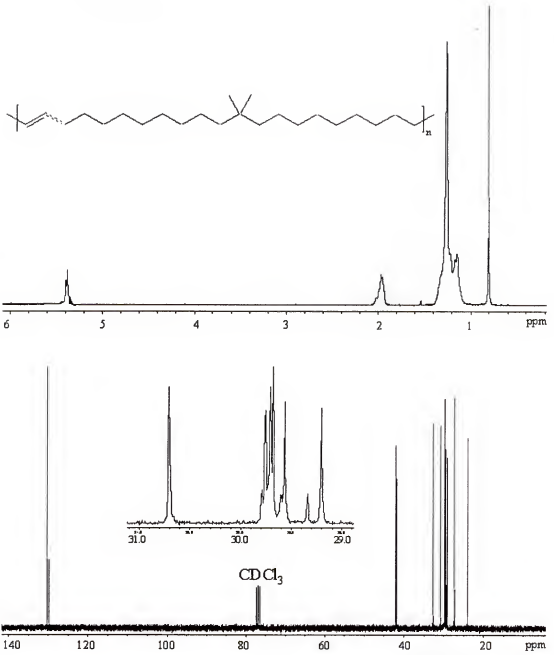

A3: ^{1}H (top) and ^{13}C (bottom) NMR spectra for the unsaturated polymer (**39c**).

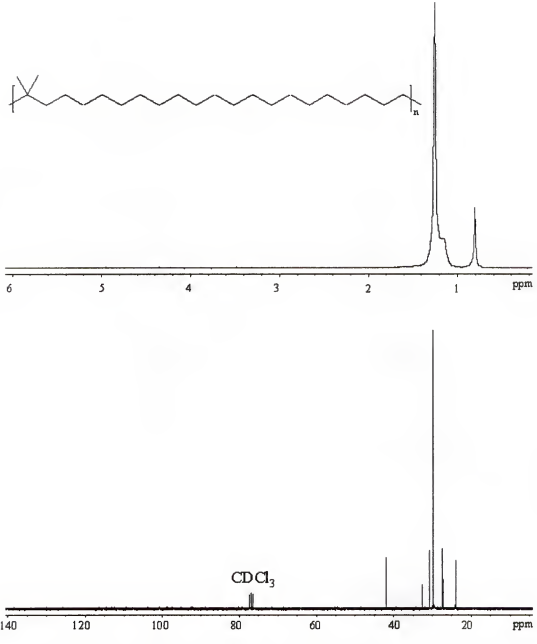

A4: ^{1}H (top) and ^{13}C (bottom) NMR spectra for the EIB model copolymer (**36c**).

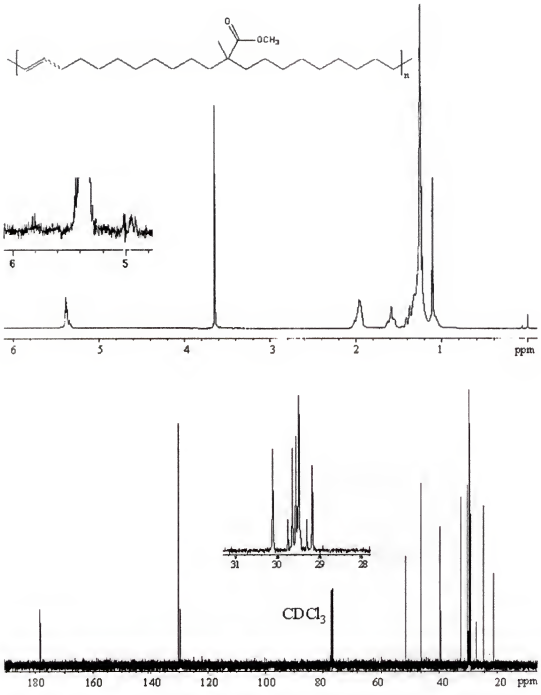

A5: ^{1}H (top) and ^{13}C (bottom) NMR spectra for the unsaturated polymer (**40**).

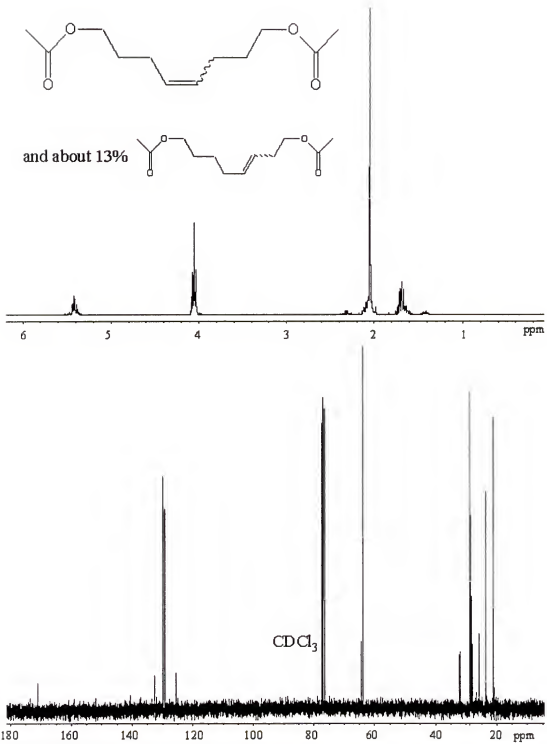

A6: ^{1}H (top) and ^{13}C (bottom) NMR spectra for MR **43b**.

APPENDIX B
ADDITIONAL IR SPECTRA

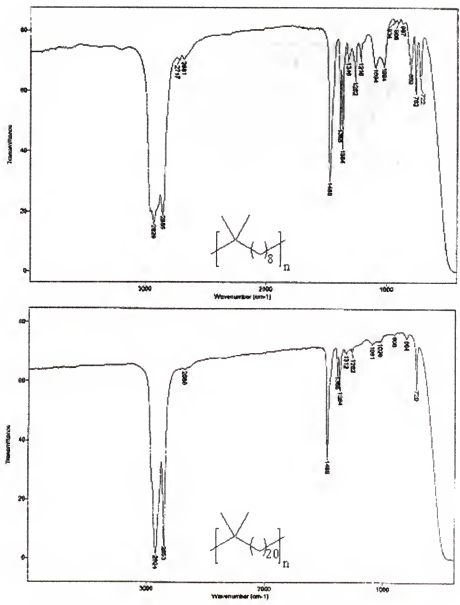

B1: IR Spectra for the EIB model copolymers **36a** (top) and **36c** (bottom).

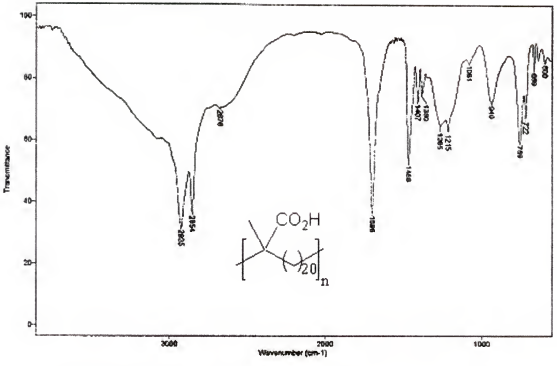

B2: IR Spectrum for the EMAA model copolymer (**38**).

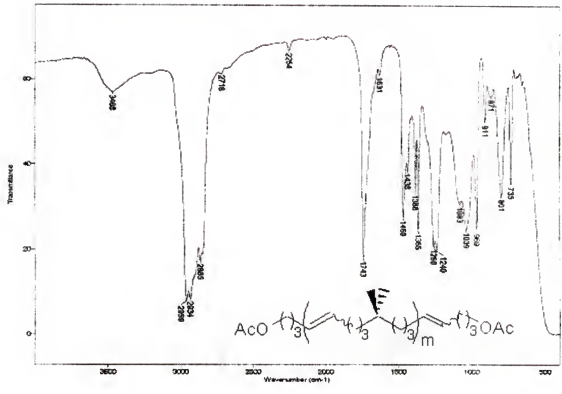

B3: IR Spectra for the unsaturated telechelic diacetate **44b** made using the polymerization-depolymerization method.

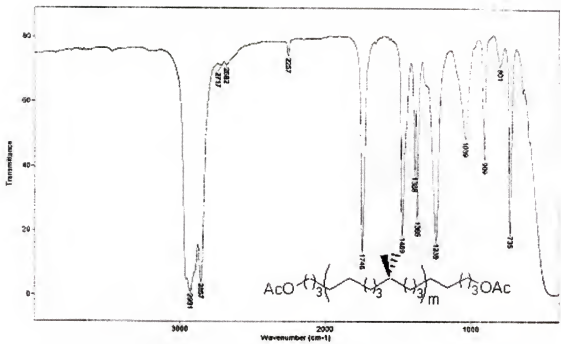

B4: IR spectrum for the saturated telechelic diacetate **45b**.

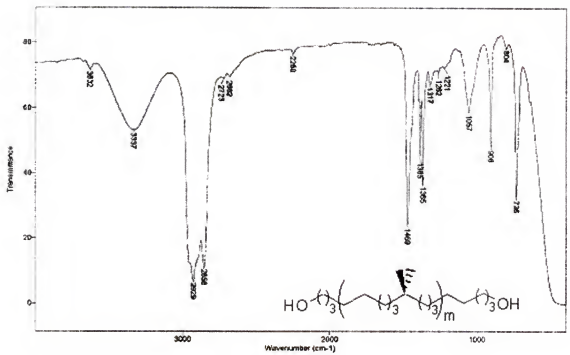

B5: IR spectrum for the telechelic diol **42b**.

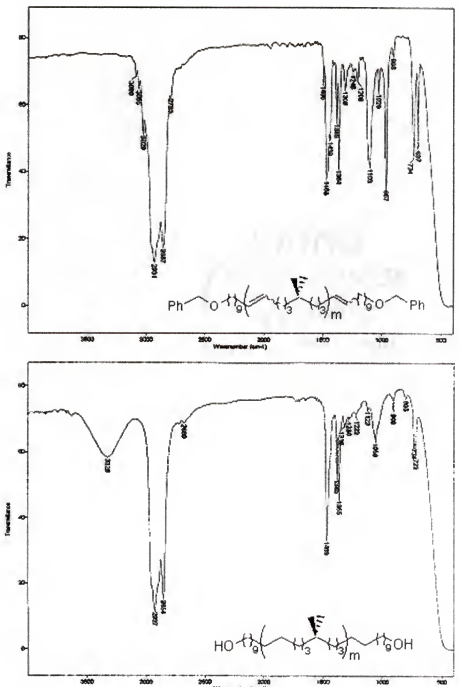

B6: IR spectra for the unsaturated telechelic di(benzyl ether) **47** (top) and the telechelic diol **42c** made using catalyst **2**.

LIST OF REFERENCES

(1) Calderon, N.; Ofstead, E. A.; Judy, W. A. *Journal of Polymer Science Part a-1-Polymer Chemistry* **1967**, *5*, 2209.

(2) Calderon, N.; Chen, H. Y.; Scott, K. W. *Tetrahedron Letters* **1967**, 3327.

(3) Ivin, K. J.; Mol, J. C. In *Olefin Metathesis and Metathesis Polymerization*; Academic Press: San Diego, 1997.

(4) Calderon, N.; Ofstead, E. A.; Ward, J. P.; Judy, W. A.; Scott, K. W. *Journal of the American Chemical Society* **1968**, *90*, 4133.

(5) Calderon, N. *Accounts of Chemical Research* **1972**, *5*, 127.

(6) Calderon, N.; Ofstead, E. A.; Judy, W. A. *Angewandte Chemie-International Edition in English* **1976**, *15*, 401-409.

(7) Eleuterio, H. S. In *US Patent*, 1963.

(8) Crabtree, R. H. In *The Organometallic Chemistry of the Transition Metals*; 3rd ed.; Wiley and Sons: New York, 2001.

(9) Eleuterio, H. S. *Journal of Molecular Catalysis* **1991**, *65*, 55-61.

(10) Eleuterio, H. *Chemtech* **1991**, *21*, 92-95.

(11) Banks, R. L. *Chemtech* **1986**, *16*, 112-117.

(12) Dallasta, G. *Makromolekulare Chemie* **1972**, *154*, 1.

(13) Natta, G.; Dallasta, G.; Donegani, G.; Mazzanti, G. *Angewandte Chemie-International Edition* **1964**, *3*, 723.

(14) Herisson, J. L.; Chauvin, Y. *Makromolekulare Chemie* **1971**, *141*, 161.

(15) Schrock, R. R. *Science* **1983**, *219*, 13-18.

(16) Schrock, R. R.; Depue, R. T.; Feldman, J.; Schaverien, C. J.; Dewan, J. C.; Liu, A. H. *Journal of the American Chemical Society* **1988**, *110*, 1423-1435.

(17) Schrock, R. R.; Depue, R. T.; Feldman, J.; Yap, K. B.; Yang, D. C.; Davis, W. M.; Park, L.; Dimare, M.; Schofield, M.; Anhaus, J.; Walborsky, E.; Evitt, E.; Kruger, C.; Betz, P. *Organometallics* **1990**, *9*, 2262-2275.

(18) Schrock, R. R.; Murdzek, J. S.; Bazan, G. C.; Robbins, J.; Dimare, M.; Oregan, M. *Journal of the American Chemical Society* **1990**, *112*, 3875-3886.

(19) Sharp, P. R.; Holmes, S. J.; Schrock, R. R.; Churchill, M. R.; Wasserman, H. J. *Journal of the American Chemical Society* **1981**, *103*, 965-966.

(20) Feldman, J.; Schrock, R. R. *Progress in Inorganic Chemistry* **1991**, *39*, 1-74.

(21) Lindmarkhamberg, M.; Wagener, K. B. *Macromolecules* **1987**, *20*, 2949-2951.

(22) Wagener, K. B.; Nel, J. G.; Konzelman, J.; Boncella, J. M. *Macromolecules* **1990**, *23*, 5155-5157.

(23) Marsella, M. J.; Maynard, H. D.; Grubbs, R. H. *Angewandte Chemie-International Edition in English* **1997**, *36*, 1101-1103.

(24) Dias, E. L.; Nguyen, S. T.; Grubbs, R. H. *Journal of the American Chemical Society* **1997**, *119*, 3887-3897.

(25) Dias, E. L.; Grubbs, R. H. *Organometallics* **1998**, *17*, 2758-2767.

(26) Schwab, P.; France, M. B.; Ziller, J. W.; Grubbs, R. H. *Angewandte Chemie-International Edition in English* **1995**, *34*, 2039-2041.

(27) Schwab, P., Grubbs, R.H. and Ziller, J.W. *Journal of the American Chemical Society* **1996**, *118*, 100-110.

(28) Trnka, T. M.; Grubbs, R. H. *Accounts of Chemical Research* **2001**, *34*, 18-29.

(29) Nguyen, S. T.; Grubbs, R. H.; Ziller, J. W. *Journal of the American Chemical Society* **1993**, *115*, 9858-9859.

(30) Rinehart, R. E.; Smith, H. P. *Journal of Polymer Science Part B-Polymer Letters* **1965**, *3*, 1049.

(31) Michelot, F. W.; Keaveney, W. P. *Journal of Polymer Science Part a-General Papers* **1965**, *3*, 895.

(32) Weskamp, T.; Schattenmann, W. C.; Spiegler, M.; Herrmann, W. A. *Angewandte Chemie-International Edition* **1998**, *37*, 2490-2493.

(33) Weskamp, T.; Kohl, F. J.; Hieringer, W.; Gleich, D.; Herrmann, W. A. *Angewandte Chemie-International Edition* **1999**, *38*, 2416-2419.

(34) Herrmann, W. A.; Kocher, C. *Angewandte Chemie-International Edition in English* **1997**, *36*, 2163-2187.

(35) Huang, J. K.; Stevens, E. D.; Nolan, S. P.; Petersen, J. L. *Journal of the American Chemical Society* **1999**, *121*, 2674-2678.

(36) Scholl, M.; Ding, S.; Lee, C. W.; Grubbs, R. H. *Organic Letters* **1999**, *1*, 953-956.

(37) Scholl, M.; Trnka, T. M.; Morgan, J. P.; Grubbs, R. H. *Tetrahedron Letters* **1999**, *40*, 2247-2250.

(38) Sanford, M. S.; Henling, L. M.; Day, M. W.; Grubbs, R. H. *Angewandte Chemie-International Edition* **2000**, *39*, 3451.

(39) Bielawski, C. W.; Grubbs, R. H. *Angewandte Chemie-International Edition* **2000**, *39*, 2903-2906.

(40) Chatterjee, A. K.; Grubbs, R. H. *Organic Letters* **1999**, *1*, 1751-1753.

(41) Wagener, K. B.; Boncella, J. M.; Nel, J. G.; Duttweiler, R. P.; Hillmyer, M. A. *Makromolekulare Chemie-Macromolecular Chemistry and Physics* **1990**, *191*, 365-374.

(42) Wolfe, P. S.; Wagener, K. B. *Macromolecular Rapid Communications* **1998**, *19*, 305-308.

(43) Wolfe, P. S.; Wagener, K. B. *Macromolecules* **1999**, *32*, 7961-7967.

(44) Wagener, K. B.; Smith, D. W. *Macromolecules* **1991**, *24*, 6073-6078.

(45) Wagener, K. B.; Brzezinska, K. *Macromolecules* **1991**, *24*, 5273-5277.

(46) Wagener, K. B.; Boncella, J. M.; Nel, J. G. *Macromolecules* **1991**, *24*, 2649-2657.

(47) Wagener, K. B.; Patton, J. T. *Macromolecules* **1993**, *26*, 249-253.

(48) Wagener, K. B.; Brzezinska, K.; Anderson, J. D.; Younkin, T. R.; Steppe, K.; DeBoer, W. *Macromolecules* **1997**, *30*, 7363-7369.

(49) Tindall, D.; Pawlow, J. H.; Wagener, K. B. In *Topics in Organometallic Chemistry: Alkene Metathesis in Organic Synthesis*; Furstner, A., Ed.; Springer: Berlin, 1998.

(50) Schrock, R. R. In *Ring Opening Polymerization*; Bruneile, D. J., Ed.; Hanser: Munich, 1993.

(51) Portmess, J. D.; Wagener, K. B. *Journal of Polymer Science Part a-Polymer Chemistry* **1996**, *34*, 1353-1357.

(52) Davidson, T. A.; Wagener, K. B. In *Synthesis of Polymers*; Schluter, A. D., Ed.; Wiley: Weinheim, 1999.

(53) Grubbs, R. H.; Miller, S. J.; Fu, G. C. *Accounts of Chemical Research* **1995**, *28*, 446-452.

(54) Grubbs, R. H.; Chang, S. *Tetrahedron* **1998**, *54*, 4413-4450.

(55) Grubbs, R. H.; Khosravi, E. In *Synthesis of Polymers*; Schluter, A. D., Ed.; Wiley: Weinheim, 1999.

(56) Brzezinska, K. R.; Schitter, R.; Wagener, K. B. *Journal of Polymer Science Part a-Polymer Chemistry* **2000**, *38*, 1544-1550.

(57) Odian, G. In *Principles of Polymerization*; 3rd ed.; John Wiley and Sons: New York, 1991.

(58) Wagener, K. B.; Valenti, D.; Hahn, S. F. *Macromolecules* **1997**, *30*, 6688-6690.

(59) Cummings, S. K.; Smith, D. W.; Wagener, K. B. *Macromolecular Rapid Communications* **1995**, *16*, 347-355.

(60) Wagener, K. B.; Brzezinska, K.; Anderson, J. D.; Dilocker, S. *Journal of Polymer Science Part a-Polymer Chemistry* **1997**, *35*, 3441-3449.

(61) Lehman, S. E.; Wagener, K. B. *Macromolecules* **2002**, *35*, 48-53.

(62) Sanford, M. S.; Love, J. A.; Grubbs, R. H. *Journal of the American Chemical Society* **2001**, *123*, 6543-6554.

(63) Sanford, M. S.; Ulman, M.; Grubbs, R. H. *Journal of the American Chemical Society* **2001**, *123*, 749-750.

(64) Lehman, S. E.; Schwendeman, J. E.; O'Donell, P. M.; Wagener, K. B. *Inorganica Chimica Acta, accepted for publication* .

(65) Furniss, B. S.; Hannaford, A. J.; Smith, P. W. G.; Tatchell, A. R. In *Vogel's Textbook of Practical Organic Chemistry*; 5th ed.; Longman Group and Wiley and Sons: New York, 1989.

(66) Shriver, D. F.; Drezdon, M. A. In *The Manipulation of Air Sensitive Compounds*; 2nd ed.; Wiley and Sons: New York, 1986.

(67) Perrin, D. D.; Armarego, W. L. F. In *Purification of Laboratory Chemicals*; 3rd ed.; Pergamon Press: New York, 1988.

(68) Maynard, H. D.; Grubbs, R. H. *Tetrahedron Letters* **1999**, *40*, 4137-4140.

(69) Ogara, J. E.; Portmess, J. D.; Wagener, K. B. *Macromolecules* **1993**, *26*, 2837-2841.

(70) Ogara, J. E.; Wagener, K. B.; Hahn, S. F. *Abstracts of Papers of the American Chemical Society* **1993**, *206*, 60-POLY.

(71) Smith, J. A.; Brzezinska, K. R.; Valenti, D. J.; Wagener, K. B. *Macromolecules* **2000**, *33*, 3781-3794.

(72) Schwendeman, J. E.; Watson, M. D.; Smith, J. A.; Brzezinska, K. R.; Wagener, K. B. In *Ring Opening Metathesis Polymerization and Related Chemistry*; Khosravi, E., Szymanska-Buzar, T., Eds.; Kluwer Academic Publishers: Netherlands, 2002.

(73) Watson, M. D.; Wagener, K. B. *Macromolecules* **2000**, *33*, 8963-8970.

(74) Watson, M. D.; Wagener, K. B. *Macromolecules* **2000**, *33*, 5411-5417.

(75) Watson, M. D.; Wagener, K. B. *Macromolecules* **2000**, *33*, 3196-3201.

(76) Watson, M. D.; Wagener, K. B. *Macromolecules* **2000**, *33*, 1494-1496.

(77) Marmo, J. C.; Wagener, K. B. *Macromolecules* **1993**, *26*, 2137-2138.

(78) Marmo, J. C.; Wagener, K. B. *Macromolecules* **1995**, *28*, 2602-2606.

(79) Ogara, J. E.; Wagener, K. B. *Makromolekulare Chemie-Rapid Communications* **1993**, *14*, 657-662.

(80) Brzezinska, K. R.; Wagener, K. B.; Burns, G. T. *Journal of Polymer Science Part a-Polymer Chemistry* **1999**, *37*, 849-856.

(81) Brzezinska, K. R.; Deming, T. J. *Macromolecules* **2001**, *34*, 4348-4354.

(82) Smith, D. W.; Wagener, K. B. *Macromolecules* **1993**, *26*, 3533-3537.

(83) Anderson, J. D.; Cummings, S. K.; Portmess, J. D.; Wagener, K. B. *Abstracts of Papers of the American Chemical Society* **1995**, *210*, 67-POLY.

(84) Cummings, S.; Ginsburg, E.; Miller, R.; Portmess, J.; Smith, D. W.; Wagener, K. In *Step Growth Polymers for High Performance Materials: New Synthetic Methods*; Hedrick, J. L., Labadie, J. W., Eds.; American Chemical Society: Washington, D.C., 1996.

(85) Church, A. C.; Pawlow, J. H.; Wagener, K. B. *Abstracts of Papers of the American Chemical Society* **1999**, *217*, 086-POLY.

(86) Church, A. C.; Pawlow, J. H.; Wagener, K. B. *Abstracts of Papers of the American Chemical Society* **2001**, *221*, 350-POLY.

(87) Smith, D. W.; Wagener, K. B. *Macromolecules* **1993**, *26*, 1633-1642.

(88) Wolfe, P. S.; Gomez, F. J.; Wagener, K. B. *Abstracts of Papers of the American Chemical Society* **1997**, *213*, 156-PMSE.

(89) Wolfe, P. S.; Gomez, F. J.; Wagener, K. B. *Macromolecules* **1997**, *30*, 714-717.

(90) Gomez, F. J.; Wagener, K. B. *Abstracts of Papers of the American Chemical Society* **1998**, *216*, 141-POLY.

(91) Gomez, F. J.; Wagener, K. B. *Journal of Organometallic Chemistry* **1999**, *592*, 271-277.

(92) Allcock, H. R.; Kellam, E. C.; Hofmann, M. A. *Macromolecules* **2001**, *34*, 5140-5146.

(93) Allcock, H. R.; Kellam, E. C. *Macromolecules* **2002**, *35*, 40-47.

(94) O'Donnell, P. M.; Brzezinska, K.; Powell, D.; Wagener, K. B. *Macromolecules* **2001**, *34*, 6845-6849.

(95) Tsuie, B.; Wagener, K. B.; Reynolds, J. R. *Abstracts of Papers of the American Chemical Society* **1999**, *218*, 182-POLY.

(96) Tao, D.; Wagener, K. B. *Macromolecules* **1994**, *27*, 1281-1283.

(97) Schlick, H.; Stelzer, F.; Tasch, S.; Leising, G. *Journal of Molecular Catalysis a-Chemical* **2000**, *160*, 71-84.

(98) Walba, D. M.; Keller, P.; Shao, R. F.; Clark, N. A.; Hillmyer, M.; Grubbs, R. H. *Journal of the American Chemical Society* **1996**, *118*, 2740-2741.

(99) Joo, S. H.; Yun, Y. K.; Jin, J. I.; Kim, D. C.; Zin, W. C. *Macromolecules* **2000**, *33*, 6704-6712.

(100) Hopkins, T. E.; Pawlow, J. H.; Koren, D. L.; Deters, K. S.; Solivan, S. M.; Davis, J. A.; Gomez, F. J.; Wagener, K. B. *Macromolecules* **2001**, *34*, 7920-7922.

(101) Hoffman, J. D. *Polymer* **1982**, *23*, 656-670.

(102) Hoffman, J. D. *Polymer* **1983**, *24*, 3-26.

(103) Schwendeman, J.; Wagener, K. B.; Sparer, R.; Benz, M. E. *Abstracts of Papers of the American Chemical Society* **2002**, *43(1)*, 282-POLY.

(104) Nunomoto, S.; Kawakami, Y.; Yamashita, Y. *Journal of Organic Chemistry* **1983**, *48*, 1912-1914.

(105) Olah, G. A.; Gupta, B. G. B.; Malhotra, R.; Narang, S. C. *Journal of Organic Chemistry* **1980**, *45*, 1638-1639.

(106) Wu, Z.; Grubbs, R. H. *Macromolecules* **1995**, *28*, 3502-3508.

(107) Reetz, M. T.; Westermann, J.; Steinbach, R. *Journal of the Chemical Society-Chemical Communications* **1981**, 237-239.

(108) Reetz, M. T.; Westermann, J. *Journal of Organic Chemistry* **1983**, *48*, 254-255.

(109) Reetz, M. T.; Westermann, J.; Kyung, S. H. *Chemische Berichte-Recueil* **1985**, *118*, 1050-1057.

(110) Reetz, M. T. *Angewandte Chemie-International Edition in English* **1991**, *30*, 1531-1546.

(111) Allcock, H. R.; Lampe, F. W. *Contemporary Polymer Chemistry*; 2nd ed.; Prentice Hall, Inc.: Englewood Cliffs, NJ, 1990.

(112) Meisters, A.; Mole, T. *Australian Journal of Chemistry* **1974**, *27*, 1665-1672.

(113) Coates, G. W.; Waymouth, R. M. In *Comprehensive Organometallic Chemistry II*; Abel, E. W., Stone, F. G. A., Wilkinson, G., Hegedus, L., Eds.; Pergamon Press: New York, 1995; Vol. 12.

(114) Mecking, S.; Johnson, L. K.; Wang, L.; Brookhart, M. *Journal of the American Chemical Society* **1998**, *120*, 888-899.

(115) Younkin, T. R.; Conner, E. F.; Henderson, J. I.; Friedrich, S. K.; Grubbs, R. H.; Bansleben, D. A. *Science* **2000**, *287*, 460-462.

(116) Shaffer, T. D.; Canich, J. A. M.; Squire, K. R. *Macromolecules* **1998**, *31*, 5145-5147.

(117) Kesti, M. R.; Waymouth, R. M. *Journal of the American Chemical Society* **1992**, *114*, 3565-3567.

(118) Wunderlich, B. *Macromolecular Physics*; vol. 3, Academic Press: New York, pp. 275-278, 1980.

(119) Wunderlich, B. *Journal of Chemical Physics* **1958**, *29*, 1395-1404.

(120) Ma, L.; Bin, Y.; Sakai, Y.; Chen, Q.; Kurosu, H.; Matsuo, M. *Macromolecules* **2001**, *34*, 4802-4814.

(121) Johnson, L. K.; Mecking, S.; Brookhart, M. *Journal of the American Chemical Society* **1996**, *118*, 267-268.

(122) Younkin, T. R.; Connor, E. F.; Henderson, J. I.; Friedrich, S. K.; Grubbs, R. H.; Bansleben, D. A. *Science* **2000**, *287*, 460-462.

(123) Yokota, K.; Hirabayashi, T. *Macromolecules* **1981**, *14*, 1613-1616.

(124) Kutsumizu, S.; Tadano, K.; Matsuda, Y.; Goto, M.; Tachino, H.; Hara, H.; Hirasawa, E.; Tagawa, H.; Muroga, Y.; Yano, S. *Macromolecules* **2000**, *33*, 9044-9053.

(125) Macknight, W. J.; Taggart, W. P.; McKenna, L. *Journal of Polymer Science Part C-Polymer Symposium* **1974**, 83-96.

(126) Lee, J. Y.; Painter, P. C.; Coleman, M. M. *Macromolecules* **1988**, *21*, 346-354.

(127) Yokota, K. *Progress in Polymer Science* **1999**, *24*, 517-563.

(128) Inai, Y.; Kato, S. I.; Hirabayashi, T.; Yokota, K. *Journal of Polymer Science Part a-Polymer Chemistry* **1996**, *34*, 2341-2348.

(129) Smith, J. A. Ph. D. Dissertation, University of Florida, 2002.

(130) Earnest, T. R.; Macknight, W. J. *Journal of Polymer Science Part B-Polymer Physics* **1978**, *16*, 143-157.

(131) Hillmyer, M. A.; Grubbs, R. H. *Macromolecules* **1993**, *26*, 872-874.

(132) Ivan, B.; Kennedy, J. P.; Chang, V. S. C. *Journal of Polymer Science: Polymer Chemistry Edition* **1980**, *18*, 3177-3191.

(133) Podesva, J.; Spevacek, J.; Dybal, J. *Journal of Applied Polymer Science* **1999**, *74*, 3214-3224.

(134) Podesva, J.; Holler, P. *Journal of Applied Polymer Science* **1999**, *74*, 3203-3213.

(135) Plank, H.; Syre, I.; Dauner, M.; Egbers, G. *Polyurethanes in Biomedical Engineering II*; Elsevier: Amstredam, 1987.

(136) Hillmyer, M. A.; Nguyen, S. T.; Grubbs, R. H. *Macromolecules* **1997**, *30*, 718-721.

(137) Maughon, B. R.; Grubbs, R. H. *Macromolecules* **1997**, *30*, 3459-3469.

(138) Maughon, B. R.; Morita, T.; Bielawski, C. W.; Grubbs, R. H. *Macromolecules* **2000**, *33*, 1929-1935.

(139) Blackwell, H. E.; O'Leary, D. J.; Chatterjee, A. K.; Washenfelder, R. A.; Bussmann, D. A.; Grubbs, R. H. *Journal of the American Chemical Society* **2000**, *122*, 58-71.

(140) Bielawski, C. W.; Scherman, O. A.; Grubbs, R. H. *Polymer* **2001**, *42*, 4939-4945.

(141) Kennedy, J. P. *Macromolecular Symposia* **2001**, *175*, 127-131.

(142) Kennedy, J. P. *Journal of Polymer Science Part a-Polymer Chemistry* **1999**, *37*, 2285-2293.

(143) Bazan, G. C.; Oskam, J. H.; Cho, H. N.; Park, L. Y.; Schrock, R. R. *Journal of the American Chemical Society* **1991**, *113*, 6899-6907.

(144) Schwab, P.; Grubbs, R. H.; Ziller, J. W. *Journal of the American Chemical Society* **1996**, *118*, 100-110.

BIOGRAPHICAL SKETCH

I was born on March 29, 1973, and grew up in Pittsburgh, Pennsylvania, with my parents and two brothers. After graduating from high school at Sewickley Academy in 1991, I began my secondary education at Purdue University, where I majored in chemical engineering. I soon found that chemistry and my home were closer to my heart, so I finished my undergraduate career in chemistry at the Pennsylvania State University, Behrend College. My interest in making practical and useful things with my knowledge of science prompted me to study polymer materials. I came to the University of Florida in 1997 for its excellent polymer program, beautiful climate, and the quality and energy of its faculty members, like Prof. Wagener. Shortly thereafter I met the love of my life. Irina, and then I met the sweetest little girl that I have ever known, my daughter Laura.

I certify that I have read this study and that in my opinion it conforms to acceptable standards of scholarly presentation and is fully adequate, in scope and quality, as a dissertation for the degree of Doctor of Philosophy.

Kenneth Wagener
Professor of Chemistry

I certify that I have read this study and that in my opinion it conforms to acceptable standards of scholarly presentation and is fully adequate, in scope and quality, as a dissertation for the degree of Doctor of Philosophy.

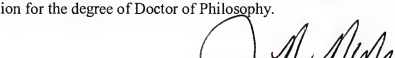

John Reynolds
Professor of Chemistry

I certify that I have read this study and that in my opinion it conforms to acceptable standards of scholarly presentation and is fully adequate, in scope and quality, as a dissertation for the degree of Doctor of Philosophy.

David Richardson
Professor of Chemistry

I certify that I have read this study and that in my opinion it conforms to acceptable standards of scholarly presentation and is fully adequate, in scope and quality, as a dissertation for the degree of Doctor of Philosophy.

Eric Enholm
Professor of Chemistry

I certify that I have read this study and that in my opinion it conforms to acceptable standards of scholarly presentation and is fully adequate, in scope and quality, as a dissertation for the degree of Doctor of Philosophy.

Anthony Brennan
Professor of Materials Science and Engineering

This dissertation was submitted to the Graduate Faculty of the Department of Chemistry in the College of Liberal Arts and Sciences and to the Graduate School and was accepted as partial fulfillment of the requirements for the degree of Doctor of Philosophy.

December 2002

_____

Dean, Graduate School